

---


Electronic Theses and Dissertations, 2004-2019

---

2014

## Treatment-Specific Approaches for Analysis and Control of Left Ventricular Assist Devices

George Faragallah  
*University of Central Florida*

 Part of the [Electrical and Electronics Commons](#)  
Find similar works at: <https://stars.library.ucf.edu/etd>  
University of Central Florida Libraries <http://library.ucf.edu>

This Doctoral Dissertation (Open Access) is brought to you for free and open access by STARS. It has been accepted for inclusion in Electronic Theses and Dissertations, 2004-2019 by an authorized administrator of STARS. For more information, please contact [STARS@ucf.edu](mailto:STARS@ucf.edu).

---

### STARS Citation

Faragallah, George, "Treatment-Specific Approaches for Analysis and Control of Left Ventricular Assist Devices" (2014). *Electronic Theses and Dissertations, 2004-2019*. 4774.  
<https://stars.library.ucf.edu/etd/4774>

# **TREATMENT-SPECIFIC APPROACHES FOR ANALYSIS AND CONTROL OF LEFT VENTRICULAR ASSIST DEVICES**

by:

**GEORGE FARAGALLAH**  
B.S. Cairo University, 2005  
M.S. University of Central Florida, 2009

A dissertation submitted in partial fulfillment of the requirements  
for the degree of Doctor of Philosophy  
in the department of Electrical Engineering and Computer Science  
in the College of Engineering and Computer Science  
at the University of Central Florida  
Orlando, Florida

Fall Term  
2014

Major Professor: Marwan A. Simaan

© 2014 George Faragallah

## **ABSTRACT**

A Left Ventricular Assist Device (LVAD) is a mechanical pump that helps patients with heart failure conditions. This rotary pump works in parallel to the ailing heart and provides an alternative path for blood flow from the weak left ventricle to the aorta. The LVAD is controlled by the power supplied to the pump motor. An increase in the pump motor power increases the pump speed and the pump flow. The LVAD is typically controlled at a fixed setting of pump power. This basically means that the controller does not react to any change in the activity level of the patient. An important engineering challenge is to develop an LVAD feedback controller that can automatically adjust its pump motor power so that the resulting pump flow matches the physiological demand of the patient. To this end, the development of a mathematical model that can be used to accurately simulate the interaction between the cardiovascular system of the patient and the LVAD is essential for the controller design. The use of such a dynamic model helps engineers and physicians in testing their theories, assessing the effectiveness of prescribed treatments, and understanding in depth the characteristics of this coupled bio-mechanical system.

The first contribution of this dissertation is the development of a pump power-based model for the cardiovascular-LVAD system. Previously, the mathematical models in the literature assume availability of the pump speed as an independent control variable. In reality, however, the device is controlled by pump motor power which, in turn, produces the rotational pump speed. The nonlinear relationship between the supplied power and the speed is derived, and interesting observations about the pump speed signal are documented.

The second contribution is the development of a feedback controller for patients using an LVAD as either a destination therapy or a bridge to transplant device. The main objective of

designing this controller is to provide a physiological demand of the patient equivalent of that of a healthy individual. Since the device is implanted for a long period of time, this objective is chosen to allow the patient to live a life as close to normal as possible.

The third contribution is an analysis of the aortic valve dynamics under the support of an LVAD. The aortic valve may experience a permanent closure when the LVAD pump power is increased too much. The permanent closure of the aortic valve can be very harmful to the patients using the device as a bridge to recovery treatments. The analysis illustrates the various changes in the hemodynamic variables of the patient as a result of aortic valve closing. The results establish the relationship between the activity level and the heart failure severity with respect to the duration of the aortic valve opening.

## ACKNOWLEDGMENTS

The writing of this dissertation marks a great milestone in my academic and professional career. I wouldn't be able to reach this point in my research without the people who guided and helped me during my academic venture. I was fortunate to have the opportunity to pursue my research at the University of Central Florida. The time I spent there was both rewarding and invaluable in my advancement. I'm extremely thankful to my advisor, Dr. Marwan Simaan. His support was instrumental to my success, without him I wouldn't be where I am today. During this time, Dr. Simaan taught me many lessons in life, academia, and research. I would like to extend a thank you to my committee members: Dr. Eduardo Divo for being available on numerous occasions when I really needed help, Dr. Zhihua Qu and Dr. Michael Haralambous enabled me to broaden my knowledge in control theory through many useful classes, and Dr. Alain Kassab for his experience in the mechanical engineering aspects of my research.

I am also thankful to my colleagues in the Control Lab, especially Yu Wang, as we collaborated on many areas of this research. I cannot forget the tremendous help I received from the administrative staff in the Electrical Engineering department; their response to my inquiries and assistance in filing the forms showed how much they care about the students. I appreciate the financial support I received from the National Science Foundation to complete my research (Grant number: ECCS-0852440).

Most importantly, a special "Thank You" to my family for their support and inspiration from thousands of miles away: My parents, Gamil and Marsil, for their love and patience; and my cousin Dr. Rafik Hanna and his family for believing in me when I had doubts in my ability to

complete my research. Finally, I thank all the great friends that I met during my time at UCF, especially soon-to-be Dr. Spencer Farrar and his family.

# TABLE OF CONTENTS

LIST OF FIGURES .....	x
LIST OF TABLES .....	xiv
CHAPTER 1: THE CARDIOVASCULAR SYSTEM MODEL.....	1
1.1. The Cardiovascular System .....	1
1.2. The Cardiac Cycle.....	5
1.2.1. Isovolumic Relaxation .....	5
1.2.2. Filling.....	5
1.2.3. Isovolumic Contraction.....	6
1.2.4. Ejection .....	6
1.3. Electrical Analogue of the Cardiovascular System .....	10
1.4. The Cardiovascular System Model .....	12
1.5. Summary .....	20
CHAPTER 2: THE LEFT VENTRICULAR ASSIST DEVICES .....	22
2.1. Heart Failure .....	22
2.2. Left Ventricular Assist Devices .....	24
2.2.1. LVAD Generations .....	24
2.2.2. LVAD Components .....	25
2.2.3. LVAD treatment strategies .....	26



2.3. The Left Ventricular Assist Device Model .....	29
2.4. The Combined Cardiovascular-LVAD Model.....	32
2.5. Summary .....	35
<b>CHAPTER 3: NEW POWER-BASED CONTROL MODEL OF THE PUMP OF THE LEFT VENTRICULAR ASSIST DEVICES .....</b>	<b>36</b>
3.1. The Power-Based Pump Model .....	36
3.2. Simulation Results .....	40
3.3. Summary .....	44
<b>CHAPTER 4: A FEEDBACK CONTROLLER TO DELIVER PHYSIOLOGICAL DEMAND FOR LVAD PATIENTS.....</b>	<b>49</b>
4.1. The Physiological Demand of LVAD Patients .....	49
4.2. Development of the Feedback Controller .....	55
4.3. Simulation results.....	59
4.4. Summary .....	63
<b>CHAPTER 5: ENGINEERING ANALYSIS OF THE AORTIC VALVE DYNAMICS IN PATIENTS WITH LEFT VENTRICULAR ASSIST DEVICES .....</b>	<b>64</b>
5.1. Method for data collection .....	64
5.2. Simulation results.....	67
5.3. Summary .....	82

CHAPTER 6: AORTIC VALVE DYNAMICS IN BRIDGE TO RECOVERY TREATMENTS .....	83
6.1. Aortic valve permanent closure problems .....	83
6.2. Aortic valve performance .....	88
6.3. Preliminary results in detecting the aortic valve opening .....	95
6.4. Summary .....	104
CHAPTER 7: SUMMARY, CONCLUSION AND FUTURE WORK .....	105
7.1. Summary and conclusion .....	105
7.2. Future work .....	109
REFERENCES .....	111

## LIST OF FIGURES

Figure 1.1: Human Circulatory System. ....	4
Figure 1.2: Cross Section of a Beating heart .....	7
Figure 1.3: Cardiac Cycle .....	8
Figure 1.4: Fifth Order Circuit Model That Represents the Cardiovascular System.....	14
Figure 1.5: Elastance Function of healthy, mild heart failure and severe heart failure Left Ventricle.....	18
Figure 2.1: Schematic of a rotary LVAD.....	28
Figure 2.2: LVAD Pump Model.....	31
Figure 2.3: Combined Cardiovascular and LVAD Model.....	34
Figure 3.1: Pump speed signal as a function of time when the pump motor power is increased linearly .....	45
Figure 3.2: Pump speed signal during normal operation (left), pump speed signal during suction (right) .....	45
Figure 3.3: Pump flow with the pump motor power increasing linearly .....	46
Figure 3.4: Left ventricular pressure for different values of $E_{\max}$ and constant $P_E = 2.16 \text{ W}$ .....	46
Figure 3.5: Pump speed for different values of $E_{\max}$ and constant $P_E = 2.16 \text{ W}$ . ....	47
Figure 3.6: Pump flow for different values of $E_{\max}$ and constant $i(t) = 2.16 \text{ W}$ .....	47
Figure 4.1: Pump speed signal for different $R_s$ , with no change to the controller parameters.....	54

Figure 4.2: Pump flow signal for different $R_s$ , with no change to the controller parameters.....	54
Figure 4.3:Block diagram for the feedback controller.....	58
Figure 4.4: Pump Flow signal as $R_s$ Changes from 1 to 0.5 mmHg.s/ml.....	61
Figure 4.5: Lower and Upper Brackets of the Fibonacci Search to Estimate $R_s$ .....	61
Figure 4.6: Lower and Upper Brackets of the Fibonacci Search to Estimate $P_E$ .....	62
Figure 5.1: Change of aortic valve flow rate with ump motor power.....	70
Figure 5.2. Pump Flow as a function of pump motor power .....	70
Figure 5.3. Left ventricle pressure as a function of pump power .....	71
Figure 5.4. Aortic pressure as a function of pump power.....	71
Figure 5.5: Waveforms for the case of inactive patient with mild heart failure. (a) Aortic valve flow, (b) pump flow, (c) Left ventricle pressure and (d) Aortic pressure.....	74
Figure 5.6: Waveforms for the case of very active patient with mild heart failure. (a) Aortic valve flow, (b) pump flow, (c) Left ventricle pressure and (d) Aortic pressure.....	75
Figure 5.7: Waveforms for the case of inactive patient with moderate heart failure. (a) Aortic valve flow, (b) pump flow, (c) Left ventricle pressure and (d) Aortic pressure. ....	76
Figure 5.8: Waveforms for the case of moderately active patient with moderate heart failure. (a) Aortic valve flow, (b) pump flow, (c) Left ventricle pressure and (d) Aortic pressure.....	77
Figure 5.9: Waveforms for the case of very active patient with moderate heart failure. (a) Aortic valve flow, (b) pump flow, (c) Left ventricle pressure and (d) Aortic pressure. ....	78

Figure 5.10: Waveforms for the case of inactive patient with severe heart failure. (a) Aortic valve flow, (b) pump flow, (c) Left ventricle pressure and (d) Aortic pressure.....	79
Figure 5.11: Waveforms for the case of moderately active patient with severe heart failure. (a) Aortic valve flow, (b) pump flow, (c) Left ventricle pressure and (d) Aortic pressure.....	80
Figure 5.12: Waveforms for the case of very active patient with severe heart failure. (a) Aortic valve flow, (b) pump flow, (c) Left ventricle pressure and (d) Aortic pressure.....	81
Figure 6.1: Aortic Valve Stenosis (source: <a href="http://www.medindia.net">www.medindia.net</a> ) .....	87
Figure 6.2: Coronary Circulation (source: <a href="http://www.wikipedia.com">www.wikipedia.com</a> ) .....	87
Figure 6.3. Aortic valve opening time as a percentage of the cardiac cycle for mild heart failure .....	90
Figure 6.4. Aortic valve opening time as a percentage of the cardiac cycle for moderate heart failure .....	90
Figure 6.5. Aortic valve opening time as a percentage of the cardiac cycle for severe heart failure .....	91
Figure 6.6: Systemic vascular current signal for mild heart failure with moderate level of activity. Pump motor power values shown are (a) $P_E=1.4W$ , (b) $P_E=1.1W$ , (c) $P_E=0.8W$ , (d) $P_E=0.6W$ and (e) $P_E=0.3W$ .....	99
Figure 6.7: Systemic vascular of patient with mild heart failure and different levels of activity: (a) active, (b) moderately active, and (c) inactive.....	100

Figure 6.8: Systemic vascular of patient with moderate heart failure and different levels of activity: (a) active, (b) moderately active, and (c) inactive. .... 101

Figure 6.9: Systemic vascular of patient with severe heart failure and different levels of activity: (a) active, (b) moderately active, and (c) inactive. .... 102

Figure 6.10:  $I_{RS}$  for mild heart failure and moderate level of activity.  $P_E$  range is from 0.2W to 1.6W ..... 103

Figure 6.11: Systemic vascular flow for healthy heart with no LVAD used..... 103

## LIST OF TABLES

Table 1.1: Phases of the Cardiac Cycle .....	7
Table 1.2: Model Parameters [8]-[10] .....	14
Table 1.3: State Variables in the Cardiovascular Model .....	21
Table 2.1: Model Parameters for the LVAD .....	31
Table 3.1: Model Parameters for the Current-Based Model.....	39
Table 3.2: Results when $E_{\max}$ is varied from 1.00 to 0.25, while $P_E$ is kept constant.....	48
Table 4.1: Aortic flow comparison between aortic flow of a healthy heart, mild heart failure with no support and mild heart failure with constant LVAD support, for different activity levels.....	53
Table 5.1: Nine different cases representing combination of three levels of heart failure and three levels of patient activity. ....	66
Table 5.2: Critical pump power ( $P_E^c$ ) values of the nine different cases. ....	82
Table 6.1: pump power ( $P_E$ ) and pump speed ( $\omega$ ) values of the nine different cases to keep the aortic valve open during 15% of the duration of the corresponding cardiac cycle.....	94
Table 6.2: Blood flow required for healthy patient and blood flow produced for the nine different when the aortic valve open during 15% of the duration of the corresponding cardiac cycle .....	94

## CHAPTER 1: THE CARDIOVASCULAR SYSTEM MODEL

The development of mathematical models requires complete understanding of the process that is being modeled. For this reason, we begin this chapter by giving a brief overview of the cardiovascular system. Much emphasis is given to the heart and the cardiac cycle because they are responsible for regulating the blood flow. The similarities between the dynamics of blood through blood vessels and Ohm's law for electrical circuits are outlined. This is followed by introducing the lumped-parameter electrical circuit model of the cardiovascular system. Then using control theory laws, the model is then formulated in the space state representation form.

### 1.1. The Cardiovascular System

The cardiovascular system consists of blood, blood vessels and the heart. In general terms, the main task of the cardiovascular system is to satisfy, for each individual cell of the organism, the requirements of metabolism for  $O_2$  and other substrates. At the same time  $CO_2$  and the other end products of metabolism have to be removed [1].

First part of the cardiovascular system is the blood. Blood is a viscous fluid that represents about 8% of the total body weight. On the average, males have blood volume of 5 to 6 liters, while females have 4 to 5 liters. Blood is constantly circulating the human body through blood vessels. Its flow through the blood vessels is powered by the force created by the pumping action of the heart. The flow in the straight blood vessels is mostly a laminar flow, but it turns to turbulent when it is distributed at the branching points in the vessels to reach the different organs of the body. Hence, the main function of the blood is to carry oxygen, nourishments, electrolytes,



hormones and vitamins to the body tissues; and collect carbon dioxide and waste away from them. Additional functions for the blood include: protecting the body from infections (helping the immune system); regulating the temperature of the body; and stopping the bleeding of open wounds (coagulation).

Second part of the cardiovascular system is the blood vessels. They are the channels through which blood reaches the body tissues. Blood vessels form two main distribution networks: the first is the systemic circulation which carries the oxygenated blood from the left side of the heart to the rest of the body and then the oxygen-depleted blood goes back to the right side of the heart; and the second is the pulmonary circulation, which carries the oxygen-depleted blood from the right side of the heart to the lungs for oxygen exchange and then carries the oxygen rich blood back to the left side of the heart. Together they are called the circulatory system and they form a closed loop system which starts and ends at the heart. Figure 1.1 shows the cardiovascular system. The blood vessels where the oxygenated blood flow is shown in red while blue indicates the vessels that carry the deoxygenated blood. In addition to the two main circulations, there is the coronary circulation. Its task is to supply the oxygenated blood to the heart muscle. The blood vessels of the coronary circulation run on the surface or deep into the heart muscle. Most of the blood delivery to the heart muscle happens when the heart muscle is relaxed, because that is when the vessels can increase their diameter.

In terms of their structure and function, the blood vessels can be classified into three main groups: arteries; capillaries and veins. Arteries carry blood away from the heart, either to body tissues (called systemic arteries) or to the lungs (called pulmonary arteries). The largest artery, in terms of diameter, is the aorta which carries the oxygenated blood as it leaves the left ventricle

and then it branches out to smaller arteries. These smaller arteries branch to even smaller blood vessels called arterioles; they help regulate the blood flow into the tissue capillaries. Capillaries have the smallest diameter among blood vessels. They are considered to be the link between arteries and veins. Their task is to facilitate the exchange of material between the blood and the tissue cells. Veins are the blood vessels that carry blood towards the heart. As opposed to the arteries, the blood flows first in veins with the smallest diameter (called venules) after it leaves the capillaries, then it flows into veins that has larger diameter. It finally reaches the two main, and largest diameter, veins: superior vena cava; and inferior vena cave, together they are called venae cavae.

Finally, the third part of the cardiovascular system is the heart. It is a muscular organ that weighs about 250~300 grams [2], and is located behind and slightly left to the breastbone. Its main task is to pump blood into the blood vessels which, in turn, deliver the blood to the various organs in the body [3].

The heart can be divided to four chambers: right atrium, right ventricle (together can be called right heart), left atrium and left ventricle (together can be called left heart), see Figure 1.2.

The two atria are thin-walled chambers that receive blood from the veins, where the two ventricles are thick-walled chambers that can pump blood into the arteries. The flow is regulated through four valves: two in the left heart (mitral and aortic valve); and two in the right heart (tricuspid and pulmonary valve). Mitral and tricuspid valves are the atria and the ventricles, where the aortic and pulmonary valves are between the ventricles and the arteries. The right and left hearts work in concert to pump blood it into the circulatory system. The sequence of events taking place inside the heart to achieve this task is called the cardiac cycle [3].

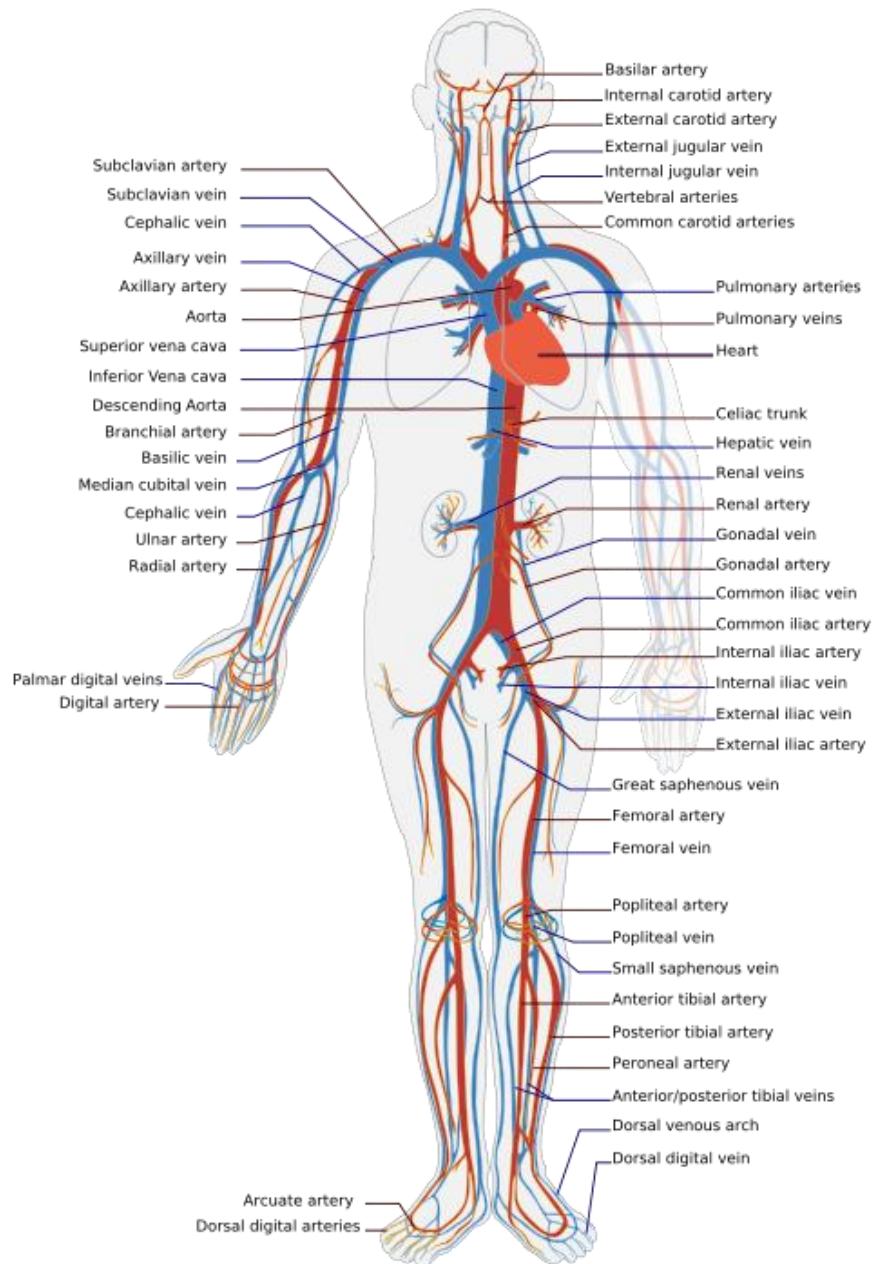


Figure 1.1: Human Circulatory System.

([http://en.wikipedia.org/wiki/File:Circulatory\\_System\\_en.svg](http://en.wikipedia.org/wiki/File:Circulatory_System_en.svg))

## 1.2. The Cardiac Cycle

The cardiac cycle is a term that refers to the sequence of events related to the heart from the beginning of one heartbeat to the beginning of the next one. In literature there are different ways to divide the cardiac cycle into phases. Some references use two main phases, while others can be more specific and list as many as eight different phases. However, when the focus is on the dynamics of the valve, using four phases can fully describe the cardiac cycle, as seen in Table 1.1.

The cardiac cycle is better explained by following the blood pressure, blood flow and the state of the valves in each phase. Focusing on the left heart side, the four phases are:

### 1.2.1. Isovolumic Relaxation

In this phase, the ventricle relaxes and its pressure is rapidly decreasing without any change in the blood volume inside the ventricle, hence the name isovolumic. This happens due to the closure of the mitral and the aortic valve in this phase. Blood from the pulmonary veins fills the left atrium and that causes a gradual increase in the left atrial pressure, but is still lower than the left ventricle pressure and that keeps the mitral valve closed during the entire phase. Across the aortic valve the aortic pressure is higher than the left ventricle pressure and that leads to the closure of the aortic valve.

### 1.2.2. Filling

In this phase, the left ventricle pressure continues to decrease until its value is lower than the left atrial pressure. This change in the pressure difference leads to the opening of the mitral valve and the blood flowing from the left atrium to fill the left ventricle. Initially the blood from

the atrium flows rapidly, but then it slows down until the filling is complete. The left ventricle pressure is increasing in a very small rate during this phase, but still lower than the aortic pressure, hence the aortic valve remains to be closed.

### 1.2.3. Isovolumic Contraction

The mitral valve closes when the pressure in the left ventricle exceeds the left atrial pressure. Now both valves are closed again, but in this phase the left ventricle pressure is rapidly increasing (i.e. the ventricle muscle is contracting). The aortic pressure continues to decrease because of the closure of the aortic valve.

### 1.2.4. Ejection

As the pressure inside the left ventricle continues to build up and exceeds the aortic pressure, the aortic valve opens in response to this change in pressure. This causes the blood to be ejected (pumped) from the left ventricle into the aorta. As the blood volume inside the ventricle starts decreases, the blood is ejected in a slower rate until it stops when the pressure in the ventricle is lower than that in the aorta. The mitral valve state remains unchanged (i.e. closed) during this phase.

Figure 1.3 shows the pressure and volume measurements of the left heart during two cardiac cycles. Note that the same sequence of events happens simultaneously in the right heart, but pressures of the right ventricle, right atrium and the pulmonary artery are lower than that of the left ventricle, left atrium and the aorta, respectively. The reason is that the left ventricle is stronger than the right ventricle, as it needs to pump blood to the whole body whereas the right ventricle pumps blood to the lungs.

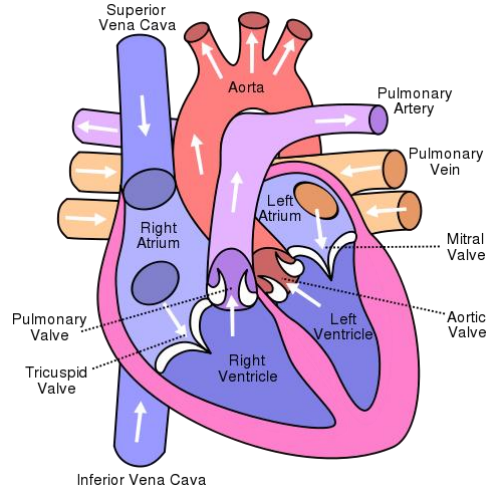


Figure 1.2: Cross Section of a Beating heart

([http://upload.wikimedia.org/wikipedia/commons/e/e5/Diagram\\_of\\_the\\_human\\_heart\\_\(cropped\).svg](http://upload.wikimedia.org/wikipedia/commons/e/e5/Diagram_of_the_human_heart_(cropped).svg))

Table 1.1: Phases of the Cardiac Cycle

Modes	Valves		Phases
	Mitral/Tricuspid	Aortic/Pulmonary	
1	Closed	Closed	Isovolumic Relaxation
2	Open	Closed	Filling
1	Closed	Closed	Isovolumic Contraction
3	Closed	Open	Ejection
-	Open	Open	Not Feasible

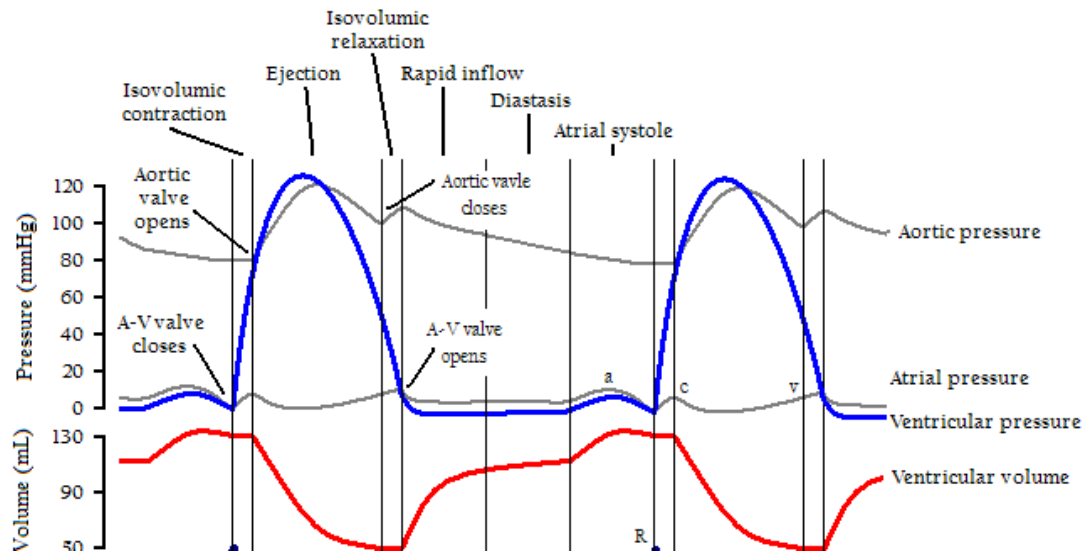


Figure 1.3: Cardiac Cycle

(Source: [http://en.wikipedia.org/wiki/File:Cardiac\\_Cycle\\_Left\\_Ventricle.PNG](http://en.wikipedia.org/wiki/File:Cardiac_Cycle_Left_Ventricle.PNG))

It is important to give formal definitions for some parameters and concepts related to the cardiac cycle since they will be used repeatedly in this dissertation [4]:

1. Heart Rate ( $HR$ ): is the number of heartbeats per unit time, commonly known as beats per minute (bpm). When calculating  $HR$  in bpm, Equation(1.1) can be used:

$$HR = \frac{60}{t_c} \quad (1.1)$$

Where  $t_c$  is the time interval for one cardiac cycle.

2. Systole: means the contraction of the heart and it describes the events that happen during the isovolumic contraction and ejection phases of the cardiac cycle.
3. End Systolic Volume ( $ESV$ ): is the blood volume inside the ventricle at the end of the systole. It is the lowest volume of blood during the cardiac cycle, thus it can be used clinically to measure the ventricle ability to pump blood.
4. Diastole: means the relaxation of the heart and it describes the events that happen during the isovolumic relaxation and filling phases of the cardiac cycle.
5. End Diastolic Volume ( $EDV$ ): is the blood volume inside the ventricle at the end of the diastole.
6. Stroke Volume ( $SV$ ): is the blood volume that is pumped by the ventricle in one beat. It can be calculated as the difference between the end-diastolic volume of blood and the end-systolic volume of blood.

$$SV = EDV - ESV \quad (1.2)$$

7. Cardiac Output ( $CO$ ): Is the blood volume ejected by the ventricle per unit time. It is common to use the units of ml/s or l/min.



$$CO = SV * HR \quad (1.3)$$

8. Ejection Fraction (EF): Is the fraction of the end diastolic volume that is pumped during every heartbeat. In other words, what percentage of the blood volume stored in the ventricle, during the isovolumic contraction, is pumped to the aorta during the ejection phase.

$$E_f = \frac{SV}{EDV} = \frac{EDV - ESV}{EDV} \quad (1.4)$$

### 1.3. Electrical Analogue of the Cardiovascular System

There are many similarities between the flow of blood into blood vessels and the electric current passing through conductors. The blood flow ( $Q$ ) depends on two factors: the pressure difference ( $\Delta P$ ) between the two ends of the blood vessel, and the impediment (resistance) ( $R_{vasc}$ ) to the blood flow through the vessel. Equation (1.5) describes such relation:

$$Q = \frac{\Delta P}{R_{vasc}} \quad (1.5)$$

This expression is similar to Ohm's law which describes the relation between the electric current ( $I$ ) and the voltage difference ( $V$ ) and electric resistance  $R$  of the conductor as described in Equation(1.6):

$$I = \frac{V}{R} \quad (1.6)$$

The volume-pressure relationship is called the vascular compliance, and it is a measure of the ability of a blood vessel wall to expand and contract in response to changes in pressure. It is important to model the vascular compliance for large arteries and veins, the compliance effect

can be neglected, however, in small arteries. The compliance is described in Equation (1.7) as the change of volume ( $\Delta Vol$ ) (The volume is denoted as  $\Delta Vol$  to avoid any confusion with the voltage) divided by the change in pressure ( $\Delta P$ ):

$$C_{vasc} = \frac{\Delta Vol}{\Delta P} \quad (1.7)$$

In order to relate the flow rate to the compliance, Equation (1.7) can be rearranged and then the derivative is taken in respect to time for both sides.

$$\frac{dVol(t)}{dt} = Q(t) = C \frac{dP}{dt} \quad (1.8)$$

The capacitance can be used to model the vascular compliance since it describes how much charge ( $\Delta q$ ) can be stored on a capacitor for a given voltage as in Equation(1.9). The relationship between the current and the voltage applied on a capacitor is described by Equation(1.10):

$$C = \frac{\Delta q}{\Delta V} \quad (1.9)$$

$$i(t) = C \frac{dv(t)}{dt} \quad (1.10)$$

The blood inertance ( $L_{vasc}$ ) relates the pressure drop with the rate of change of flow as in Equation(1.11). When the blood is subjected to a pressure difference the velocity of the blood changes and, in turns, the flow rate changes. In large blood vessels the inertance has more effect, while in small arteries it is the resistance that is more effective [7].

$$P(t) = L_{vasc} \frac{dQ(t)}{dt} \quad (1.11)$$

The blood inertance can be modeled using the concept of inductance in electric circuits. The relationship between the self-inductance of an inductor ( $L$ ), current passing through it and voltage is:

$$v(t) = L \frac{di(t)}{dt} \quad (1.12)$$

Equations (1.6), (1.10) and (1.12) can be used to model the hemodynamic relations described in Equations (1.5), (1.8) and (1.11), respectively.

#### 1.4. The Cardiovascular System Model

A mathematical model is a complete and consistent set of mathematical equations that can describe an entity. This entity may be physical, mechanical, biological, physiological or conceptual [5]. In many disciplines there is a need to use such models to experiment theories before they are applied to real world applications. This testing and simulation process helps engineers modify and improve their designs with the least amount of loss in time, money, effort or in some cases life. Additionally, a model can help in describing the underlying changes in the entity (the inverse problem) using the input-output data relation in the model. Lately, there has been a rapid advancement in the modeling of biomedical applications, thanks to the use of technology to collect and process huge amount of data needed to develop an accurate model [1].

The entity in our research is the cardiovascular system which can be first modeled into a lumped-parameter electrical circuit model and then using laws from circuit theory we can translate it into a set of differential equations [6].

Various models have been developed in the literature during the last few decades. The model complexity is determined primarily by the application for which the model is used. In this

chapter a lumped-parameter circuit model is used which describes only the left side of the heart with the systemic circulation. The reasons behind not modeling the pulmonary circulation and the right heart are related to the application discussed in this dissertation, and these reasons will be explained in more details in the next chapters.

The model used in this dissertation is an electrical circuit model that was developed in [8]-[10], and is shown in Figure 1.4. In Table 1.2 all the parameters of the model are listed along with their physiological meaning and a standard value is given (when applicable).

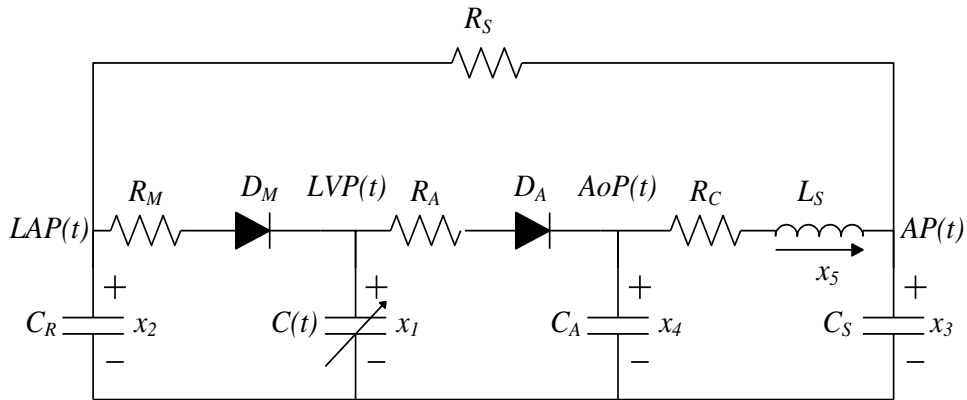


Figure 1.4: Fifth Order Circuit Model That Represents the Cardiovascular System

Table 1.2: Model Parameters [8]-[10]

Parameters	Value	Physiological Meaning
Resistances (mmHg · s/ml)		
$R_S$	1.0000	Systemic Vascular Resistance (SVR)
$R_M$	0.0050	Mitral valve resistance
$R_A$	0.0010	Aortic valve resistance
$R_C$	0.0398	Characteristic resistance
Compliances (ml/mmHg)		
$C(t)$	Time-varying	Left ventricle compliance
$C_R$	4.4000	left atrial compliance
$C_S$	1.3300	
$C_A$	0.0800	
Inertances (mmHg · s <sup>2</sup> /ml)		
$L_S$	0.0005	Inertance of blood in aorta
Valves (no units)		
$D_M$	-	Mitral valve
$D_A$	-	Aortic valve

The parameters listed in Table 1.2 are well explained and an algorithm for the estimation process is provided in [11]. It is important, however, to explain three of the parameters in more details since these parameters will be used extensively in this dissertation.

1. Systemic Vascular Resistance:

Systemic Vascular Resistance (*SVR*), also referred to as  $R_s$  in Figure 1.4, is the total resistance of the systemic circulation to the blood flow. When *SVR* increases, arterial pressure also increases which, in turn, reduces the cardiac output, and vice versa [12]. The overall diameter of the blood vessels in the systemic circulation is the most important factor that affects *SVR*. As a result of a complex physiological process, *SVR* decreases during exercise allowing more blood flow into the circulation, but *SVR* increases during rest[13],[14].

The pressure difference across the systemic circulation equals the mean arterial pressure (*MAP*) minus the central venous pressure (*CVP*) (it is the pressure inside the vena cava, and it determines the amount of blood returned to the heart), and the total blood flow is the cardiac output (*CO*) [15]. Using these variables in Equation (1.5) yields an expression for determining *SVR*:

$$SVR = \frac{MAP - CVP}{CO} \quad (1.13)$$

Usually the value of *CVP* is very small and can be neglected, which reduces Equation (1.13) into:

$$SVR = \frac{MAP}{CO} \quad (1.14)$$

*SVR* is represented in the model by an electrical resistance  $R_s$ . The value for  $R_s$  can be varied to simulate different level of activates for the body. Small values of  $R_s$  are used to simulate high level of activity (such as fast walking or running, for example), while high values are used to simulate low level of activity (such as rest or sleeping, for example). In our model, we use a value of  $R_s = 1.0 \text{ mmHg} \cdot \text{s/ml}$  to represent a normal activity level.

## 2. Left Ventricular Compliance

The elastance function  $E(t)$  is a measure of how the left ventricle reacts according to the four phases of the cardiac cycles mentioned in Table 1.1.  $E(t)$  is the time-varying parameter that can be calculated by Equation(1.15) and it describes the relationship of left ventricle pressure  $LVP(t)$  to the left ventricle volume  $LVV(t)$  and a reference volume  $V_o$  [16],[17]. The Left Ventricle compliance  $C(t)$  is the reciprocal of the elastance function of the heart.

$$E(t) = \frac{LVP(t)}{LVV(t) - V_o} \quad (1.15)$$

$$C(t) = \frac{1}{E(t)} \quad (1.16)$$

The left ventricle can be viewed as an elastic bag that expands and contracts based on the differential pressure on it.

The elastance function  $E(t)$  can be approximated mathematically. In our work we use the expression(1.17):

$$E(t) = (E_{\max} - E_{\min})E_n(t) + E_{\min} \quad (1.17)$$

Where  $E_n(t_n)$  is the normalized elastance (also called “double hill” function) represented by the following expression [18]:

$$E_n(t_n) = 1.55 * \left[ \frac{\left(\frac{t_n}{0.7}\right)^{1.9}}{1 + \left(\frac{t_n}{0.7}\right)^{1.9}} \right] * \left[ \frac{1}{1 + \left(\frac{t_n}{1.17}\right)^{21.9}} \right] \quad (1.18)$$

In (1.18),  $t_n = t/T_{\max}$ ,  $T_{\max} = 0.2 + 0.15 * t_c$  and  $t_c$  is the cardiac cycle interval, i.e.,  $t_c = 60/HR$ , where  $HR$  is the heart-rate. Notice that  $E(t)$  is a re-scaled version of  $E_n(t_n)$  and the constants  $E_{\max}$  and  $E_{\min}$  are related to the end-systolic pressure volume relationship (ESPVR) and the end-diastolic pressure volume relationship (EDPVR) respectively. For a healthy heart  $E_{\max} = 2$  mmHg/ml and  $E_{\min} = 0.06$  mmHg/ml, but for a heart with a cardiovascular disease  $E_{\max}$  can be assigned a value less than 2 mmHg/ml to simulate such case. The lower the  $E_{\max}$  value, the less elastance the ventricle has, hence simulating a more severe heart disease.

Figure 1.5 shows the elastance function of the left ventricle over one cardiac cycle for three different cases: (1) Healthy heart ( $E_{\max} = 2$  mmHg/ml) shown in the plot as red solid line, (2) Heart with mild heart failure condition ( $E_{\max} = 1$  mmHg/ml) shown in the plot as blue solid line with dotted data markers, and (3) Heart with severe heart failure condition ( $E_{\max} = 0.25$  mmHg/ml) shown in the plot as black dashed line. All plots are considered for  $HR = 60$  beat/min which results in a cardiac cycle time of  $t_c = 1$  s.



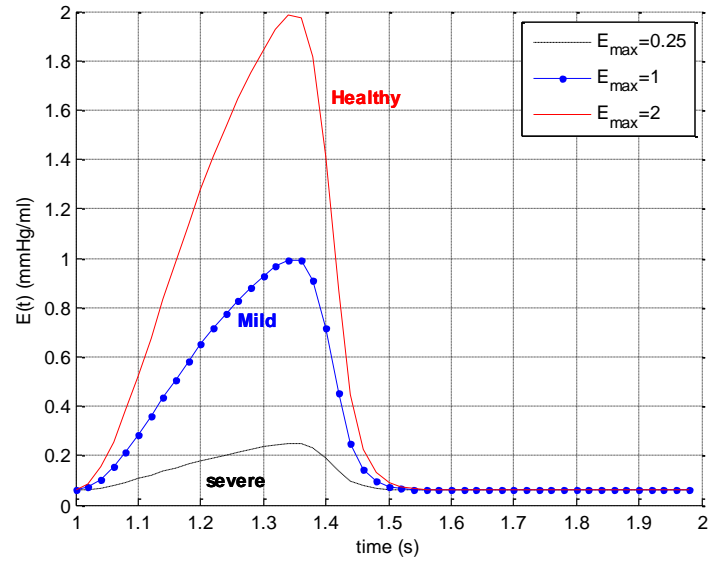


Figure 1.5: Elastance Function of healthy, mild heart failure and severe heart failure Left Ventricle

### 3. Mitral and Aortic Valves

The mitral and aortic valves are represented by two non-ideal diodes consisting of a resistance  $R_M$  and ideal diode  $D_M$  for the mitral valve, and resistance  $R_A$  and ideal diode  $D_A$  for the aortic valve, as shown in Figure 1.4.

Any Ideal diode is either short circuit or open circuit depending on the voltage across it. If the diode is short circuit, it can simulate the valve being open, and for a closed valve, the diode is open circuit.

The differential equations that govern the circuit model in Figure 1.4 have been derived in [8]. The state space representation of the model is shown in Equation(1.19) with the state variables of the system listed in Table 1.3.

$$\begin{bmatrix} \dot{x}_1 \\ \dot{x}_2 \\ \dot{x}_3 \\ \dot{x}_4 \\ \dot{x}_5 \end{bmatrix} = \begin{bmatrix} \frac{-\dot{C}(t)}{C(t)} & 0 & 0 & 0 & 0 \\ 0 & \frac{-1}{R_S C_R} & \frac{1}{R_S C_R} & 0 & 0 \\ 0 & \frac{1}{R_S C_S} & \frac{-1}{R_S C_S} & 0 & \frac{1}{C_S} \\ 0 & 0 & 0 & 0 & \frac{-1}{C_A} \\ 0 & 0 & \frac{-1}{L_S} & \frac{1}{L_S} & \frac{-R_C}{L_S} \end{bmatrix} \begin{bmatrix} x_1 \\ x_2 \\ x_3 \\ x_4 \\ x_5 \end{bmatrix} + \begin{bmatrix} \frac{1}{C(t)} & \frac{-1}{C(t)} \\ \frac{-1}{C_R} & 0 \\ 0 & 0 \\ 0 & \frac{1}{C_A} \\ 0 & 0 \end{bmatrix} \begin{bmatrix} \frac{1}{R_M} r(x_2 - x_1) \\ \frac{1}{R_A} r(x_1 - x_4) \end{bmatrix} \quad (1.19)$$

Note that in (1.19) the non-linearity caused by the diodes is represented by the ramp function  $r(\xi)$  described in(1.20):

$$r(\xi) = \begin{cases} \xi & \text{if } \xi \geq 0 \\ 0 & \text{if } \xi < 0 \end{cases} \quad (1.20)$$

This ramp function  $r(\xi)$  allows the model to simulate the four phases of the cardiac cycle. For instance in the contraction and relaxation phases,  $LVP$  is greater than  $LAP$  and  $AoP$  is greater than  $LVP$ , and this causes both valves to be closed. This translates in the model to  $x_1(t)$  is greater than  $x_2(t)$  and  $x_4(t)$  is greater than  $x_1(t)$ , and, in turn, the two ramp function  $r(x_2 - x_1)$  and  $r(x_1 - x_4)$  are equal to zero making  $D_M$  and  $D_A$  open circuit, respectively. In the filling phase, however,  $x_1(t)$  is greater than  $x_4(t)$ , and this leads  $r(x_1 - x_4)$  to have a value equals to the voltage difference across the diode  $D_M$  and its resistance  $R_M$ . Similarly, in the ejection phase  $r(x_2 - x_1)$  will have a value equals to the voltage difference across the diode  $D_A$  and its resistance  $R_A$ .

### 1.5. Summary

In this chapter, we reviewed the cardiovascular system and in particular the heart. The events that happen during the cardiac cycle is outlined and important medical definitions are given. A lumped-parameter model of the cardiovascular system of a healthy subject is presented. Using Kirchhoff's voltage and current laws, five differential equations were formulated to give the mathematical model that can accurately represent the left side of the heart and the systemic circulation. The reasons for not including the pulmonary circulation and the right heart in the model are related to the application of this research. As it will be clearer from chapter 2, the engineering problem we discuss in this dissertation is focused on patients with left-sided heart failure. Assuming that the pulmonary circulation and the right heart are healthy helps in making the model less complex. It still, however, accurately models the left heart and the systemic circulation.

Table 1.3: State Variables in the Cardiovascular Model

Variables	Names	Physiological Meaning (unit)
$x_1(t)$	$LVP(t)$	Left Ventricular Pressure (mmHg)
$x_2(t)$	$LAP(t)$	Left Atrial Pressure (mmHg)
$x_3(t)$	$AP(t)$	Arterial Pressure (mmHg)
$x_4(t)$	$AoP(t)$	Aortic Pressure (mmHg)
$x_5(t)$	$Q_T(t)$	Total Flow (ml/s)

## CHAPTER 2: THE LEFT VENTRICULAR ASSIST DEVICES

The Left Ventricular Assist Device (LVAD) is one of the available treatment options for heart failure patients. It is mechanical pump that is connected between the left ventricle and the aorta, and helps in providing adequate blood flow to the patient. Developing a mathematical model for the LVAD can help researchers and engineers to understand and test their theories before they are applied to patients. The chapter begins with a brief introduction of the heart failure problem. Details about the LVAD types, its construction and the different treatments for which it can be used, are given. Then The LVAD pump is represented by a 1<sup>st</sup> order circuit model. The pump model is combined with the 5<sup>th</sup> order cardiovascular model from the previous chapter to form the complete cardiovascular-LVAD model.

### 2.1. Heart Failure

The American Heart Association (AHA) estimates that 5.8 million patients above the age of 20 in the United States are suffering from Heart Failure [19], a condition in which the heart is no longer able to pump enough blood to meet the physiological needs of the body. It is a chronic, progressive condition that is difficult to detect at the early stages because, at first, the heart and the body work together to try to make up for the inadequate blood supply. The heart can compensate by pumping faster than usual or developing more muscle mass to pump stronger, while the body can narrow the blood vessels to raise the blood pressure and can divert the blood from less vital tissue to more important ones. These measures taken by both the heart and the body are only temporary. Once they cannot keep up with the workload, symptoms such as exercise intolerance and fatigue start to appear.

Heart failure can occur due to: diseases that can damage the heart –including coronary heart disease, high blood pressure, and diabetes- are common causes of heart failure; and/or unhealthy habits like smoking, being overweight, unhealthy food diet, and physical inactivity.

Heart failure can affect the right side of the heart (called right-sided heart failure), the left side of the heart (called left-sided heart failure), or both sides (called bi-ventricular heart failure) [21]. In this dissertation, the focus is on the left-sided heart failure and its treatment. Left-sided heart failure can be further divided into two types: systolic failure, which is the inability of the ventricle to contract normally to pump enough blood into the circulation; and diastolic failure, which is the inability of the ventricle to relax normally to be filled with blood during the relaxation phase.

The estimated total of direct and indirect cost of heart failure in the United States for 2008 is \$34.8 billion dollars with the greatest share being hospitalization. Treatments that can lead to patients being discharged from hospitals faster can reduce this cost, and hence there is more research and funds aimed at these treatments. The next section will explain how the LVAD is one of these treatments that can cut the cost of heart failure. Other treatments for heart failure include: medications, bypass surgery, heart valve surgery, and heart transplant. For severe heart failure patients, heart transplant is the best long term therapy. In the United States there are 100,000 patients suitable for heart transplant, but only 2200 operations performed annually due to the shortage in available donors [20]. The unbalance between donors and recipients presses the need for alternative treatments that can replace heart transplant or temporarily support the patient for usual long periods of time on the transplant list.

## 2.2. Left Ventricular Assist Devices

The LVAD is a mechanical pump that is connected between the left ventricle and the aorta through two cannulae. It is designed to help the left ventricle of the patient in pumping blood in higher rates from the weak ventricle to the aorta. The LVAD pump is implanted just below the diaphragm in the abdomen. A tube that passes through the skin connects the pump with a system controller unit and the battery pack that provides power, both are wearable devices.

### 2.2.1. LVAD Generations

The LVAD is classified into two generations based on the pump technology used in them. The first generation pumps are pulsatile pumps, which mimic the pumping action of the heart. In detail, the pulsatile pumps consist of two mechanical valves and a pusher-plate pump. When blood fills the ventricle, it creates pressure forcing one of the pump valves to open and then blood fills the pumping chamber. After the valve closes, a force will be applied rapidly to push the plates to decrease the pump chamber volume. The pressure increase inside the chamber causes the blood to be pumped through the second mechanical valve into the aorta. These pumps have the drawbacks of being less durable, bulky and noisy. In addition, they cause bleeding, infections, thrombo-embolic events and technical failures [22].

The second generation, however, is a continuous flow pumps that don't operate on the fill-and-empty concept, but rather has blood flowing through the pump continuously [23]. They are smaller in size, produce less noise and much more durable than the first generation pumps. It is better mainly because it contains less moving parts and no mechanical valves are needed, hence less maintenance and lower probability of malfunction occurring. The flow is generated by

the motion of a central rotor that contains permanent magnets and controlled by electric current that runs through coils contained in the pump housing. Unlike the first generation, the second generation pumps change the hemodynamic conditions of the patients because of the continuous flow doesn't resemble the intermittent flow by the native heart [24]. Continuous flow pumps used in the LVAD are either centrifugal pumps or axial pumps. The centrifugal pumps are shaped in a way that the blood –or generally speaking, any fluid– enters the pump chamber perpendicular to the rotor axis direction and the blades cause the blood to accelerate circumferentially and exit through an outlet. In the axial flow pumps, the blood flows in the same direction of the axis of the rotor.

The pump used later in the model, explained in sections 3 and 4, is a second generation axial flow pump.

### 2.2.2. LVAD Components

Regardless of the pump technology used, the LVAD has the following important components [22], [25]:

1. Inlet cannula: a tube that connects the left ventricle to the pump. It is surgically attached to the walls of the left ventricle during the operation of implanting the LVAD.
2. A mechanical pump: this is considered as the main part of the LVAD system. And it is well explained in the previous section.
3. Outlet cannula: a tube that connects the pump chamber to the ascending aorta.
4. Controller: its function is to control motor power and speed, provide redundant system operation, monitor the performance of the system, records and store events in memory, and to give warnings and alarms when necessary. Under the current technology the



controller is set to provide constant flow rate that meets the baseline physiological demand of the patient [49]. A feedback controller that can respond to the changes in the physiological state of the patient is essential for the advancement in the LVAD treatment. In addition, the controller should be able to detect and avoid the suction phenomenon. Suction happens when the pump speed is too high that it attempts to draw more blood from the ventricle than available. This can cause severe damage to the heart muscle.

5. Power source: a set of two rechargeable batteries that can be worn by the patient with a shoulder strap. One battery supply the power to the controller unit and the other is a backup. The battery level can be monitored from the screen of the controller unit.
6. Driveline: it is a thin tube that runs from the controller unit and passes through the skin to the pump in order to provide the current needed to control the rotational speed of the pump.

Figure 2.1 shows all the components of an LVAD, note that the pump in this figure is an axial flow pump, but the figure can be applicable for any other types of pump.

### 2.2.3. LVAD treatment strategies

There are three different types of treatment where the LVAD can be used. Two are intended for temporary support: bridge to transplant and bridge to recovery. The third treatment is aimed at permanent support and it is called destination therapy.

First type of treatment is Bridge to Transplant (BTT). In this type of treatment, the LVAD is used to maintain and improve the ventricular function and perfusion in patients waiting for heart transplant. It is essential to use this kind of the support because of the long waiting period between getting on the recipient list and the availability of a suitable heart. BTT is used

for patients hospitalized with end-stage heart failure. The LVAD allows those patients to be discharged from the hospital and return home while waiting for the donor heart.

Second is Bridge to Recovery (BTR). This is a new application for the LVAD. It was recently observed that the LVAD support for some patients is accompanied by hemodynamic and physiologic changes that are indicative of recovery [28]. Some studies credit the continuous unloading of the left ventricle as a factor that can help the reverse remodeling process (i.e. recovery) [29], [30].

Third and final type is Destination Therapy (DT). In some cases heart transplant operations are not possible due to age or condition. In such cases the LVAD is suitable adjunct therapy to heart transplant and is used to support the heart failure patients for the rest of their lives [22]. As a result of recent studies [32],[33] showing that the LVAD has a better two-year survival rate over medical therapy, the FDA approved the LVAD for DT in the US.

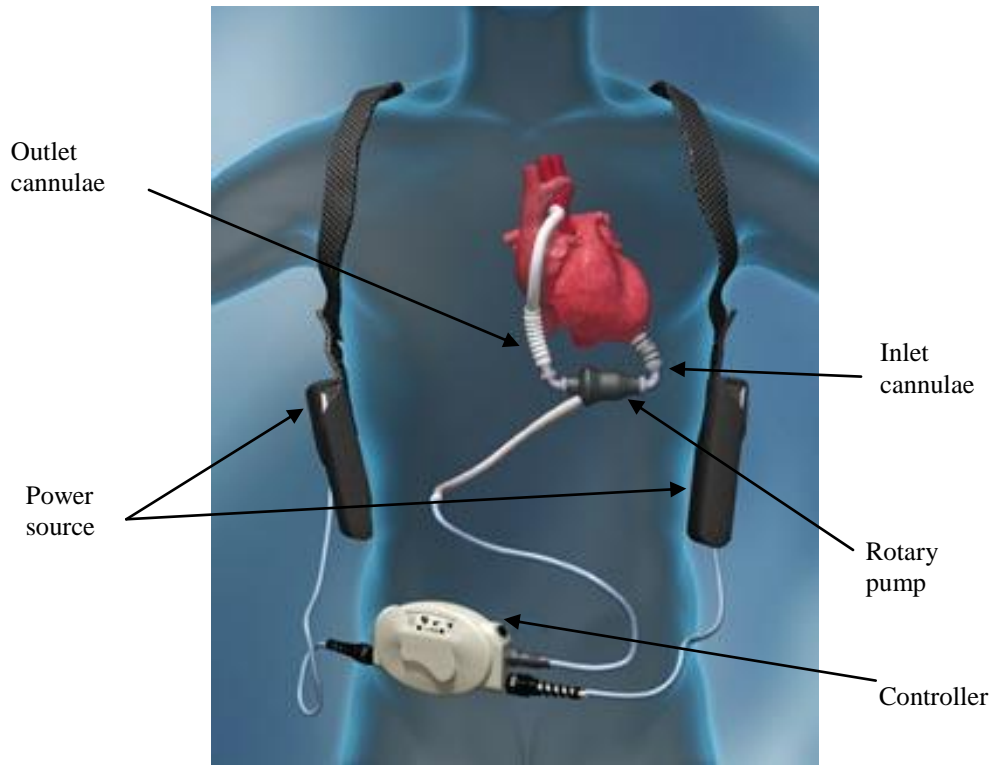


Figure 2.1: Schematic of a rotary LVAD  
(source: Thoratec)

### 2.3. The Left Ventricular Assist Device Model

The LVAD pump considered in this dissertation is a second generation axial-flow blood pump that is driven by a DC motor. The rotation of the impellor of the pump causes a high pressure difference that forces the blood to flow from the inlet cannula to the outlet cannula [34]. This pressure difference between the left ventricle and the aorta can be expressed as the sum of pressure differences across the inlet cannula  $H_i$ , the pump  $H_p$  and the outlet cannula  $H_o$ , that is:

$$LVP(t) - AoP(t) = H_i + H_p + H_o \quad (2.1)$$

The terms on the right hand side in Equation (2.1) are defined in [35] as:

$$H_i = R_i Q_p(t) + L_i \frac{dQ_p(t)}{dt} \quad (2.2)$$

$$H_p = R_p Q_p(t) + L_p \frac{dQ_p(t)}{dt} - \beta \omega^2(t) \quad (2.3)$$

$$H_o = R_o Q_p(t) + L_o \frac{dQ_p(t)}{dt} \quad (2.4)$$

The parameter  $\beta$  is a pump-dependent constant and  $\omega(t)$  is the pump rotational speed.

The parameters  $R_p$ ,  $R_i$  and  $R_o$  represent the resistances and  $L_p$ ,  $L_i$  and  $L_o$  represents the inertances of the pump, inlet cannula and outlet cannula, respectively.

We note, however, that when suction occurs another term needs to be added to Equation(2.1) to account for the resistance of the flow due to suction. In case of suction Equation(2.1) will be:

$$LVP(t) - AoP(t) = H_i + H_p + H_o + R_k Q_p(t) \quad (2.5)$$

$R_k$  is a function of  $LVP(t)$  because when suction happens  $LVP$  decreases significantly causing the blood volume inside the ventricle to decrease. This phenomenon can be represented by a non-linear resistance [50] in the form of:

$$R_k = \begin{cases} 0 & \text{if } LVP(t) > \bar{x}_1 \\ \alpha(LVP(t) - \bar{x}_1) & \text{if } LVP(t) \leq \bar{x}_1 \end{cases} \quad (2.6)$$

In Equation(2.6),  $\alpha$  is a cannula-dependent scaling factor and  $\bar{x}_1$  is a suction threshold. If  $LVP$  is less than or equal this threshold, then the value of  $R_k$  will increase linearly as a function of the difference between  $LVP$  and  $\bar{x}_1$ .

Using Equations(2.3), (2.2) and (2.4) to simplify (2.5) yields:

$$LVP(t) - AoP(t) = R^* Q_p(t) - L^* \frac{dQ_p(t)}{dt} - \beta \omega^2(t) \quad (2.7)$$

Where:

$$R^* = R_k + R_p + R_i + R_o \quad (2.8)$$

And

$$L^* = L_p + L_i + L_o \quad (2.9)$$

Figure 2.2 shows the circuit model for the LVAD pump and Table 2.1 lists all the parameters in the LVAD along with a typical value and the physiological meaning for each.

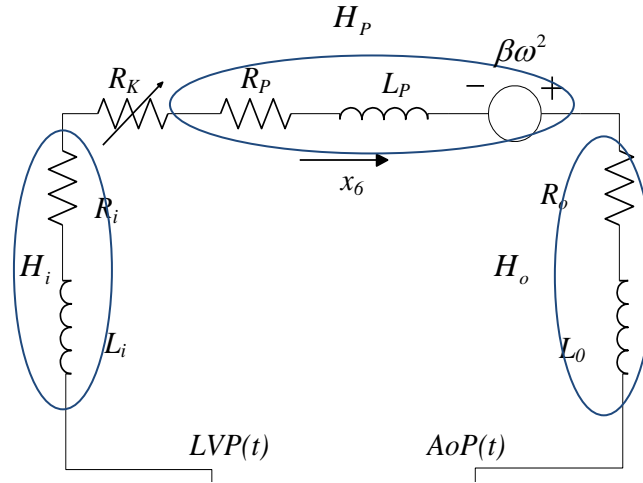


Figure 2.2: LVAD Pump Model

Table 2.1: Model Parameters for the LVAD

Parameters	Value	Physiological Meaning
Resistances (mmHg • s/ml)		
$R_i$	0.0677	Inlet resistance of cannulae
$R_p$	0.17070	Pump resistance
$R_o$	0.0677	Outlet resistance of cannulae
$R_K$	see (2.6)	Suction resistance with parameters: $\alpha = -3.5\text{s/ml}$ and $\bar{x}_1 = 1\text{mmHg}$
Inertances (mmHg • s <sup>2</sup> /ml)		
$L_i$	0.0127	Inlet inertance of cannulae
$L_p$	0.02177	Pump inertance
$L_o$	0.0127	Outlet inertance of cannulae
Constants (mmHg/rpm <sup>2</sup> )		
$\beta$	$9.9025 \cdot 10^{-7}$	Pump-dependent constant

#### 2.4. The Combined Cardiovascular-LVAD Model

A combined model of the LVAD and cardiovascular system has been derived in [8]. By adding the model of the LVAD to the cardiovascular system we add one state variable corresponding to the blood flow in the pump  $Q_p(t)$ ; which we will denote as. By rearranging Equation (2.7) and replacing  $LVP(t)$ ,  $AoP(t)$  and  $Q_p(t)$  with  $x_1(t)$ ,  $x_4(t)$  and  $x_6(t)$ , respectively, the differential equation for the 1<sup>st</sup> order pump model can be written as:

$$\dot{x}_6(t) = \frac{1}{L^*} x_1(t) - \frac{1}{L^*} x_4(t) - \frac{R^*}{L^*} x_6(t) + \frac{\beta}{L^*} u(t) \quad (2.10)$$

Where  $u(t) = \omega^2(t)$  is used to denote the control variable in the model.

Combining Equations (1.19) and (2.10) yields the 6<sup>th</sup> order mathematical model that fully represents the interaction between the cardiovascular system and the LVAD. Such model can be represented, using control terminology, in the standard state-space form:

$$\dot{x}(t) = A(t) x(t) + P(t) p(x) + b u(t) \quad (2.11)$$

Where:

$$A(t) = \begin{bmatrix} \frac{-\dot{C}(t)}{C(t)} & 0 & 0 & 0 & 0 & \frac{-1}{C(t)} \\ 0 & \frac{-1}{R_S C_R} & \frac{1}{R_S C_R} & 0 & 0 & 0 \\ 0 & \frac{1}{R_S C_S} & \frac{-1}{R_S C_S} & 0 & \frac{1}{C_S} & 0 \\ 0 & 0 & 0 & 0 & \frac{-1}{C_A} & \frac{1}{C_A} \\ 0 & 0 & \frac{-1}{L_S} & \frac{1}{L_S} & \frac{-R_C}{L_S} & 0 \\ \frac{1}{L^*} & 0 & 0 & \frac{-1}{L^*} & 0 & \frac{-R^*}{L^*} \end{bmatrix} \quad (2.12)$$

$$P(t) = \begin{bmatrix} \frac{1}{C(t)} & \frac{-1}{C(t)} \\ \frac{-1}{C_R} & 0 \\ 0 & 0 \\ 0 & \frac{1}{C_A} \\ 0 & 0 \\ 0 & 0 \end{bmatrix}, \quad p(x) = \begin{bmatrix} \frac{1}{R_M} r(x_2 - x_1) \\ \frac{1}{R_A} r(x_1 - x_4) \end{bmatrix} \quad (2.13)$$

And,

$$b = \begin{bmatrix} 0 \\ 0 \\ 0 \\ 0 \\ 0 \\ \frac{\beta}{L^*} \end{bmatrix} \quad (2.14)$$

This is a non-linear time-varying model that is controlled by increasing or decreasing the rotational speed of the pump can also be regarded as a bio-mechanical coupled system where the dynamics of the heart and the pump are interconnected, each influencing the other.

Figure 2.3 shows the complete 6<sup>th</sup> order circuit model of the cardiovascular system and the LVAD pump. This model is basically the 5<sup>th</sup> order model that was presented in chapter 1 with the 1<sup>st</sup> order model of the pump connected between the ventricle and the aorta.



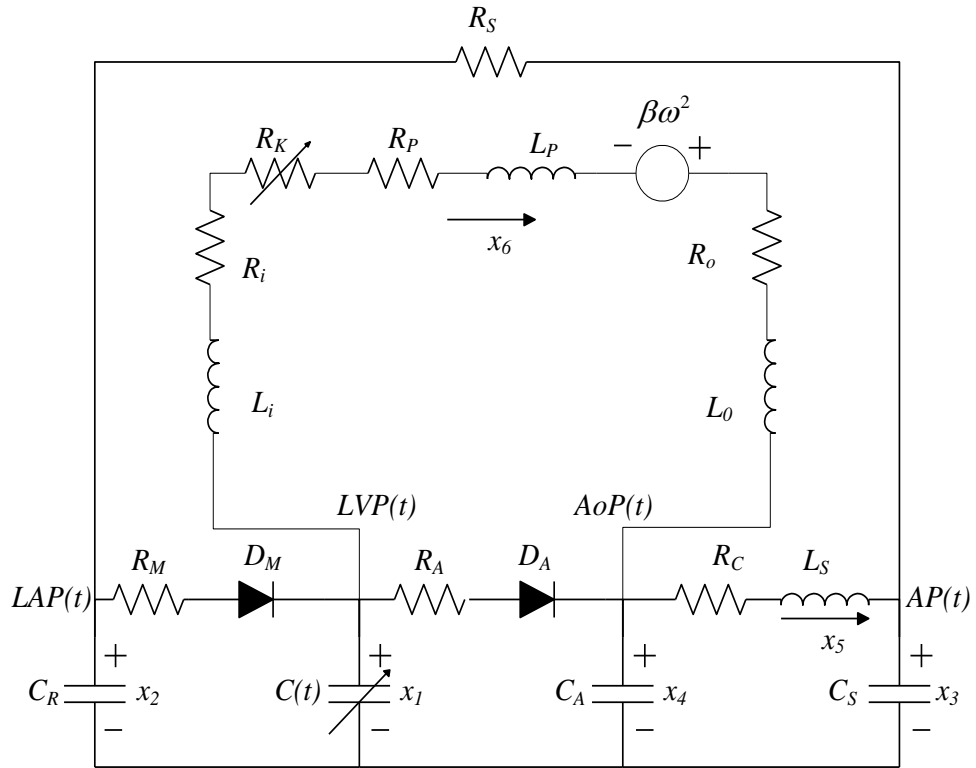


Figure 2.3: Combined Cardiovascular and LVAD Model

## 2.5. Summary

In this chapter, we presented a 1<sup>st</sup> order model to represent the pump. This model was derived from the equation that describes the pressure difference between the left ventricle and the aorta. The phenomenon of suction was accounted for by adding a nonlinear resistance  $R_K$ . During normal operation,  $R_K$  is equal to zero. When suction occurs, however,  $R_K$  represents the resistance to the flow due to the unavailability of blood in the ventricle. The pump model was added to the 5<sup>th</sup> order cardiovascular model yielding a 6<sup>th</sup> order model that can represent the combined cardiovascular-LVAD model. This model is controlled by the rotational speed of the pump. In reality, the pump is controlled by the pump motor current, which controls the pump speed. In the next chapter, we reformulated the combined cardiovascular-LVAD model in such a way so as to introduce the pump motor current instead of the pump speed as the independent control variable to the model.

## CHAPTER 3: NEW POWER-BASED CONTROL MODEL OF THE PUMP OF THE LEFT VENTRICULAR ASSIST DEVICES

The model discussed in Chapter 2 was derived based on the assumption that the pump speed is the independent control variable that is available for controlling the performance of the system. While this may be acceptable from a theoretical point of view, in practice, however, the pump is controlled by varying the electrical power supplied to the LVAD pump. In this chapter, we reformulate the 6<sup>th</sup> order model to have the pump power as the independent control variable. A relationship between the pump power and the pump speed is derived. Finally, simulation results are shown to validate the model and to explore the characteristics of the pump speed signal during normal operation and suction.

### 3.1. The Power-Based Pump Model

From the previous chapter, we know that Equation (2.7) can be written as:

$$LVP(t) - A_oP(t) = R^*Q_p(t) - L^* \frac{dQ_p(t)}{dt} - H \quad (3.1)$$

The direct relation between the electrical power delivered to the motor ( $P_E$ ) and the hydrodynamic power generated by the pump ( $P_p$ ) can be used to determine the pressure head  $H$  in (3.1) as follows:

$$P_p = \eta P_E \quad (3.2)$$

Where  $\eta$  is the electric to hydrodynamic power transfer efficiency. The hydrodynamic power can be written as the product of the density of the reference fluid  $\rho$ , acceleration of

gravity  $g$  , pump head  $H$  , and flow rate  $Q_p(t)$  through the pump. Therefore equation (3.2) can be written as:

$$\rho \cdot g \cdot H \cdot Q_p(t) = \eta P_E \quad (3.3)$$

Solving for  $H$  yields:

$$H = \delta \frac{P_E}{Q_p(t)} \quad (3.4)$$

Where  $\delta = \frac{\eta}{\rho g}$  . The parameters listed in the previous equations are defined and typical values are given in Table 3.1. Note that the LVAD used in our model assumes that all energy losses are accounted for by the pressure losses induced by  $R_p$  and  $L_p$  , and subsequently  $\eta$  is assumed to be 100%.

Substituting Equation (3.4) in (3.1) yields the state equation that governs the behavior of the LVAD pump, see Equation(3.5).

$$LVP(t) - A_oP(t) = R^*Q_p(t) - L^* \frac{dQ_p(t)}{dt} - \delta \frac{P_E}{Q_p(t)} \quad (3.5)$$

Note that  $P_E$  is the only control variable in the entire model. It can be changed by either manipulating the current  $I$  or the voltage  $V$  across the DC motor of the pump according to the relationship  $P_E = VI$  .

In order to develop a complete power-based model, a relationship has to be found between the pump power and the rotational speed of the pump. From Equation(2.7), the pump head pressure is given by:

$$H = \beta \omega^2(t) \quad (3.6)$$

Using Equations(3.4) and(3.6), and solving for the rotational pump speed [37]:

$$\omega(t) = \sqrt{\frac{\delta P_E}{\beta Q_p(t)}} \quad (3.7)$$

This relationship is highly nonlinear, and because of the dependence on  $Q_p(t)$ , a constant value of power applied to the LVAD motor will not lead to a constant rotational speed on the pump. Instead, the rotational speed of the pump will be periodic in nature as determined by equation (3.7) since  $Q_p(t)$  is periodic. This phenomenon will be further explained in the next sections. It should be noted that when referencing the rotational speed that corresponds to a value of  $P_E$ , we actually mean the average value of  $\omega(t)$  over its period.

To formulate the power-based model in the state space representation, the  $b$  matrix described in Equation(2.14) will change to:

$$b = \begin{bmatrix} 0 \\ 0 \\ 0 \\ 0 \\ 0 \\ \frac{\delta}{L x_6(t)} \end{bmatrix} \quad (3.8)$$

Note that the rest of the system described by Equations(2.11), (2.12) and (2.13) will not be changing.

Table 3.1: Model Parameters for the Current-Based Model

Parameters	Value	Physiological Meaning
$\rho$	13,600	Density of a reference fluid (kg/m <sup>3</sup> )
$g$	9.8	Acceleration of gravity (m/s <sup>2</sup> )
$\eta$	100%	Pump efficiency

### 3.2. Simulation Results

In order to observe how the pump speed signal changes over its range of operation, the 6<sup>th</sup> order power-based model is excited with a linearly increasing values of electric pump power according to the following expression:

$$P_E(t) = 0.6 + 0.12t \quad , 0 \leq t \leq 60 \quad (3.9)$$

The variable parameters in the model are set at heart rate of 60 bpm;  $R_s = 1$  mmHg·s/ml (indicating a normal activity level); and  $E_{\max} = 1$  mmHg/ml (indicating a mild heart failure condition). Such pump motor power profile allows the pump to operate first in the normal operation range and then, at  $t = 43$  s, it operates during suction.

Figure 3.1 illustrates the variations of the pump speed as the pump electric power increases. First note that the linear increase of the pump electric power is accompanied by nonlinear increase in the mean value of the rotational pump speed. It is important to note that this nonlinear relation between the speed and the power is true within the normal operation region of the pump speed. Once the pump operates in the suction region, the signature of the pump speed signal is changed.

Second, the pump speed has a superposed oscillatory component that has the same pulsatility of the heart ( $HR = 60$  bpm). This shows how the pulstaility of the heart affect the performance of the pump. This phenomenon has recently been observed in *in-vivo* data obtained through clinical studies [38]. This is the first time a mathematical model is capable of reproducing such phenomenon. This represents a breakthrough in accurately modeling this complex bio-mechanical system.

Third, the amplitude of the oscillatory component of the pump speed signal decreases as the power increase. This happens because when the pump speed increases, it withdraws blood from the ventricle faster (i.e. the rate of unloading increases). As the blood volume inside the ventricle decreases, the left ventricle pressure also decreases. Hence, the effect of the heart on the pump performance diminishes. The amplitude of the signal exhibits a sudden increase (in this example at  $t=43$  s.) at the start of suction. It can be from Figure 3.3 which shows the pump flow that suction behavior also is observed at  $t=43$  s. Such behavior is in accordance to what was reported in literature either in simulation or in *in-vivo* data [8]-[10], [39]-[42]. Furthermore, when the pump is operating during suction, a noticeable change in the characteristics and the shape of the pump speed signal can be observed. These changes are seen clearly in Figure 3.2 in which details of the results of Figure 3.1 are shown over two 5-second intervals, from  $10 \leq t < 15$  (normal) and  $45 \leq t < 50$  (suction). Such distinction in the signal shape has been used in the determination of the onset of suction using Lagrangian support vector machine method [43].

Next we need to study the effect varying  $E_{\max}$  on the hemodynamic of the patient and the pump performance. For this reason we simulated with four different value of  $E_{\max}$  to represent varying degrees of the severity of the cardiovascular disease. Starting from  $E_{\max} = 1.0$  mmHg/ml to represent a sick heart, and gradually decreasing it till  $E_{\max} = 0.25$  mmHg/ml to represent a critically sick heart. The pump motor power is kept constant ( $P_E(t) = 2.16$  W.) for each time the model is simulated with different  $E_{\max}$ . Figure 3.4 shows that as  $E_{\max}$  decreases, the pressure inside the left ventricle  $LVP(t)$  decreases, specifically during the contraction and ejection phases of the cardiac cycle. This is expected since the heart does most of its work during these two



phases. In addition, Figure 3.5 shows that the pump speed signal, at a constant  $P_E$ , is greatly affected by the value of  $E_{\max}$ . When  $E_{\max}$  is set at 1 mmHg/ml, the amplitude of the pump speed signal is 680 rpm (i.e. ~5.59% of its mean value). When  $E_{\max}$  is set at 0.25 mmHg/ml, however, the amplitude of the pump speed signal is reduced to 142 rpm (i.e. 1.17% of its mean value). Such phenomenon can be used in a less invasive approach to estimate  $E_{\max}$  for LVAD patients.

The amplitude and the change percentage are calculated according to these Equations:

$$\text{Amplitude} = \frac{1}{2}(\max(\omega) - \min(\omega)) \quad (3.10)$$

$$\text{Percentage of Change} = \frac{\text{Amplitude}}{\text{mean}(\omega)} \quad (3.11)$$

Constant monitoring for  $E_{\max}$  can help physicians in diagnostics and therapeutic decisions on heart protection and eventual weaning strategies for LVAD patients [44]. Using the pump speed and pump electric power signals can help in estimating  $E_{\max}$  without the need to use Equation (1.15) which requires access to  $LVP(t)$  and  $LVV(t)$ , both signals require invasive measurements. Algorithms to estimate  $E_{\max}$  have been developed in [46]-[47], however such algorithms assumes a healthy heart or a patient with sick heart but no LVAD implanted. Other approaches developed contractility indices for the LVAD patients, instead of estimating  $E_{\max}$ , to evaluate how good the ventricle can contract. One method used the pump flow and pump speed to develop its contractility index [48]. The pump flow needs to be measured using flow meter or to be estimated.

Fifth, Table 3.2 shows results that are compiled from Figure 3.4, Figure 3.5 and Figure 3.6. These results show that for a critically sick heart ( $E_{\max} = 0.25$ ) the average speed of the pump is higher than that of the sick heart ( $E_{\max} = 1.00$ ), while the pump flow is lower when  $E_{\max} = 0.25$ . This means that, for the same constant pump electric power, the pump has to run faster and produce lower flow rate when  $E_{\max} = 0.25$ .

It is also interesting to note that during systole the highest pump speed is for  $E_{\max} = 0.25$ , followed by  $E_{\max} = 0.50$ ,  $E_{\max} = 0.75$  and  $E_{\max} = 1.00$ , respectively. During diastole, however, this order is reversed and the highest pump speed is for  $E_{\max} = 1.00$ .

In contrast the highest flow rate during systole is for  $E_{\max} = 1.00$ , followed by  $E_{\max} = 0.75$ ,  $E_{\max} = 0.50$  and  $E_{\max} = 0.25$ , respectively. During diastole, however, this order is reversed and the highest pump speed is for  $E_{\max} = 0.25$ .

These differences between the four pump speed signals (and also the four pump flow signals) are noticeable during systole, while in diastole such differences are very small. The reason for these differences is clear when looking at Figure 3.4. The  $LVP(t)$  signals for the different cases of  $E_{\max}$  in the systole phase vary clearly. The higher the value of  $E_{\max}$ , the greater the instantaneous values of  $LVP(t)$ . This causes the dynamics of the pump and flow to be different according to the  $E_{\max}$  value. The  $LVP(t)$  during the diastole phase is almost the same for the four different cases of  $E_{\max}$ . The diastole is the relaxation phase of the left ventricle during the cardiac cycle, hence the strength of the left ventricle (i.e.  $E_{\max}$ ) has little influence on the dynamics of the pump and the flow.

### 3.3. Summary

In this chapter, we presented a combined model of the cardiovascular-LVAD system with the pump motor power as the control variable. This control variable was chosen over the pump speed because in reality the LVAD is controlled by the electric power delivered to the pump which, in turn, controls the pump speed. When the pump is controlled in terms of its speed, the actual implementation of any desired pump speed profile requires the solution of an inverse problem in order to determine the corresponding pump motor power that can yield that speed profile. Such inverse problem is difficult to solve because of the nonlinearity between the pump speed and the pump motor power, and the coupling effect between the ventricle and the pump.

A relationship between the pump motor electric power and the pump speed is derived in this chapter. This relationship shows how the pump speed is affected by the pump flow. An interesting observation is also noted about how this model can help in the development of algorithms that can estimate  $E_{\max}$ .

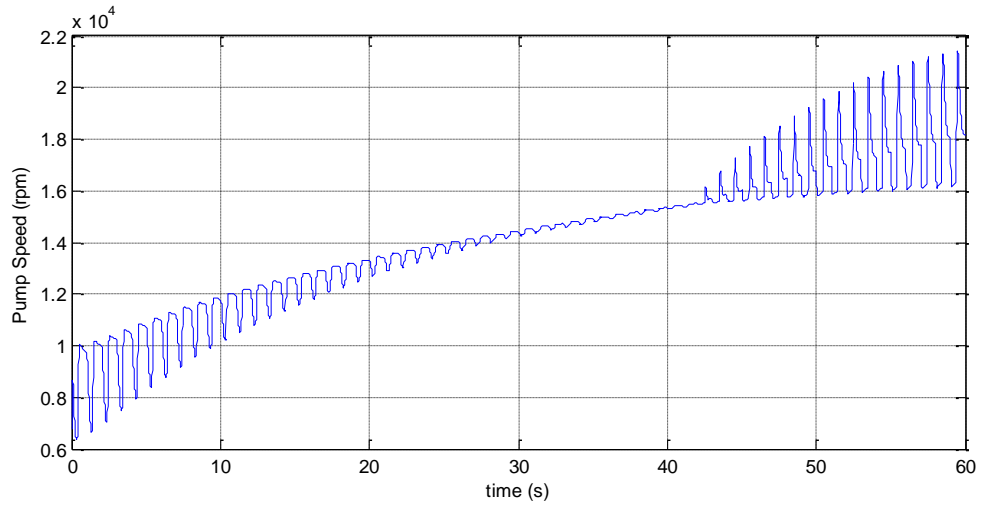


Figure 3.1: Pump speed signal as a function of time when the pump motor power is increased linearly

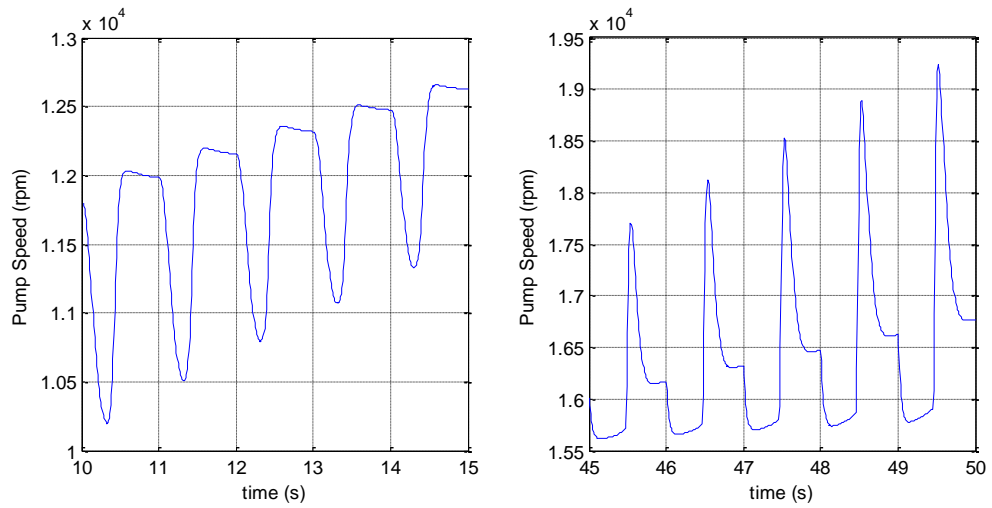


Figure 3.2: Pump speed signal during normal operation (left), pump speed signal during suction (right)

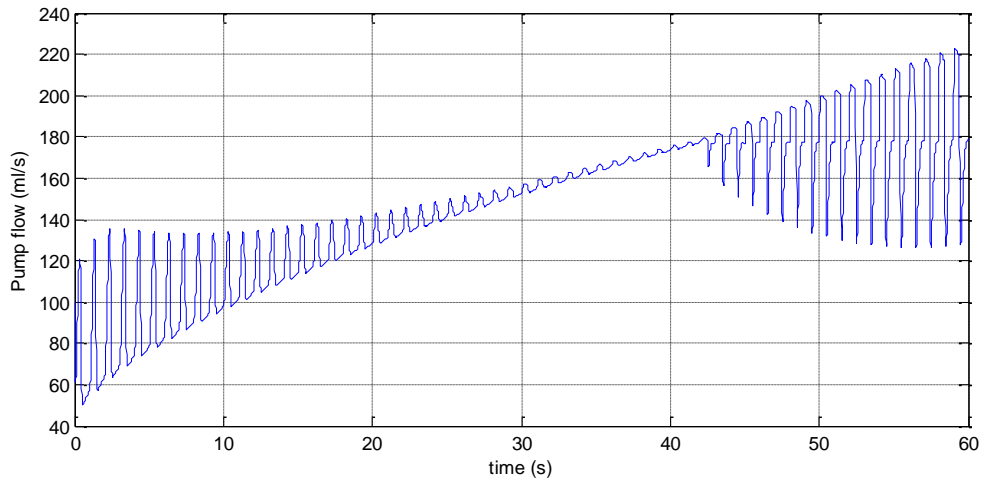


Figure 3.3: Pump flow with the pump motor power increasing linearly

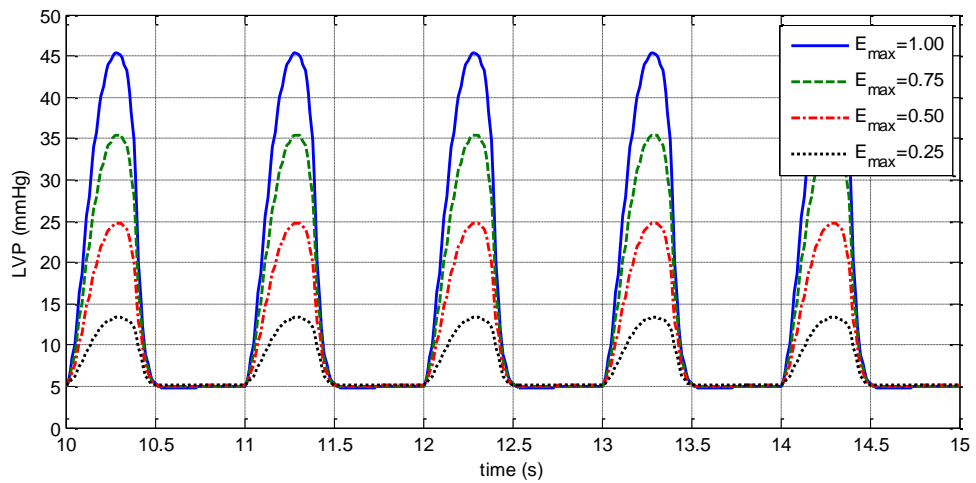


Figure 3.4: Left ventricular pressure for different values of  $E_{\max}$  and constant  $P_E = 2.16$  W.

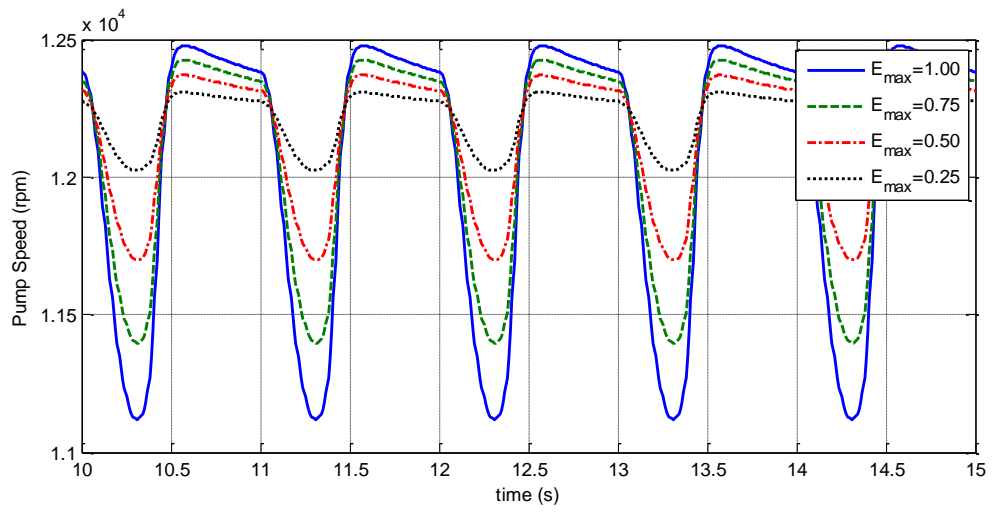


Figure 3.5: Pump speed for different values of  $E_{\max}$  and constant  $P_E = 2.16$  W.

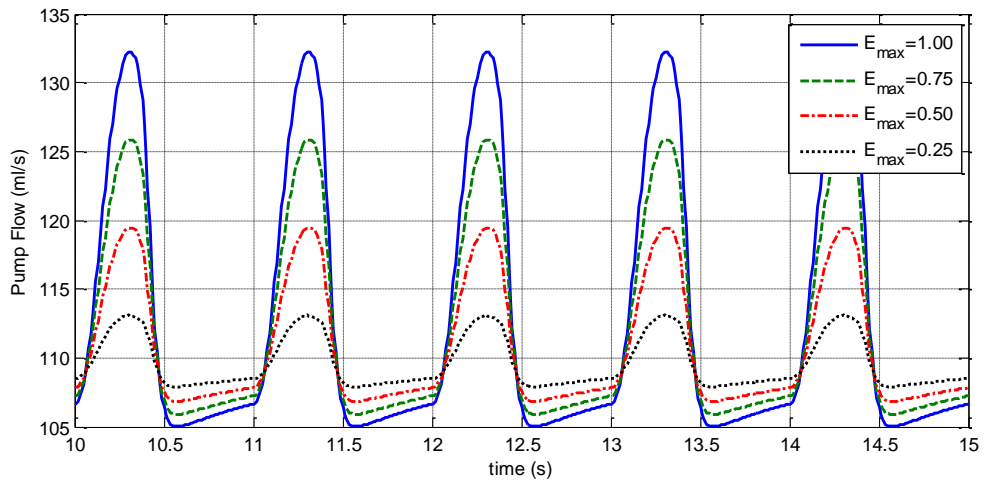


Figure 3.6: Pump flow for different values of  $E_{\max}$  and constant  $i(t) = 2.16$  W.

Table 3.2: Results when  $E_{\max}$  is varied from 1.00 to 0.25, while  $P_E$  is kept constant

	$E_{\max} = 1.00$	$E_{\max} = 0.75$	$E_{\max} = 0.50$	$E_{\max} = 0.25$
Average pump flow $Q_p$ (ml/s)	113.08	111.90	110.71	109.63
Average systole $Q_p$ (ml/s)	122.92	119.14	115.30	111.56
Average diastole $Q_p$ (ml/s)	106.01	106.70	107.43	108.25
Average pump speed $\omega$ (rpm)	12,057	12,106	12,159	12,213
Average systole $\omega$ (rpm)	11,552	11,725	11,913	12,107
Average diastole $\omega$ (rpm)	12,419	12,378	12,336	12,289

## **CHAPTER 4: A FEEDBACK CONTROLLER TO DELIVER PHYSIOLOGICAL DEMAND FOR LVAD PATIENTS**

In this chapter we develop a feedback controller that can help patients outfitted with an LVAD that is used as a destination therapy or bridge to transplant device. In both destination therapy and bridge to transplant the device is implanted for a longer period of time compared to the bridge to recovery treatments. Hence, the main objective of the controller is to provide the patient with blood flow as close as possible to that produced by a healthy heart. This allows the patient to return to a close to normal activity during the prolonged treatment period. This is accomplished by controlling the pump motor power to minimize the difference between the pump flow and the cardiac output of a healthy heart experiencing the same level of activity as the patient. Simulation results are presented to show the effectiveness of the feedback controller in matching the blood flow requirements of the patient.

### 4.1. The Physiological Demand of LVAD Patients

The physiological demand of LVAD patients is defined as the required blood flow that the body needs per minute. In a healthy heart, this is equal to the cardiac output as the heart can deliver blood to the rest of the body. For a heart failure patient, however, the heart is not strong enough to produce the cardiac output that can satisfy the physiological demand of the patient, so the LVAD is implanted to provide the patient with an increased blood flow.

For treatments that require long time period of LVAD support, the main focus should be on providing adequate support. Destination therapy and bridge to transplant fall under this category of treatments.



The problem of providing the adequate physiological demand for the LVAD patient is the fact that the level of activity of the patient is constantly changing. The LVAD pump controller needs to be able to increase or decrease the blood flow to match such changes. In addition the controller must be reliable and robust.

Under current practice [49], physicians perform a ramped speed study on the patient, while monitoring key hemodynamic data, to determine a fixed speed setting for this patient. Any change in the controller parameters during the LVAD support is done by a physician or a clinician (i.e. open loop control techniques) during routine visits or when there are indications of inadequate support [49]. As mentioned, the need to adjust the LVAD support is due to the different levels of activities experienced by the patients and their emotional changes too [50], [51]. These changes exhibited by a wide variation of the systemic vascular resistance of the LVAD patient which is represented by  $R_s$  in the mathematical model presented in chapter three [52]-[54].

Table 4.1 shows simulation results from the model to highlight the issues with the constant LVAD support. The first column shows the cardiac outputs produced by a healthy heart (i.e.  $E_{\max} = 2.00$  mmHg) for different levels of activities. These values are used as a reference for what the physiological demand of heart failure patient that is experiencing a similar level of activity. Second column in the table shows the cardiac outputs of a patient with a mild heart failure with no LVAD support. The third column shows the aortic flow (i.e. the sum of the pump flow and the flow pumped through the aortic valve by the native heart) of a mild heart failure patient with constant LVAD support. Constant LVAD support means that the pump motor power doesn't change during the entire support time. In this case the pump motor power is set at 1W.

By comparing the values in the healthy heart case and the constant LVAD support case, it is obvious that while the constant LVAD support matches the cardiac output of a healthy heart in the case of moderate activity level ( $HR = 75$ ,  $R_s = 1.0$ ), it doesn't match the cardiac output in the cases of very active and inactive levels. In the case of very active patient it is seen that the constant level of support provides 1.29 l/min less than the physiological demand of the patient. In the case of the inactive level the constant LVAD support provides 0.39 l/min more than the physiological demand, which could be negatively impacting the heart by providing more blood than needed and risking the occurrence of suction events. In addition, this means that the controller is drawing more power from the LVAD batteries than what is actually needed.

Comparing the values in the first and second column shows that the cardiac output of a mild heart failure patient with no LVAD support provides about 25% less blood flow of that of the healthy heart. The objective of the LVAD is to compensate for this 25% deficit, but with the constant LVAD support, however, this is not possible.

Table 4.1 offers an interesting observation about the aortic flows of the constant LVAD support. When the pump controller parameters are kept constant, one would expect that the flow remains constant, but it is shown that this is not true as the flow increases with the increased level of activity. This is because the cardiovascular system and the pump are coupled systems that affect each other. As the level of activity increases the heart rate increase provides more blood available to the pump, additionally, the systemic vascular resistance decreases making the blood flows faster in the circulation.

This phenomenon has been observed, both in simulation and in-vivo data, that for constant pump motor power, the mean pump flow increases when the activity level of the

patient increases, and vice versa [58]. Figure 4.1 and Figure 4.2 are obtained from simulation and they show plots of both pump speed and pump flow spontaneously reacting to changes in the systemic vascular resistance without any changes in the controller parameters. For example, the pump motor power is set at 2.16W. and  $E_{\max} = 1.0$  mmHg/ml, the mean pump flow is measured for three different values of  $R_s$ . As mentioned earlier the lower the value of  $R_s$  indicating an increase in the activity level, the higher the mean pump flow, as shown in Figure 4.2. This shows that the cardiovascular system combined with the LAVD pump can sense the change in the patient's level of activity and then react accordingly. It should be mentioned though that when the blood flow increases in a respond to an increased level of activity, such increase is not sufficient to match the physiological demand. Similarly, when the blood flow decreases when the activity level decreases, such decrease doesn't get low enough to match the demand (i.e. the pump is providing more blood than needed by the body).

Table 4.1: Aortic flow comparison between aortic flow of a healthy heart, mild heart failure with no support and mild heart failure with constant LVAD support, for different activity levels

		Aortic flow		
		Healthy heart $E_{\max} = 2.00$ mmHg	No LVAD support $E_{\max} = 1.00$ mmHg	Constant LVAD Support $E_{\max} = 1.00$ mmHg
Level of physical Activity	Very active $HR = 120\text{bpm}$ $R_s = 0.5$ mmHg.s/ml	9.25 l/min	6.86 l/min	7.96 l/min
	Moderately active $HR = 75\text{bpm}$ $R_s = 1.0$ mmHg.s/ml	5.10 l/min	3.80 l/min	5.18 l/min
	Inactive $HR = 60\text{bpm}$ $R_s = 1.2$ mmHg.s/ml	4.32 l/min	3.17 l/min	4.71 l/min

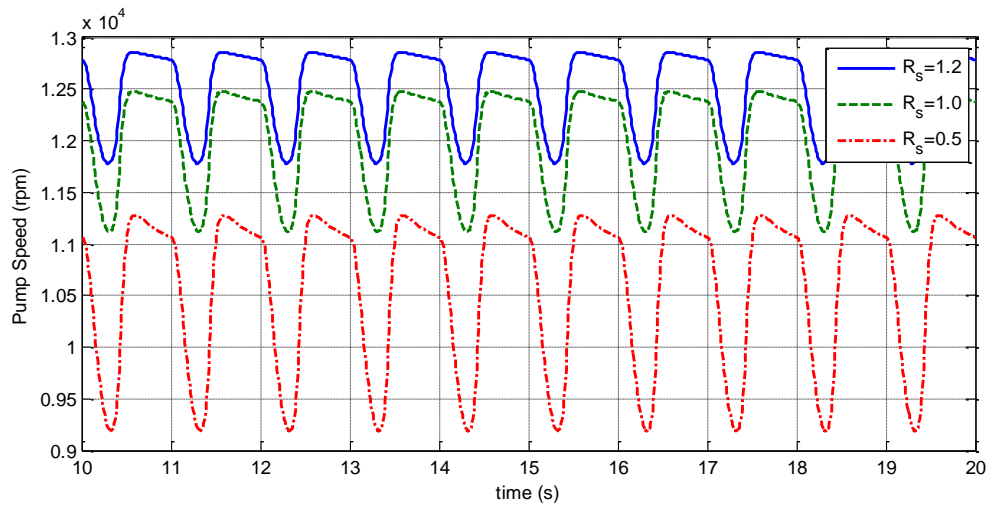


Figure 4.1: Pump speed signal for different  $R_s$ , with no change to the controller parameters

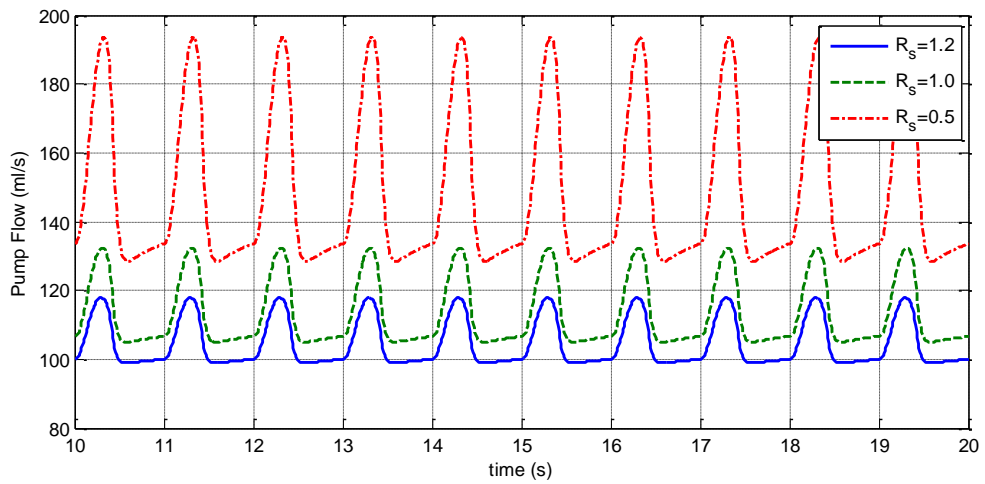


Figure 4.2: Pump flow signal for different  $R_s$ , with no change to the controller parameters

#### 4.2. Development of the Feedback Controller

The development of a feedback controller for the LVAD is an important challenge facing the increased use of such devices. Such variations in blood flow demand require a feedback controller that can automatically change the pump motor power to meet the body requirements for cardiac output and keep the mean arterial pressure within the normal limits [8]. Ideally, the development of a feedback controller requires the availability of real-time measurements of the hemodynamic of the patient. These measurements, however, are generally difficult to obtain because the placement of pressure or flow sensors, for long-term application in the human heart, is not possible under the current technology [55]. The pump flow ( $Q_p$ ) is a suitable feedback variable since it requires a flow-meter installed at one of the pump cannulae. Figure 4.3 shows a schematic of a controller that uses pump flow measurements to control the pump speed using the pump motor power.

This fact is used in estimating the level of activity of the patient by estimating  $R_s$ . This is accomplished by minimizing an error signal which is a measure of the difference between the actual pump flow measurements of the patient and the pump flow calculated based on the estimated  $R_s$ . Once  $R_s$  is estimated, the cardiac output of a healthy heart experiencing the same level of activity is determined by using the 5<sup>th</sup> order model of the healthy heart. This is followed by the manipulation of the control variable (i.e. pump motor power) to achieve the desired pump flow.

The feedback controller shown in Figure 4.3 consists of four stages:

The first stage, which is labeled “detect change in pump flow”, is used to detect changes in the activity level of the patient and prompt the controller to react to such changes. As mentioned a change in the mean pump flow signal without the pump motor power changing is an indication of a variation in the activity level of the patient. In this stage the pump flow signal is measured and the average ( $\bar{Q}_{pm}$ ) is calculated during each cardiac cycle.

The second stage, labeled “Estimate the level of activity ( $R_s$ ) using the 6<sup>th</sup> order model” involves adjusting the numerical value of  $R_s$  in the 6<sup>th</sup> order model through a recursive approach until the resulting mean pump flow from the model matches the actual mean pump flow of the patient. This is accomplished by minimizing the square of the difference between the measured and calculated mean pump flows as seen in Equation(4.1).

$$\text{minimize } J(R_s) = (\bar{Q}_{pm} - \bar{Q}_p(R_s, P_{po}))^2 \quad (4.1)$$

Where  $\bar{Q}_p$  is the mean pump flow calculated by simulating the 6<sup>th</sup> order patient-specific model. The pump motor power used in the model ( $P_{po}$ ) should be the same as the actual power supplied to the LVAD pump because the model must simulate the current state of the patient while changing  $R_s$  through a recursive algorithm to minimize the function in Equation(4.1).

During the third stage, labeled “Calculate physiological demand for the estimated  $R_s$ ”, the physiological demand or required mean pump flow under the current activity level is determined by imposing the value of  $R_s$  estimated during the previous stage into the 5<sup>th</sup> order model with  $E_{\max} = 2$  mmHg/ml to represent a healthy heart. This is done since the overall

objective of the controller is to determine the actual output of a healthy heart under the current level of activity, characterized by the estimated  $R_s$ , and try to match it with the LVAD output.

During the fourth stage, labeled “Update Pump Motor Power”, the pump motor power will be adjusted until the mean pump flow approaches the physiological demand for the current level of activity calculated in the previous stage. Again, this is accomplished by minimizing the square of the difference between the physiological demand and the adjusted mean pump flow as seen in Equation(4.2).

$$\text{minimize } f(P_E) = \left( CO - \bar{Q}_p(\hat{R}_s, P_E) \right)^2 \quad (4.2)$$

Where  $CO$  is the required blood flow for the patient,  $\hat{R}_s$  is the estimated systemic vascular resistance of the patient and  $P_E$  is changing through recursive algorithm to minimize the function in Equation(4.2). The  $P_E$  value that results in minimizing such function is the control signal that is sent to the pump to adjust its speed.



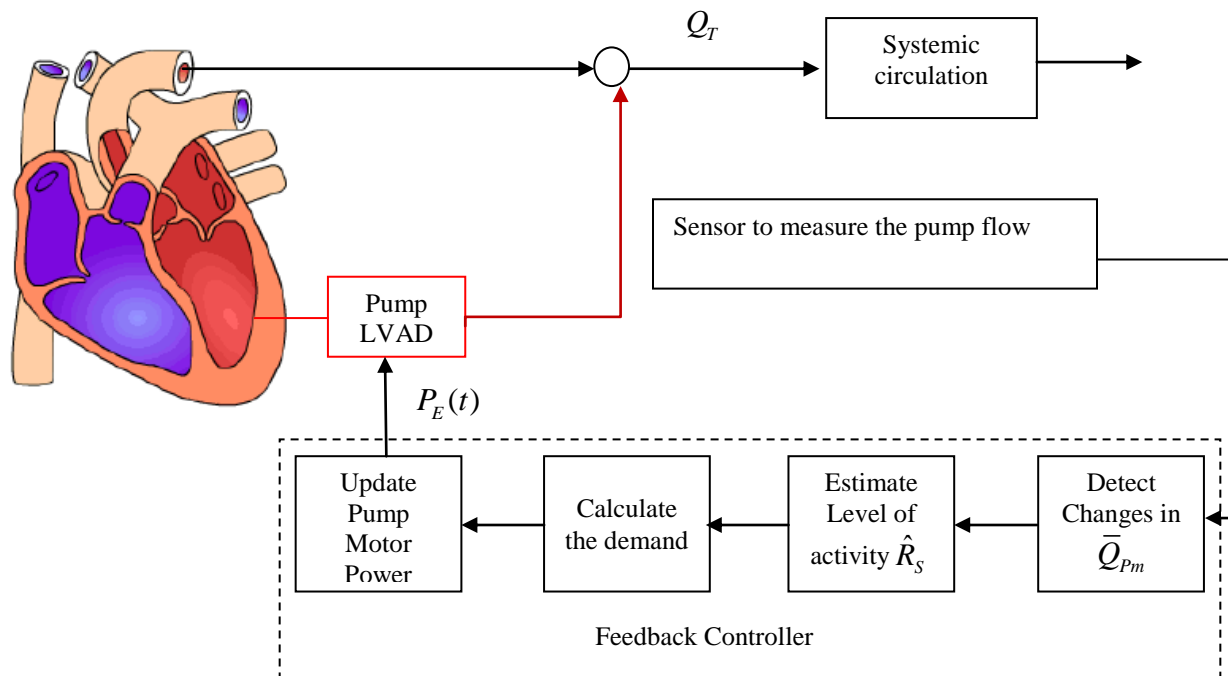


Figure 4.3:Block diagram for the feedback controller

### 4.3. Simulation results

In this section we test the feedback controlled explained in the previous section. Figure 4.1 shows a simulation example of a patient initially at rest who then becomes more physically active. This simulation is modeled by a change in  $R_s$  from 1 mmHg.s/ml to 0.5 mmHg.s/ml. at  $t = 4$ s.

The Fibonacci search algorithm is chosen to minimize the objective function in Equations(4.1) and (4.2), because of its inherent advantage of having a predefined number of iteration before the algorithm arrives at a solution. The number of iterations depends on the tolerance specified by the system [59].

The Fibonacci search was then used to estimate this change in  $R_s$  . The number of iterations required to arrive at a converged solution was predetermined based on both the possible range of  $R_s$  and the tolerance required; the former is assumed to be between 0.4 and 1.4 mmHg.s/ml while the latter was established as 0.01 mmHg.s/ml. Hence:

$$F_n > \left( \frac{1.4 - 0.4}{0.01} \right) = 100 \Rightarrow F_{11} = 144 > 100 \Rightarrow n = 11 \quad (4.3)$$

Here, the number of required iterations,  $n$  , is determined as the  $n$  th Fibonacci number larger than the search range divided by the tolerance. In this case, the 11<sup>th</sup> Fibonacci number satisfies this criterion.

Using the 6<sup>th</sup> order model the  $R_s$  will be estimated in an iterative manner. The search bracket is narrowed down at every iteration step until the convergence criterion is met after the  $n$  h iteration. This process is shown in Figure 4.5.

Although the search interval was originally set for values of  $R_s$  between 0.4 and 1.4 mmHg.s/ml, prior knowledge of the dynamics of the system allows us to start from a narrower interval. That is, it could have been assumed a priori that the increase in mean pump flow signal was evidence of a decrease in  $R_s$  and therefore start with a bracket between 0.4 and 1.0 mmHg.s/ml instead, for example, leading to a smaller number of required iterations. The value of  $R_s$  is estimated at 0.5 (Which is a correct estimation since this is the value we used in our simulation). This value will be taken and substituted in the 5<sup>th</sup> order model and the  $CO$  will be calculated over one cardiac cycle.

For the case being implemented herein, the physiological demand  $CO$  was found to be 148.9 ml/s, larger than the current mean pump flow of 115.3 ml/s achieved by a pump motor power of 1.2W. Therefore, an increase of the pump motor power is necessary to achieve the goal of meeting the physiological demand. The initial bracket for the pump motor power was then established between 1.2W and 7.8W. Figure 4.6 shows the evolution of the  $P_E$  bracket throughout the Fibonacci search algorithm.

The research presented in this chapter has limitations that should be mentioned. The simulation results are based on a constant heart rate during all different cases of activity level. This was done to observe how the pump flow changes when only the systemic vascular resistance changes. It should be noted that the changes in the systemic vascular resistance, in most cases, is associated with a change in the heart rate.

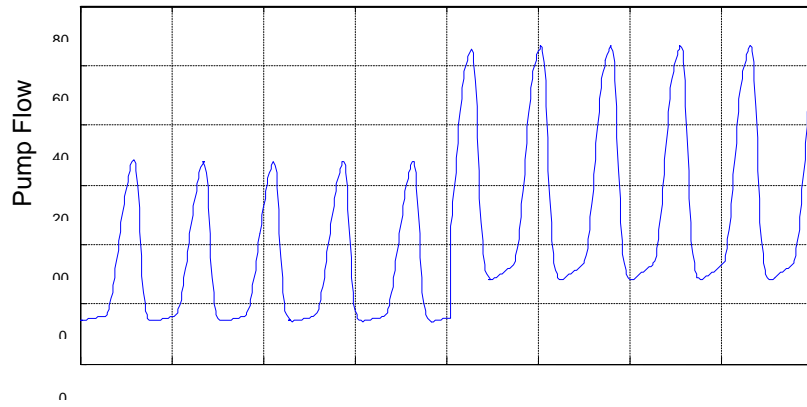


Figure 4.4: Pump Flow signal as  $R_s$  Changes from 1 to 0.5 mmHg.s/ml

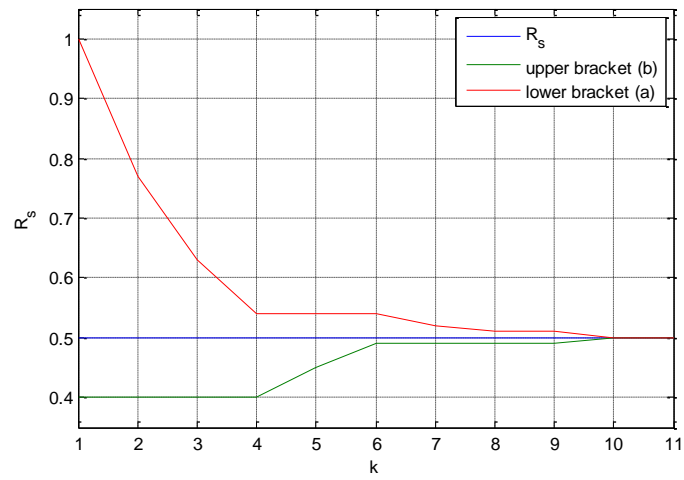


Figure 4.5: Lower and Upper Brackets of the Fibonacci Search to Estimate  $R_s$

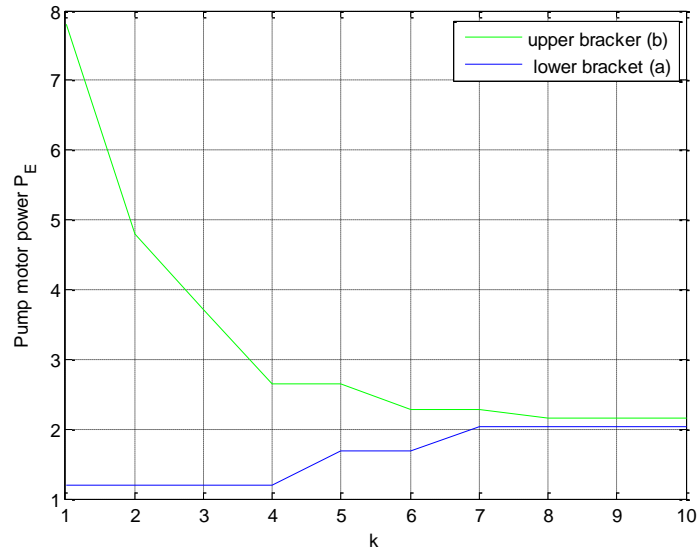


Figure 4.6: Lower and Upper Brackets of the Fibonacci Search to Estimate  $P_E$

#### 4.4. Summary

In this chapter, we developed a feedback controller that can be implemented in LVAD devices used in destination therapy and bridge to transplant. The objective of the controller is to provide the blood flow for the heart failure patient that is equivalent to the cardiac output of a healthy heart experiencing the same level of activity. The controller achieves this by estimating  $R_s$  which is a representation of the activity level. The controller uses the 5<sup>th</sup> order model to calculate the cardiac output of a healthy heart at the same level activity of the patient and set it as the targeted blood flow rate. By adjusting the pump motor power, the controller can achieve the targeted blood flow rate. A simulation example is used to illustrate the four stages performed by the controller.

## **CHAPTER 5: ENGINEERING ANALYSIS OF THE AORTIC VALVE DYNAMICS IN PATIENTS WITH LEFT VENTRICULAR ASSIST DEVICES**

The objective of this chapter is to observe the effect of the permanent closure of the valve on the hemodynamic waveforms of the LVAD patient, as well as the effect of the pump power on the dynamics of the valve. The chapter starts by explaining how the mathematical model that was presented in Chapter Three will be used to collect the data. This is followed by an analysis of the effect of the permanent closure of the aortic valve on the hemodynamic conditions of the patient. The simulation results also show the effect of the pump flow on the aortic valve. Finally, a summary is presented.

### 5.1. Method for data collection

The second generation pumps for the LVAD creates a continuous flow of blood in the aorta opposed to the pulstaile flow that is natively created by the human heart. Naturally, the pulstaile flow happens due to the aortic valve opening during the ejection phase and then closing for the remainder of the cardiac cycle. When the LVAD is present, however, the ejection phase time is shortened (i.e. aortic valve opens for a shorter duration), or in some cases is completely skipped (i.e. aortic valve closes during the entire cycle) when the pump is operating at a higher setting, the latter case is referred to as permanent closure of the aortic valve. This change in the flow pattern causes changes in the hemodynamic conditions of the patient and affects the pump performance. The permanent closure of the valve happens because the pump is unloading the left ventricle fast enough that the pressure inside the ventricle is not sufficient to force the blood to

be pumped through the aortic valve. Such permanent closure can further lead to undesirable changes in the hemodynamic conditions of the patient.

The mathematical model is used to study the effect of the aortic valve dynamics on the hemodynamic of the LVAD patient and on the pump performance characteristics. We excited the model with different values of the control variable  $P_E$  so that the effect of the pump on the aortic valve can be observed over a wide range of pump operation. It is imperative that this range includes the critical value of  $P_E$ , henceforth denoted by  $P_E^c$ , at which the permanent closure of the aortic valve first occurs. As explained in chapter three, there is a complex relation between the pump motor power and its rotational speed, so we will define the critical speed  $\omega^c$  as the pump speed when the pump motor is supplied with the critical pump power  $P_E^c$ .

In order to detect the permanent closure of the aortic, we observed the diode  $D_A$ , in Figure 2.3, which represents the aortic valve. An aortic valve that is operating normally is simulated by  $D_A$  being open (i.e., short circuit) during the ejection portion of each cardiac cycle. Permanent closure of the valve happens when  $D_A$  closes (i.e., becomes open circuit) and remains closed for the entire duration of the cardiac cycle. The case when the permanent closure occurs translates to zero flow through  $R_A$ , meaning there is no flow through the aortic valve, and that flow through the pump is equal to the total flow through the aorta (i.e.  $x_5(t) = x_6(t)$ ).

The complexity in this analysis arises from the fact that the critical pump power  $P_E^c$  depends on two physiological factors: (i) the severity of the heart failure, and (ii) the activity level of the patient. To cover a wide range of these factors, we simulated nine different cases corresponding to combinations of three different levels of heart failure (represented by three



different values of  $E_{\max}$  ) and three different levels of patient activity (represented by three different values of  $R_s$  with corresponding values of heart rate,  $HR$  ) [60]. These cases are summarized in Table 5.1

Table 5.1: Nine different cases representing combination of three levels of heart failure and three levels of patient activity.

		Level of Heart Failure		
		$E_{\max} = 1.00$ mmHg	$E_{\max} = 0.75$ mmHg	$E_{\max} = 0.50$ mmHg
Level of physical Activity	$HR = 120$ bpm $R_s = 0.5$ mmHg.s/ml	Mild Heart Failure Very Active	Moderate Heart Failure Very Active	Sever Heart Failure Very Active
	$HR = 75$ bpm $R_s = 1.0$ mmHg.s/ml	Mild Heart Failure Moderately Active	Moderate Heart Failure Moderately Active	Sever Heart Failure Moderately Active
	$HR = 60$ bpm $R_s = 1.2$ mmHg.s/ml	Mild Heart Failure Inactive	Moderate Heart Failure Inactive	Sever Heart Failure Inactive

## 5.2. Simulation results

The nine different cases described in Table 5.1 have been simulated using our model for a range of  $P_E$  starting at 0.1W and ending at 1.6W. Before summarizing the overall results, we will first describe in detail the results that correspond to only one representative case: a patient with mild heart failure and with a moderate level of activity (i.e.  $E_{\max}=1$ ,  $HR=75$  and  $R_s=1.0$ ). We will then illustrate graphically the general results encompassing all other eight cases to show the effects of the aortic valve dynamics as the severity of the heart failure as well as the activity level of the patient vary as described in Table 5.1 [60].

Figure 5.1 shows a plot of the minimum, maximum (i.e. peak) and mean values of the blood flow signal through the aortic valve as a function of  $P_E$ . It is clear from this plot that the aortic valve closure occurs at the critical value of  $P_E^c = 0.8W$  and a corresponding critical speed  $\omega^c = 9,052$  rpm. Note that the minimum values of the blood flow through the aortic valve are small negative values when pump power is below  $P_E^c$ . This small reverse flow in the aortic valve is due to the effect of the aortic compliance (denoted by  $C_A$  in Figure 2.3). Physiologically this is due to the adverse pressure gradient that is developed as the aortic flow begins to decelerate rapidly after reaching its peak which affects the low momentum fluid near the wall of the aorta causing reverse flow in the sinus region [61]. The plot in Figure 5.1 also shows that as  $P_E$  is increased starting at 0.1W, the mean value of blood flow through the aortic valve decreases, as expected, but the maximum value of the blood flow also decreases but at a very sharp and much faster rate. This happens because as pump power is increased, the pump speed will also increase resulting in a higher pressure difference between the left ventricle and aorta, which causes more

blood to flow through the pump rather than through the aortic valve. This phenomenon is more evident in Figure 5.2 which shows a plot of the pump flow signal as a function of  $P_E$ . While all values (max, mean and min) of the pump flow increase, as expected, with increasing values of  $P_E$ , the maximum value seems to exhibit a breakpoint at the critical power  $P_E^c = 0.8W$  by remaining constant with zero slope as  $P_E$  is increased beyond  $P_E^c$ . This breakpoint in the slope of the maximum values of the pump flow occurs exactly when the aortic valve closes for the entire cardiac cycle and continues to be closed as  $P_E$  is increased.

Figure 5.3 shows the left ventricle pressure as a function of  $P_E$ . It is important to notice that the minimum values of this signal almost stay constant as  $P_E$  is increased, even after  $P_E^c$  is reached. This is due to the fact that the minimum value of the left ventricle pressure happens during the filling phase, which is not greatly affected by the aortic valve dynamics. The maximum values, on the other hand, only stay constant before  $P_E^c$ ; once this critical value is reached the maximum value is decreasing at a very sharp rate. The maximum value happens during the rapid ejection of blood out of the aortic valve (i.e. early in the ejection phase). This means that as long as the aortic valve is opening during the cardiac cycle, there is enough blood volume in the ventricle to reach certain pressure that can force the aortic valve to open. Once  $P_E^c$  is exceeded, the maximum value starts to decrease due to the decrease in the blood volume inside the ventricle at the end of the filling (diastolic) phase (LVEDV). It is interesting to see the mean values are decreasing before  $P_E^c$  is reached, while the maximum and minimum values stay almost the same. The reason for that decrease is the shorter duration of the aortic valve opening

(more details on aortic valve opening duration in the next chapter), which leads to reaching the minimum value faster as the  $P_E$  increases. Once  $P_E^c$  is reached, the mean values decrease at a higher rate simply due to the aortic valve closure and the ejection phase not occurring. The mean values decrease as the maximum value decreases and  $P_E$  increases.

Figure 5.4 shows a plot of aortic pressure as a function of  $P_E$ . Prior to  $P_E^c$ , the maximum value of the aortic pressure signal is almost constant. The maximum values happen during the reduced ejection phase (i.e. later in the ejection phase). On the other hand, both the minimum and mean values are increasing as the value of  $P_E$  increases. The minimum values increase because as the  $P_E$  increases, the duration of the aortic valve opening decreases. This leads to less blood flow through the valve and more blood flowing at an increasingly higher rate through the pump. Hence, the more blood volume in the aorta during diastole, the higher the minimum values of the aortic pressure signal. After exceeding the value of  $P_E^c$ , the three values (i.e. maximum, minimum and mean) are increasing in a higher rate. Since the aortic valve is no longer opening, the pressure in the aorta is increasing as the unloading rate is increasing. If this increase continues, the aortic pressure will reach a certain level when it doesn't have any pulsatility (i.e. the signal will be flat line).

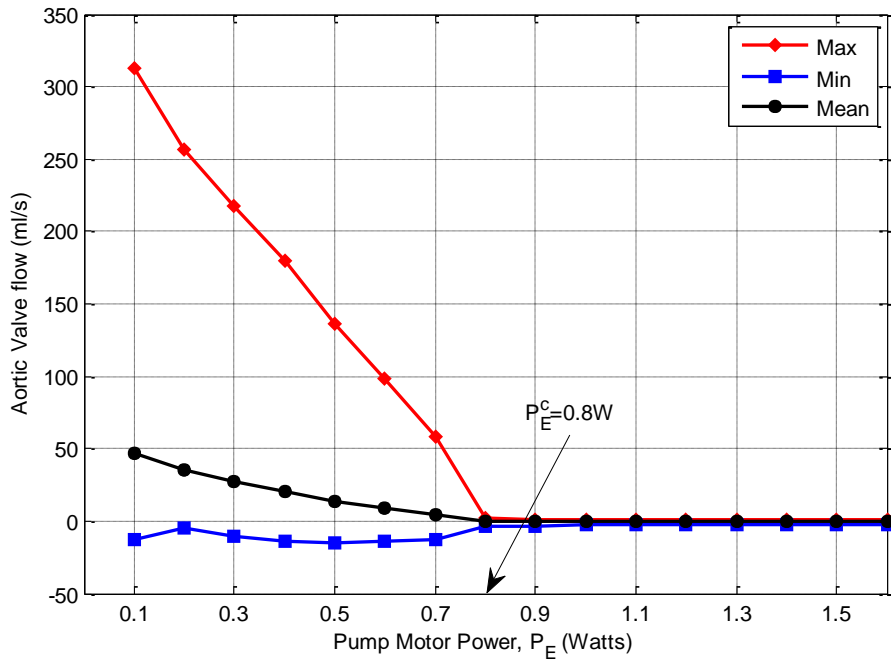


Figure 5.1: Change of aortic valve flow rate with ump motor power

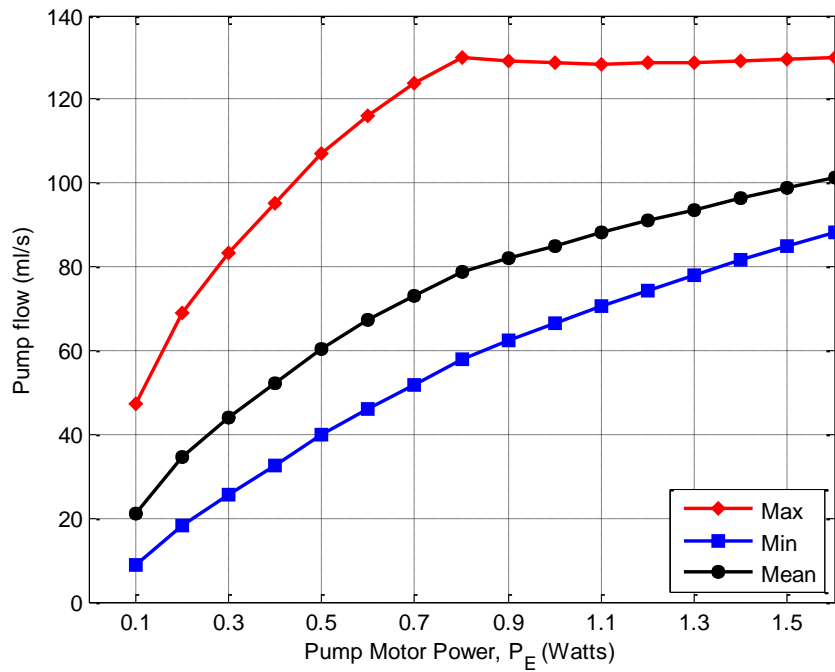


Figure 5.2. Pump Flow as a function of pump motor power

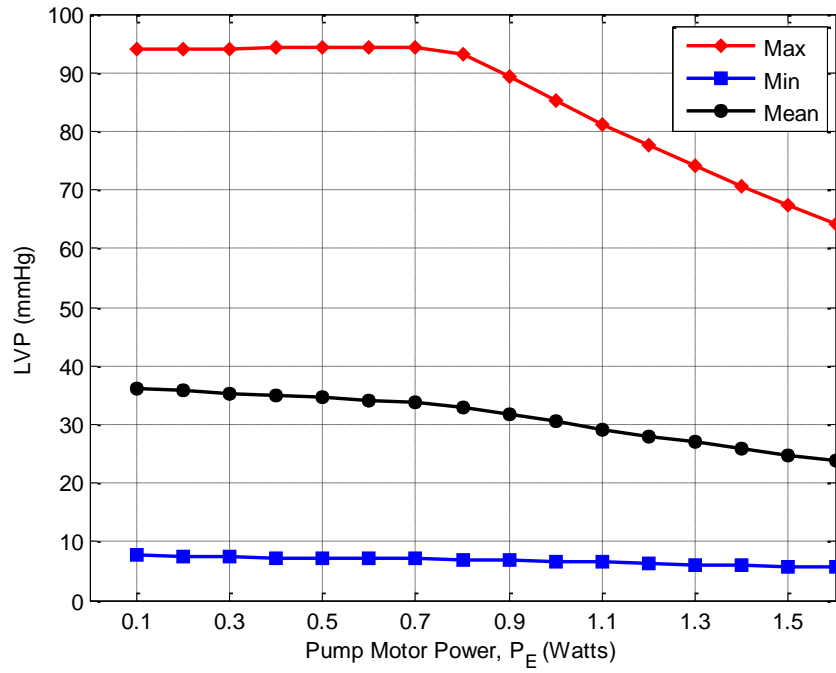


Figure 5.3. Left ventricle pressure as a function of pump power

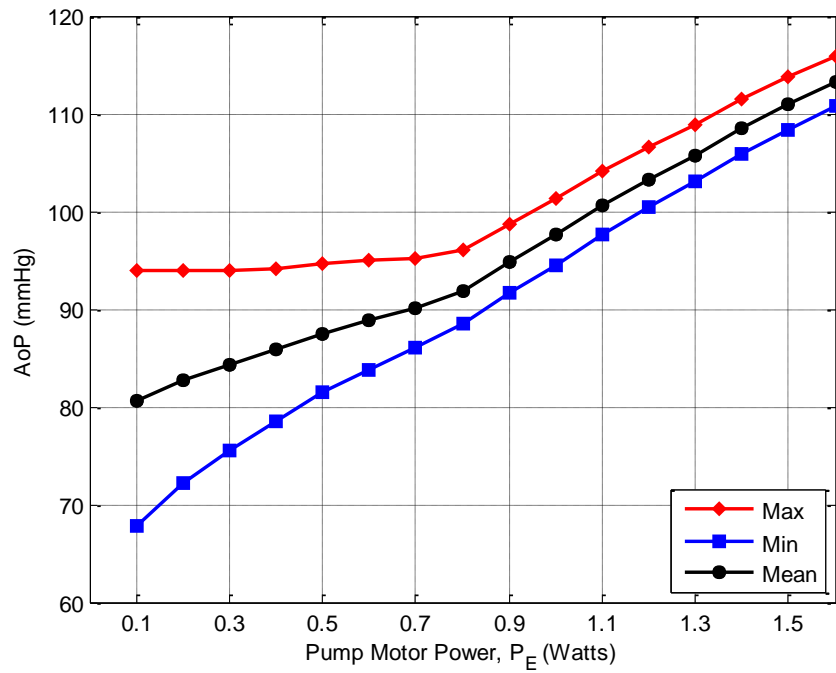


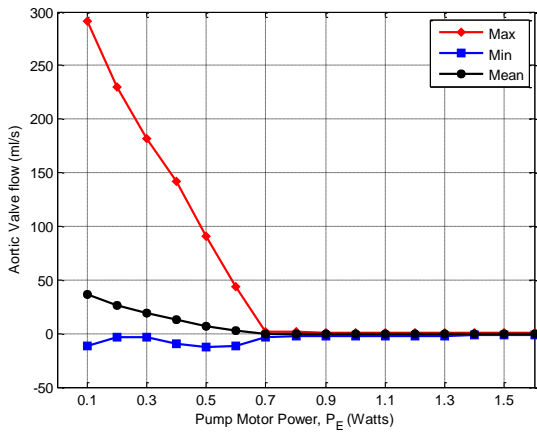
Figure 5.4. Aortic pressure as a function of pump power

Figure 5.5 through Figure 5.12 show the same waveforms for the other eight cases that were listed in Table 5.1. It is clear that all these waveforms exhibit the same characteristics as the ones listed in the case we discussed in detail previously (i.e. Mild heart failure, moderately active patient). As expected we see that the case of a mild heart failure patient with high level of activity (i.e.  $E_{\max}=1$ ,  $HR=120$  and  $R_S=0.5$ ) has a higher value of  $P_E^c$ , while the case of severe heart failure and low level of activity (i.e.  $E_{\max}=0.5$ ,  $HR=60$  and  $R_S=1.2$ ) has the lower value of  $P_E^c$ .

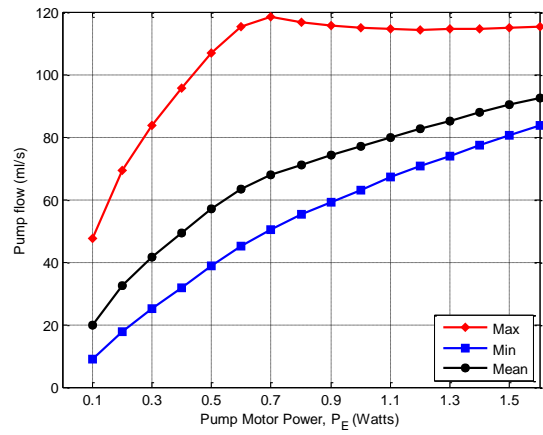
Since  $P_E^c$  and  $\omega^c$  are related by a complex nonlinear expression (see Equation(3.7)), the values of  $P_E^c$  and corresponding  $\omega^c$  for the nine cases in Table 5.1 are given in Table 5.2. The relationship between  $P_E^c$  and  $\omega^c$  is quite interesting but not surprising. First, increasing the power to the LVAD does not always necessarily mean increasing the speed. As is clear from Equation(3.7), the speed is also dependent on the rate of blood flow through the pump, which may have a compensating effect on the speed (i.e., decreasing it even if  $P_E$  is increasing). Second, for all three levels of activity, the weaker the heart, the lower the speed at which the aortic valve shuts down, as expected. For example, for an inactive patient, the aortic valve shuts down when the speed reaches 7433 rpm if the heart is severely sick, but can hold off until the speed reaches 9168 rpm if the heart is mildly sick. On the other hand, for a given level of heart failure, the lowest speed at which the aortic valve shuts down seems to vary with the level of activity. For a patient with mild heart failure, the aortic valve shuts down first when the activity level is moderate at 9052 rpm, but for a patient with moderate or severe heart failure, the valve shuts down first at 8403 rpm and 7433 rpm, respectively, when the patient is inactive. What this

essentially means is that for a given state of heart failure, if the level of activity of the patient is continuously changing, the pump should be operated at control values of power and speed that do not go above the lowest values that result in shutting down of the aortic valve. Finally, it is interesting to note that the results in Table 5.2 are minimally affected by the pump parameters in the model, suggesting that the above observations are valid for a wide range of LVADs whose pumps can be modeled as described in Chapter Three. Our analysis indicates that the critical pump speeds remain within  $\pm 0.7\%$  of the nominal values shown in Table 5.2 when the pump parameters  $R_p$  and  $L_p$  are changed by  $\pm 10\%$  from their nominal values as shown in Table 2.1.

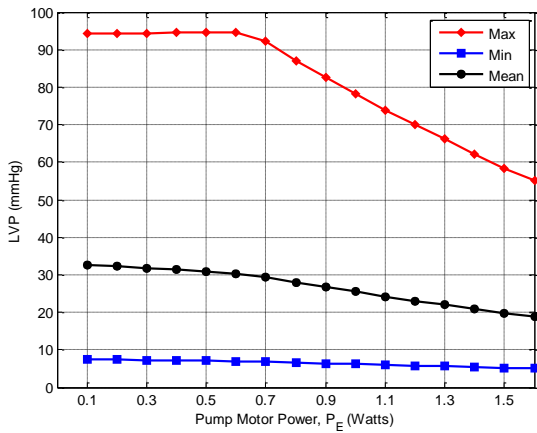




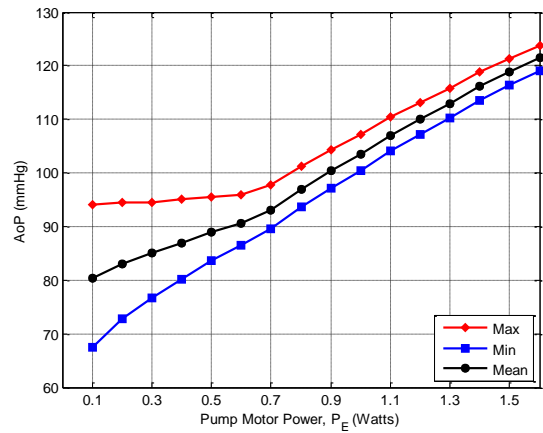
(a)



(b)

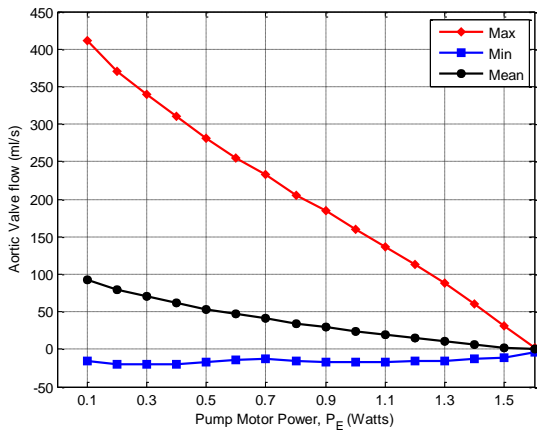


(c)

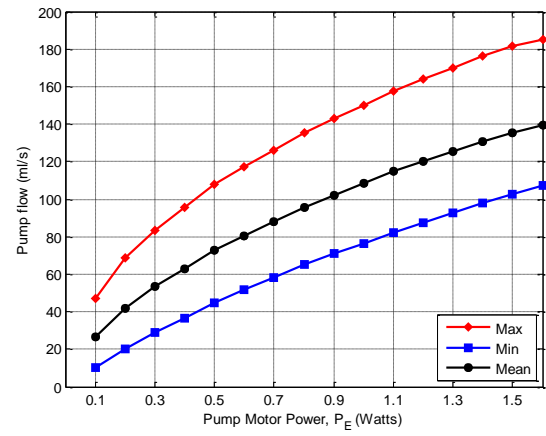


(d)

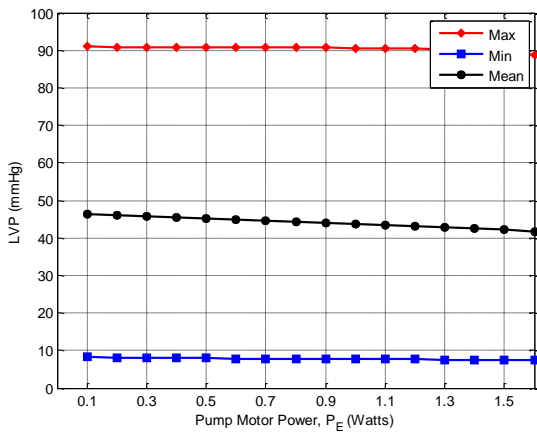
Figure 5.5: Waveforms for the case of inactive patient with mild heart failure. (a) Aortic valve flow, (b) pump flow, (c) Left ventricle pressure and (d) Aortic pressure.



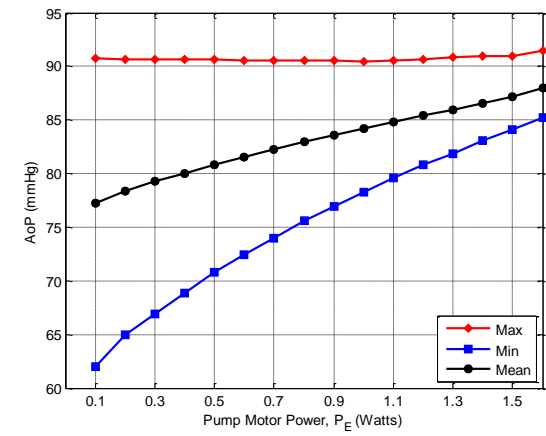
(a)



(b)

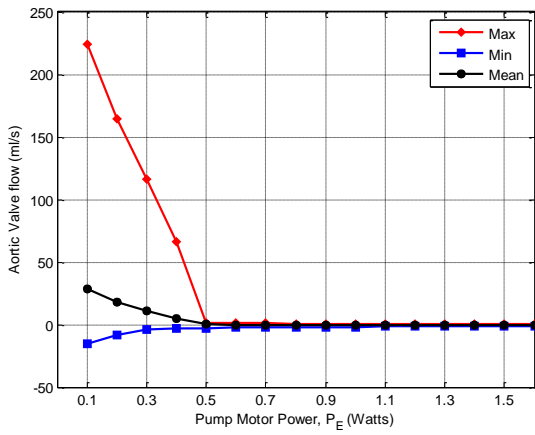


(c)

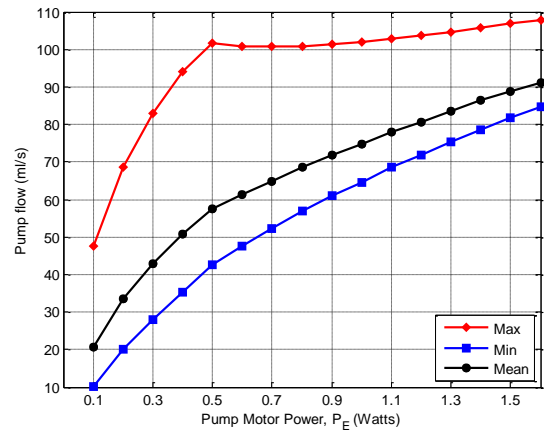


(d)

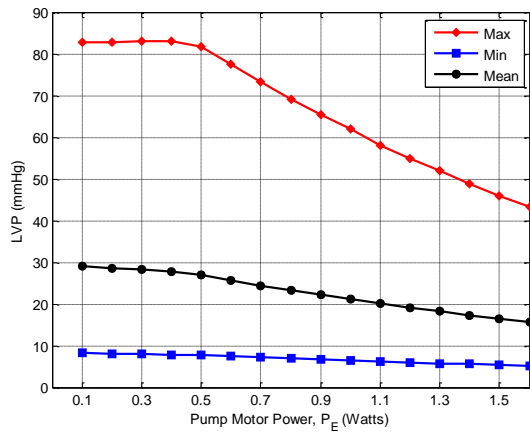
Figure 5.6: Waveforms for the case of very active patient with mild heart failure. (a) Aortic valve flow, (b) pump flow, (c) Left ventricle pressure and (d) Aortic pressure.



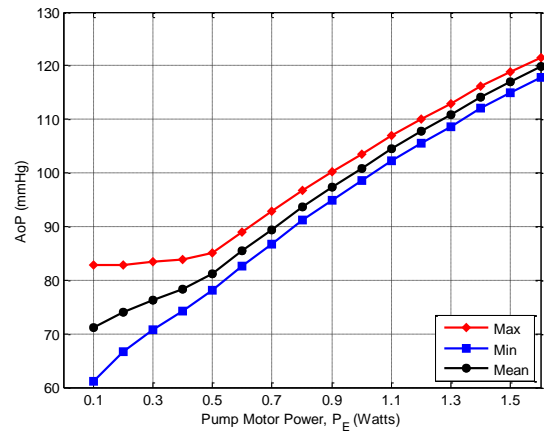
(a)



(b)

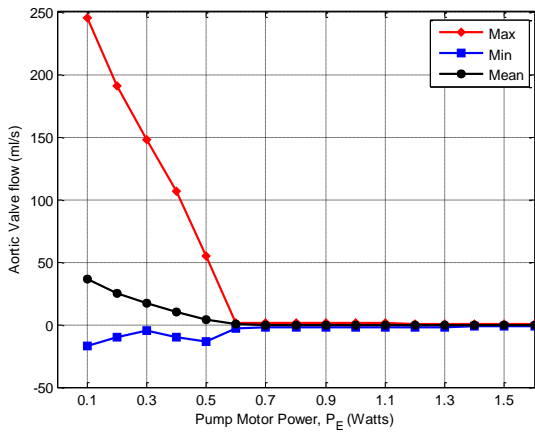


(c)

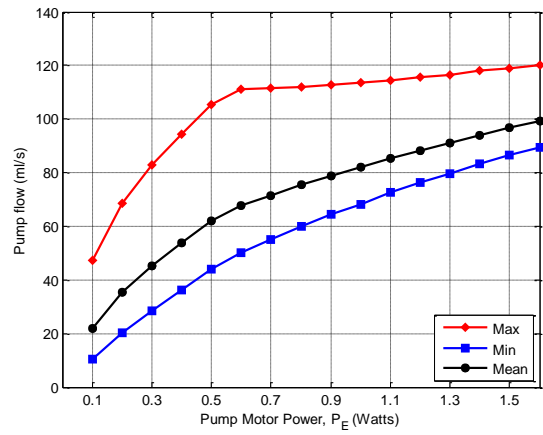


(d)

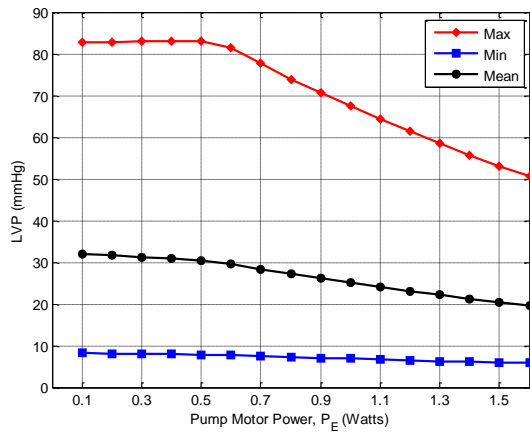
Figure 5.7: Waveforms for the case of inactive patient with moderate heart failure. (a) Aortic valve flow, (b) pump flow, (c) Left ventricle pressure and (d) Aortic pressure.



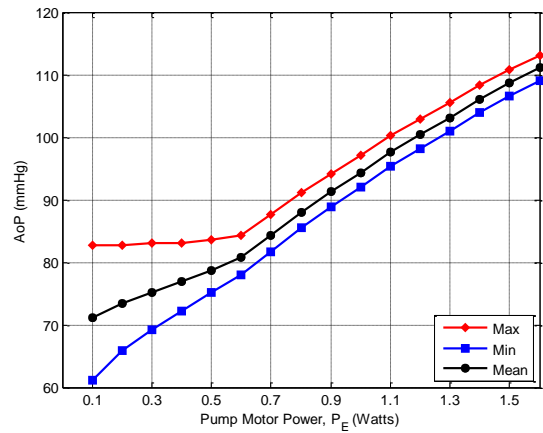
(a)



(b)

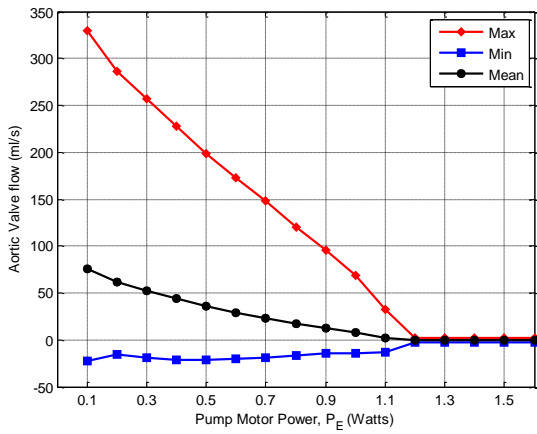


(c)

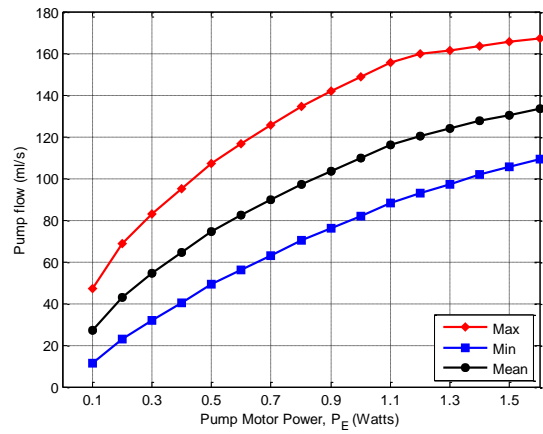


(d)

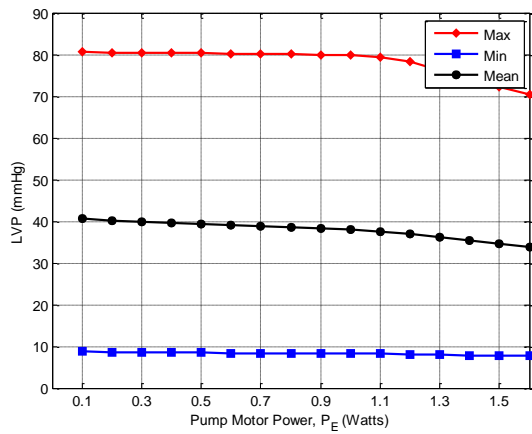
Figure 5.8: Waveforms for the case of moderately active patient with moderate heart failure. (a) Aortic valve flow, (b) pump flow, (c) Left ventricle pressure and (d) Aortic pressure.



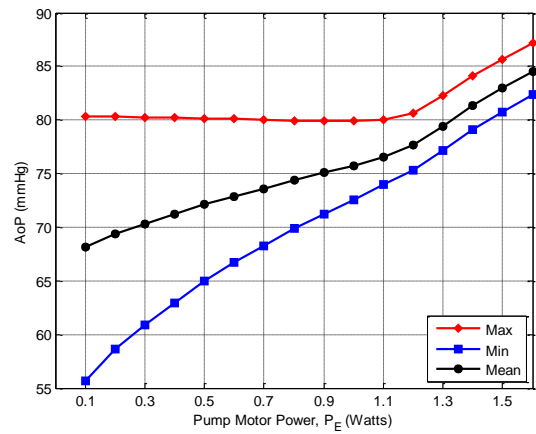
(a)



(b)

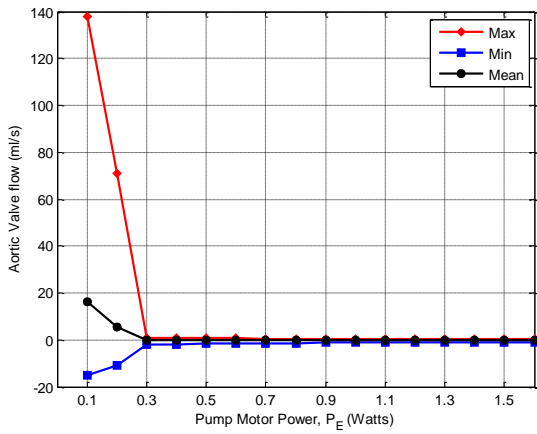


(c)

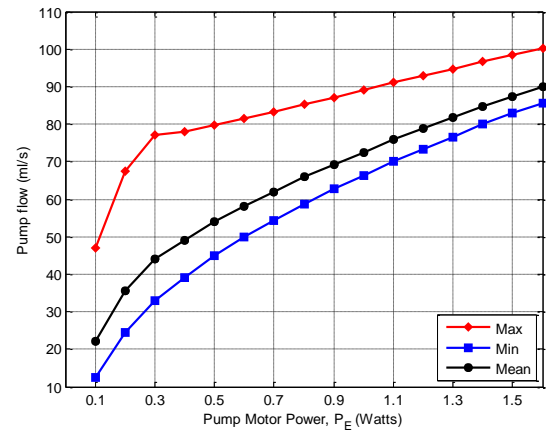


(d)

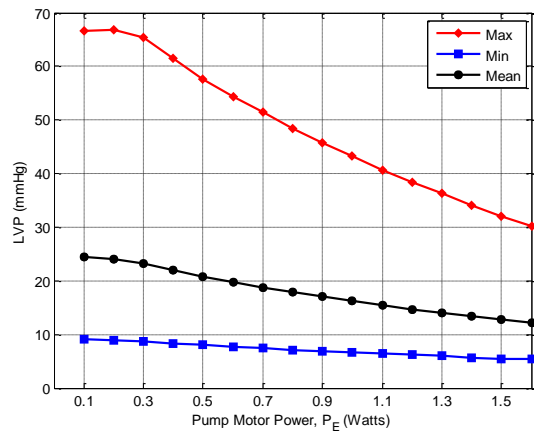
Figure 5.9: Waveforms for the case of very active patient with moderate heart failure. (a) Aortic valve flow, (b) pump flow, (c) Left ventricle pressure and (d) Aortic pressure.



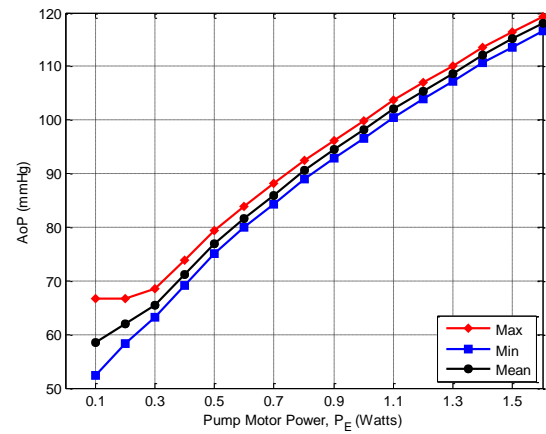
(a)



(b)

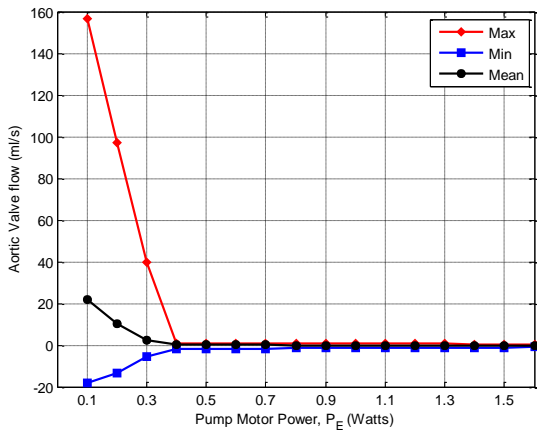


(c)

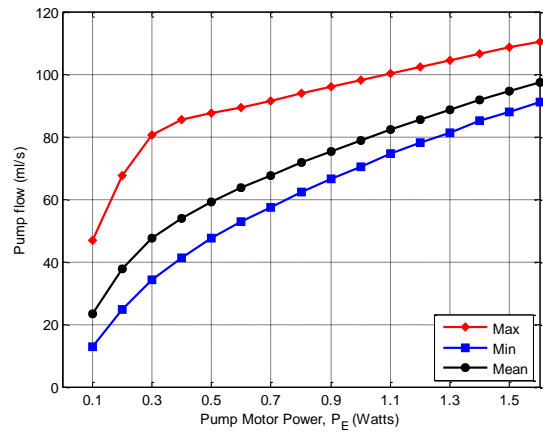


(d)

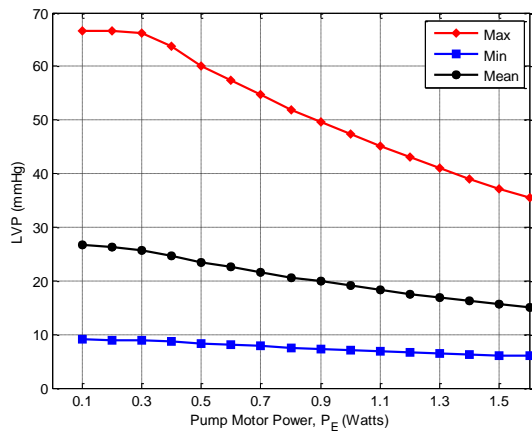
Figure 5.10: Waveforms for the case of inactive patient with severe heart failure. (a) Aortic valve flow, (b) pump flow, (c) Left ventricle pressure and (d) Aortic pressure.



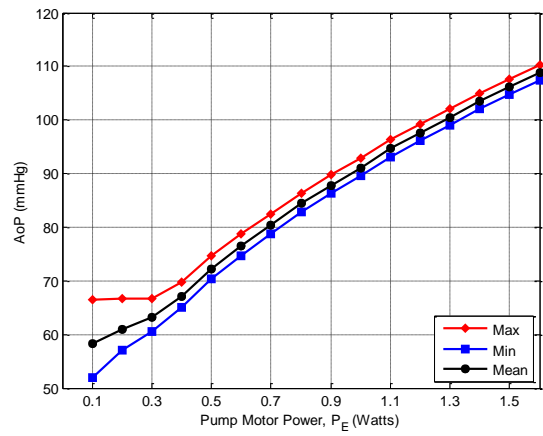
(a)



(b)

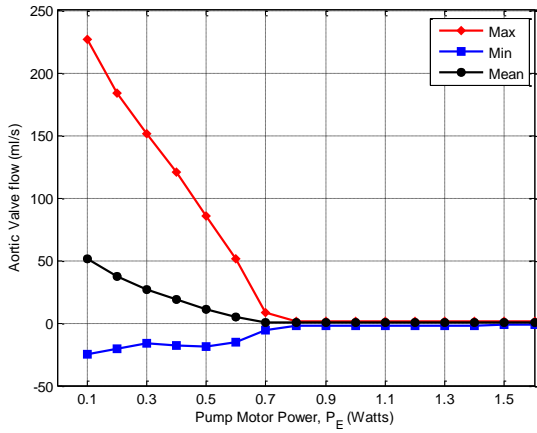


(c)

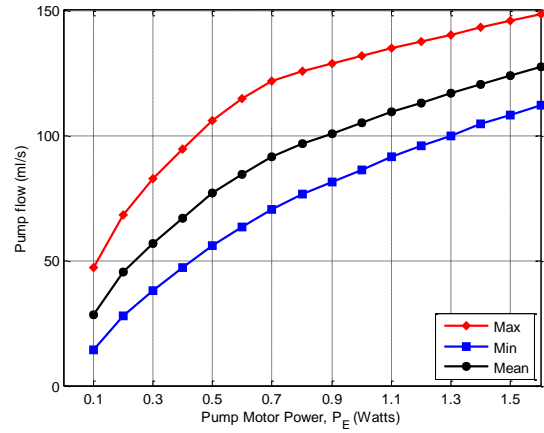


(d)

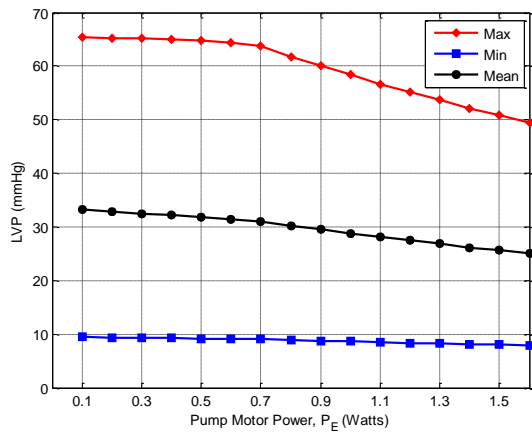
Figure 5.11: Waveforms for the case of moderately active patient with severe heart failure. (a) Aortic valve flow, (b) pump flow, (c) Left ventricle pressure and (d) Aortic pressure.



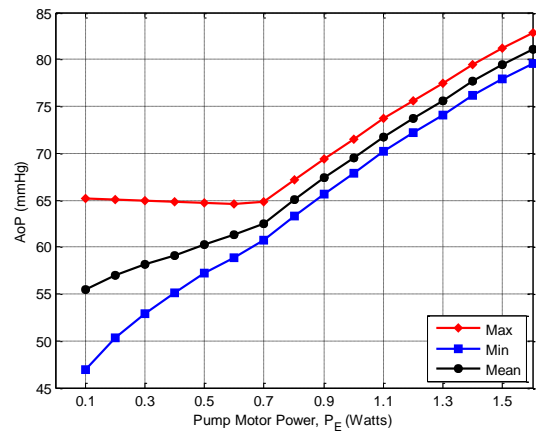
(a)



(b)



(c)



(d)

Figure 5.12: Waveforms for the case of very active patient with severe heart failure. (a) Aortic valve flow, (b) pump flow, (c) Left ventricle pressure and (d) Aortic pressure.



Table 5.2: Critical pump power ( $P_E^c$ ) values of the nine different cases.

		Level of Heart Failure		
		$E_{\max}=1.00\text{mmHg}$	$E_{\max}=0.75\text{mmHg}$	$E_{\max}=0.50\text{mmHg}$
Level of physical Activity	$HR = 120 \text{ bpm}$ $R_S = 0.5 \text{ mmHg.s/ml}$	$P_E^c = 1.6W$ $\omega^c = 9,454\text{rpm}$	$P_E^c = 1.2W$ $\omega^c = 8,825\text{rpm}$	$P_E^c = 0.7W$ $\omega^c = 7,732\text{rpm}$
	$HR = 75\text{bpm}$ $R_S = 1.0\text{mmHg.s/ml}$	$P_E^c = 0.8W$ $\omega^c = 9,052\text{rpm}$	$P_E^c = 0.6W$ $\omega^c = 8,460\text{rpm}$	$P_E^c = 0.4W$ $\omega^c = 7,694\text{rpm}$
	$HR = 60\text{bpm}$ $R_S = 1.2\text{mmHg.s/ml}$	$P_E^c = 0.7W$ $\omega^c = 9,168\text{rpm}$	$P_E^c = 0.5W$ $\omega^c = 8,403\text{rpm}$	$P_E^c = 0.3W$ $\omega^c = 7,433\text{rpm}$

### 5.3. Summary

In this chapter we introduced the importance of studying the aortic valve dynamics effect on the hemodynamic of the patient, and how the pump power affects the valve opening during the cardiac cycle. We used our mathematical model to run nine different simulations that covers a variety of patient cases to observe such changes when the aortic valve is working properly (i.e. opening and closing every cardiac cycle) and when it is in the permanent closure state. The simulation results are then presented and they show consistent waveform patterns among all the nine cases. The following chapter will continue investigating the aortic valve dynamics specifically on bridge to recovery patients.

## **CHAPTER 6: AORTIC VALVE DYNAMICS IN BRIDGE TO RECOVERY TREATMENTS**

In this chapter, we explain the necessity of studying the aortic valve dynamics during the LVAD support for bridge to recovery treatment. By using the mathematical model, we examine the aortic valve performance prior to its permanent closure for different activity levels of the patient and severity of heart failure. Additionally, LVAD power and speed control parameters that yield a given percentage of the cardiac cycle during which the aortic valve remains open are examined indicating that the severity of the heart failure is a very important factor in deciding the appropriateness of the LVAD as a bridge to recovery treatment. Then preliminary results are given to show the characteristics of the systemic circulation flow signal when the aortic valve is open and closed. Finally, a summary is presented.

### 6.1. Aortic valve permanent closure problems

The bridge to recovery treatment differs from the other two types of treatments in the sense that the native heart of the patient will have to completely support the blood flow demand on its own after the device is removed. In the bridge to transplant and the destination therapy this is not the case. In the former type the device supports the patient until the transplant is performed and the patient has a new heart, in the latter type the device is implanted permanently to support the patient with no plans for removal.

Bridge to recovery is a very critical use of the LVAD which was introduced in recent years [62],[63], and there are ongoing research activities to fully understand how the LVAD

affects the native heart of the patient. The aortic valve dynamics is an important assessment tool for indication of heart recovery and keeping normal operation of the valve can help avoiding incidents that can delay or prevent recovery.

Normal operation of the valve essentially means the opening and closing of the valve every cardiac cycle. The opening of the aortic valve is the event that starts the ejection phase. The closing of the valve marks the end of the ejection phase and the beginning of the relaxation phase (as discussed in chapter 1). When the LVAD pump is implanted, however, it disturbs this cycle by shortening the ejection phase due to the pump rapidly unloading blood from the ventricle. As explained in chapter 5, with the increased pump motor power, the aortic valve closes for the entire cardiac cycle, this is known as the permanent closure.

The permanent closure of the aortic valve of a bridge to recovery patient may cause numerous complications such as:

- 1- Changes in the hemodynamic conditions of the patient: The changes in the hemodynamic conditions of the LVAD patient can be attributed to the decreased pulsatility that is associated with the aortic valve permanent closure. This decrease in pulsatility can be seen in the pressure and the flow waveforms of LVAD patients when the valve is closed (Shown in Section 5.2). As the pump speed increases, the pulsatility decreases due to the higher rate of unloading blood from the ventricle. When the aortic valve experience permanent closure, decreased pulsatility still exists mainly because the contractions of the left ventricle. This low pulsatility can lead to aortic insufficiency and other long term vascular complications [64].

- 2- Aortic valve stenosis: It occurs to about 88% of LVAD patients [65]. Aortic stenosis is a narrowing of the aortic valve opening which can lead to a restricted blood flow from the left ventricle to the aorta. Figure 6.1 shows the differences between healthy aortic valve and aortic valve with stenosis, both during open and closed states. In the case of the aortic valve stenosis, it can be seen that the valve is not fully open in the “open state”, and it is partially closed in the “closed state”. This is a critical condition that needs to be avoided, since after the removal of the LVAD (as in bridge to recovery treatments) it is very important to have a functioning valve for the heart to continue supporting the patient’s blood flow demand on its own.
- 3- Stagnation of blood flow and thrombus formation: The stagnation of flow increases the possibility of thrombus formation [67] in the aortic root and this raises the concern because the proximity of where the coronary arteries are located. Figure 6.2 shows the two main coronary arteries starting from a point near the aortic valve. The coronary arteries are intended to feed the heart muscle with oxygenated blood from the negative flow in the aorta. The thrombus formation on the closed aortic valve will create coronary occlusion preventing blood to flow back through the coronary. This occlusion further weakens the heart muscle and increases the risk of fatal events such as cardiac arrest.

For such reasons, the aortic valve opening during every cycle is important to avoid these events. The frequent opening of the valve will maintain pulsatility in the aortic flow which will resemble that of a healthy heart, albeit the pulse magnitude will still be lower in the case of the

LVAD patient. In addition, the regular opening of the aortic valve can keep the anatomical structure of the valve preserved; hence, avoiding the aortic valve fusion and aortic valve stenosis. Finally, to avoid the risks of thrombus formation on the coronary, the flow of blood through the opened aortic valve can wash out the thrombus regularly. This can clear the way for the coronary arteries to get the oxygenated blood intended to feed the heart muscle [68].

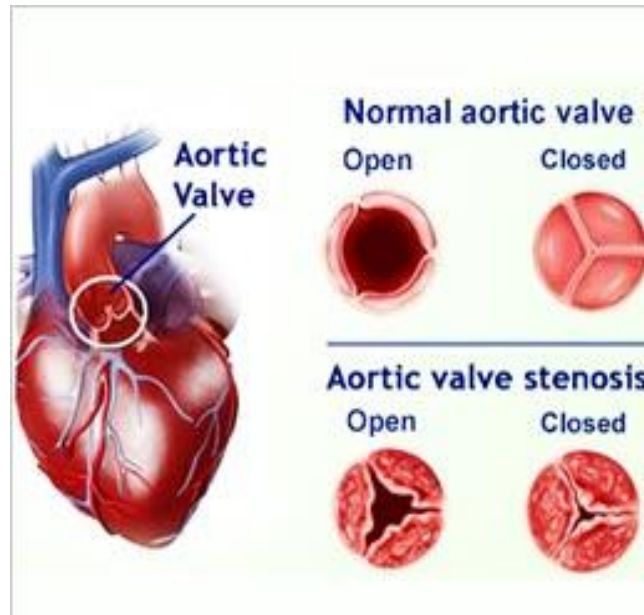


Figure 6.1: Aortic Valve Stenosis (source: [www.medindia.net](http://www.medindia.net))

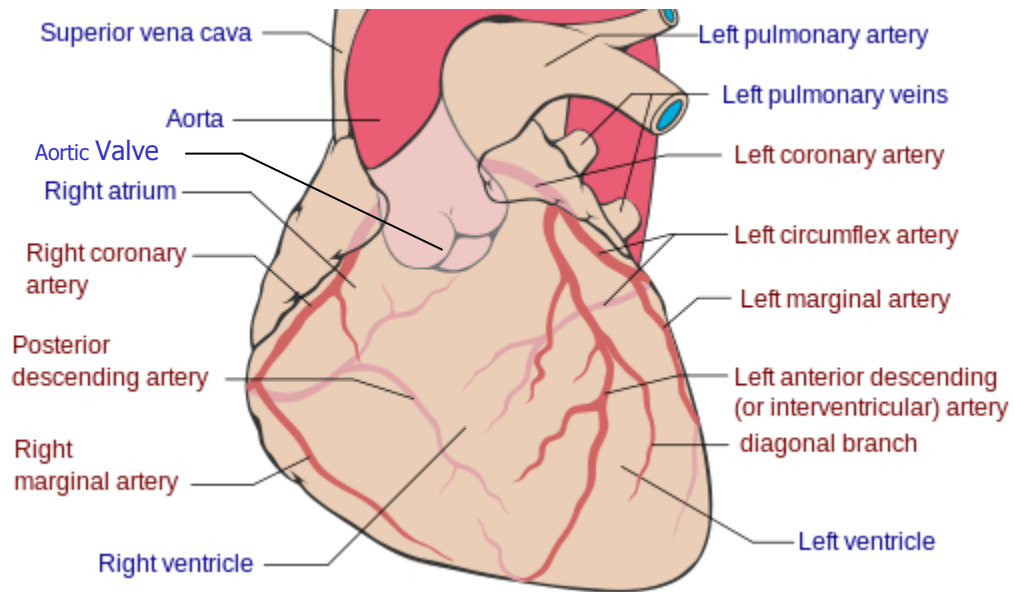


Figure 6.2: Coronary Circulation (source: [www.wikipedia.com](http://www.wikipedia.com))

## 6.2. Aortic valve performance

In the previous chapter, we defined the pump motor power level at which the aortic valve starts experiencing the permanent closure. In this chapter, however, the research is extended to look at the performance of the aortic valve prior to the time when it closes permanently. This is an important factor that needs to be examined in bridge to recovery treatments. It is well known that for a healthy heart, a normal aortic valve remains open during about 30% of the cardiac cycle while blood is ejected through the valve to the aorta [69]. In bridge to recovery LVAD treatment, clearly the aortic valve does not instantaneously switch from normal operation (i.e. being open for a portion of the cardiac cycle) to complete closure. One would expect that as the power level increase, the duration when the aortic valve remains open during a cardiac cycle will gradually decrease until permanent closure occurs at the critical values. The nine different cases used in chapter 5, and described in Table 5.1, were used to obtain the percentage of the aortic valve duration before its permanent closure. Figure 6.3-Figure 6.5 show plots of the percentage of the cardiac cycle during which the aortic valve remains open for the mild, moderate and severe heart conditions respectively plotted against the pump power. Each of these figures includes the three different cases of the activity level of the patient. It is interesting to note that, as expected, for an LVAD used as a bridge to recovery the range of flexibility in the control variable is widest when the heart failure condition is mildest (as in Figure 6.3). In fact, for a very active patient with mild heart failure, the valve remains active - being open during about 10% of the cardiac cycle - even when  $P_E$  reaches a value of 1.5W. On the other hand, when the condition of the patient is severe (as in Figure 6.5) it is extremely difficult to control the power delivered to the LVAD in such a way as to keep the aortic valve operating properly. The range

of control over which the valve remains operating properly is very narrow; lower than  $0.3W$ ,  $0.4W$  and  $0.7W$  for inactive, moderately active and very active patient, respectively. Comparing the three figures, it is important to note that regardless of the severity of heart failure, the more active the patient the larger  $P_E^c$  will be.

It is interesting to note that at very low pump motor power setting (i.e.  $P_E=0.1W$ ), the aortic valve opening duration percentage is roughly within 35%-40% of the cardiac cycle for the very active case, regardless of the heart failure severity. When the heart failure is severe, however, the rate of decrease in the opening percentage decreases rapidly, and it closes permanently at  $0.7W$ . In the mild heart failure case, the decrease in the opening percentage of the valve is much slower than the other two cases, where the permanent closure occurs at  $1.6W$ . This observation is also true for the cases of moderately active and Inactive, which their aortic valve opening percentages start at 20%-25% and 18%-23% of the cardiac cycle at  $P_E=0.1W$ , respectively.



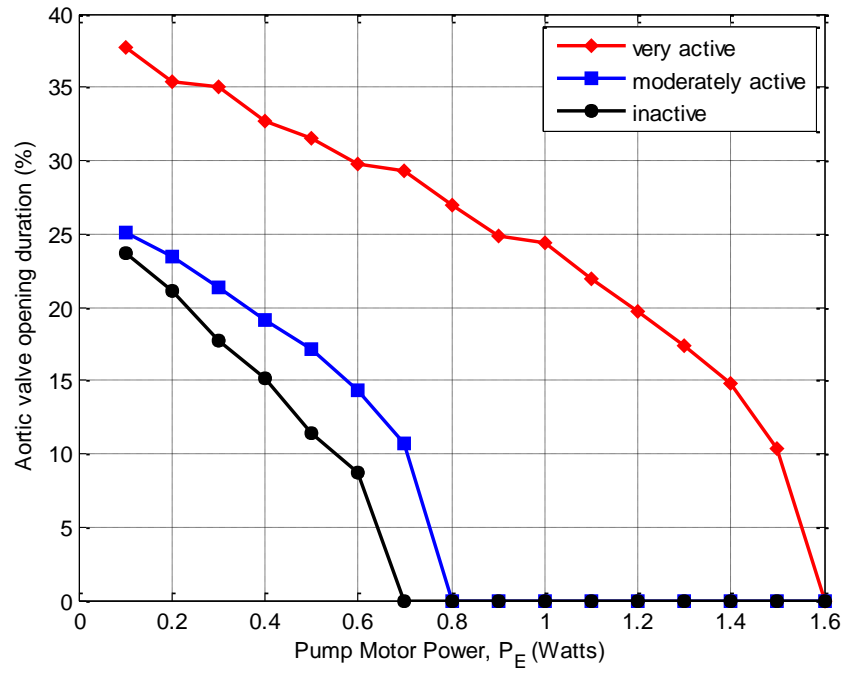


Figure 6.3. Aortic valve opening time as a percentage of the cardiac cycle for mild heart failure

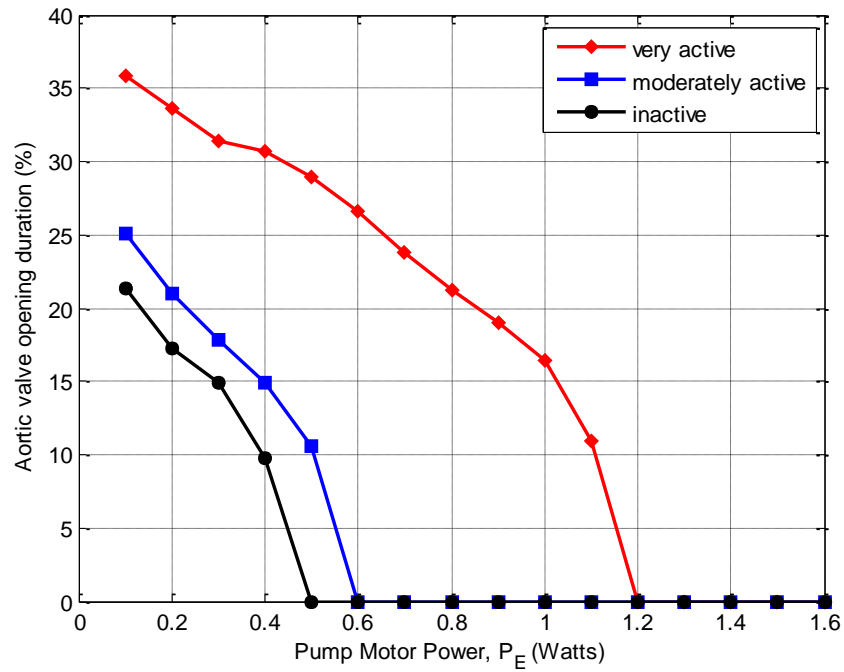


Figure 6.4. Aortic valve opening time as a percentage of the cardiac cycle for moderate heart failure

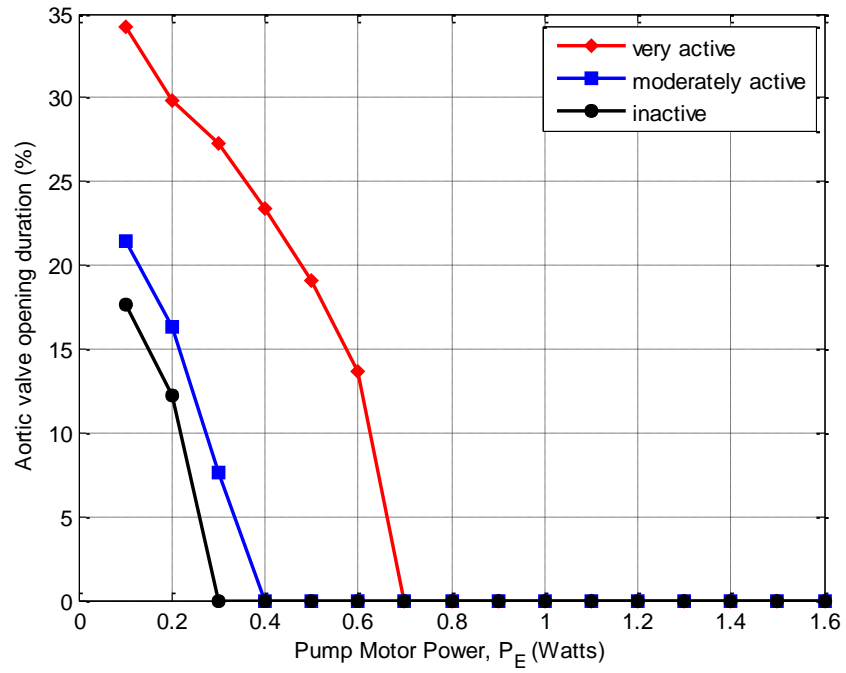


Figure 6.5. Aortic valve opening time as a percentage of the cardiac cycle for severe heart failure

Generally speaking, it would be preferable to operate the LVAD at control values that result in a specified percentage of the cardiac cycle for the aortic valve to remain open. As an illustrative example, Table 6.1 shows the power requirements and resulting pump speeds that yield conditions where the aortic valve remains open for 15% of the duration of the corresponding cardiac cycle. The 15% was selected as a guideline because it represents half of the opening duration percentage of an aortic valve of a healthy individual. In addition, at 15% we can see clearly from the figures that the aortic valve will open during the cardiac cycle for each of the nine cases. Clearly all of these values are below the critical values given in Table 5.2 and may be used as guidelines for controlling the LVAD pump.

One aspect of the results of interest is the level of cardiac support provided to the circulatory system in a bridge-to-recovery LVAD treatment. Table 6.2 shows the total blood flow rate in the circulatory system when the LVAD is operated to keep the aortic valve open for 15% of the duration of the corresponding cardiac cycle (i.e., using the control values shown in Table 6.1). The total rate of blood that flows in the circulatory system of a healthy person (with  $E_{\max} = 2$ ) at the same three levels of activity defined in Table 5.1 are also shown in Table 6.2. This table also shows the percentages for each of the nine blood flow rates with respect to the corresponding blood flow rate of a healthy heart. Note that in the case of mild heart failure, the total blood flow rate supplied to the circulatory system ranges between 87% and 91% of the blood flow rate required by a healthy heart. For the moderate heart failure case, this range is between 74% and 77%, and for the severe heart failure case, this range is between 56% and 59%. It is interesting to note that in each of these three cases, the range is very narrow (3 to 4%), indicating that the LVAD's ability to meet the patient's need for blood flow is not much affected

by the level of patient's activity level. However, for each level of activity, the LVAD's ability to meet the patient's blood need is highly dependent on the patient's heart failure condition. These percentages cover a much wider range (30 to 32%) depending on the patient's heart condition. It is also important to note that in the severe heart failure case, the LVAD is only able to provide a little more than one half (56% to 59%) of required blood flow to sustain the patient's needs, leading to the intuitive conclusion that the LVAD may not be appropriate as a bridge to recovery treatment for patients with severe heart failure.

Table 6.1: pump power ( $P_E$ ) and pump speed ( $\omega$ ) values of the nine different cases to keep the aortic valve open during 15% of the duration of the corresponding cardiac cycle.

		Level of Heart Failure		
		$E_{\max} = 1.00$	$E_{\max} = 0.75$	$E_{\max} = 0.50$
Level of physical Activity	$HR = 120\text{bpm}$ $R_S = 0.5\text{mmHg.s/ml}$	$P_E = 1.39W$ $\omega = 9,141\text{rpm}$	$P_E = 1.02W$ $\omega = 8,503\text{rpm}$	$P_E = 0.59W$ $\omega = 7,470\text{rpm}$
	$HR = 75\text{bpm}$ $R_S = 1.0\text{mmHg.s/ml}$	$P_E = 0.57W$ $\omega = 8,553\text{rpm}$	$P_E = 0.4W$ $\omega = 7,838\text{rpm}$	$P_E = 0.23W$ $\omega = 6,917\text{rpm}$
	$HR = 60\text{bpm}$ $R_S = 1.2\text{mmHg.s/ml}$	$P_E = 0.4W$ $\omega = 8,338\text{rpm}$	$P_E = 0.28W$ $\omega = 7,693\text{rpm}$	$P_E = 0.14W$ $\omega = 6,672\text{rpm}$

Table 6.2: Blood flow required for healthy patient and blood flow produced for the nine different when the aortic valve open during 15% of the duration of the corresponding cardiac cycle

		Blood flow for healthy heart and different levels of heart failure			
		$E_{\max} = 2.00$	$E_{\max} = 1.00$	$E_{\max} = 0.75$	$E_{\max} = 0.50$
		mmHg	mmHg	mmHg	mmHg
Level of physical Activity	$HR = 120\text{bpm}$ $R_S = 0.5\text{mmHg.s/ml}$	9.30 l/min 100%	8.22 l/min 88%	7.04 l/min 76%	5.39 l/min 58%
	$HR = 75\text{bpm}$ $R_S = 1.0\text{mmHg.s/ml}$	4.90 l/min 100%	4.46 l/min 91%	3.77 l/min 77%	2.88 l/min 59%
	$HR = 60\text{bpm}$ $R_S = 1.2\text{mmHg.s/ml}$	4.30 l/min 100%	3.74 l/min 87%	3.18 l/min 74%	5.40 l/min 56%

### 6.3. Preliminary results in detecting the aortic valve opening

In order to be able to maintain regular opening of the aortic valve during LVAD support, a feedback controller that can keep the pump motor power below the critical value ( $P_E^c$ ) must be developed. This controller should utilize a feedback variable from the pump signals or the cardiovascular system to detect the opening (or the permanent closure) of the aortic valve. In this research we present the systemic vascular flow as a good candidate to be the feedback signal. This signal is selected mainly because of two reasons: (1) measuring this signal can be done easily in real time through a flow sensor cuff placed on the arm of the patient, and (2) This signal pattern noticeably changes when the aortic valve experiences permanent closure.

The systemic vascular flow (denoted as  $I_{RS}$ ) is the total flow through the systemic circulation and is represented in the mathematical model as the current that flows through  $R_s$  (see Figure 2.3) this flow can be calculated in the model as:

$$I_{RS} = \frac{x_3(t) - x_2(t)}{R_s} \quad (6.1)$$

Or alternatively as:

$$I_{RS} = x_5(t) - C_s \frac{dx_3(t)}{dt} \quad (6.2)$$

Figure 6.6 shows the systemic vascular flow signals for the case of a mild heart failure and moderate level of activity, within three cardiac cycles, for different values of  $P_E$ . In Figure 6.6 (a) – (c) (blue plots) the pump motor power values used are 1.4W, 1.1W and 0.8W, respectively. All these values are high enough to cause the permanent closure of the aortic valve

(see Figure 6.3 and Table 5.2), in fact one of the pump motor power values ( $P_E = 0.8W$ ) is the critical pump motor power ( $P_E^c$ ). The systemic vascular flow signals in these three plots have two peaks during each cardiac cycle; one of these peaks is distinctively higher than the other. This is remarkably different than the signals shown when lower pump motor power values (i.e. less than  $P_E^c$ ) are used. Figure 6.6 (d)-(e) show the systemic vascular flow (in red plots) when pump motor power is set to 0.6W and 0.3W, respectively. In these cases, the difference between the two peaks in value is much smaller than the previous cases [70].

Figure 6.7-Figure 6.9 show that this signal pattern is consistent in all the nine cases we presented in Table 5.1. The three figures represent the three level of heart failure severity, while each figure has three subplots to represent the three levels of activity: (a) active, (b) moderately active, and (c) inactive. The range and step increase of the pump motor power in each case were changed to guarantee that the critical pump power ( $P_E^c$ ) value is used (shown in dashed blue trace), in addition to two other values (shown in dashed blue trace also) greater than  $P_E^c$  and other two below  $P_E^c$  (shown in solid red trace).

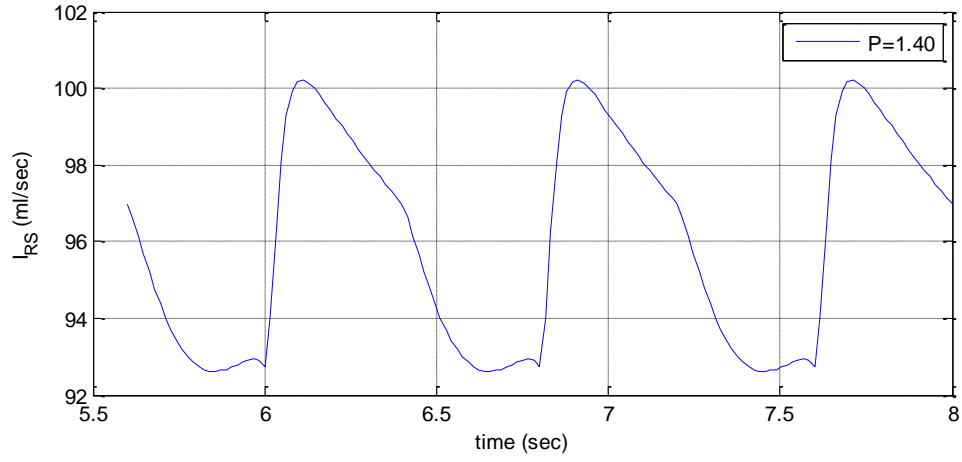
These plots further support the claim that it is easier to detect the aortic valve opening and develop a controller for keeping the aortic valve dynamics normal in patients with mild heart failure. As seen in Figure 6.7-Figure 6.9, the vertical separation between the two peaks when the patient has a mild heart failure is greater than that of the other two cases of heart failure severity. Additionally, within each level of heart failure severity, this vertical separation increases as the level of activity increases. This concludes to the fact that an active patient with mild heart failure

is the most obvious case (between the nine cases) for a controller to easily detect the aortic valve permanent closure occurrences.

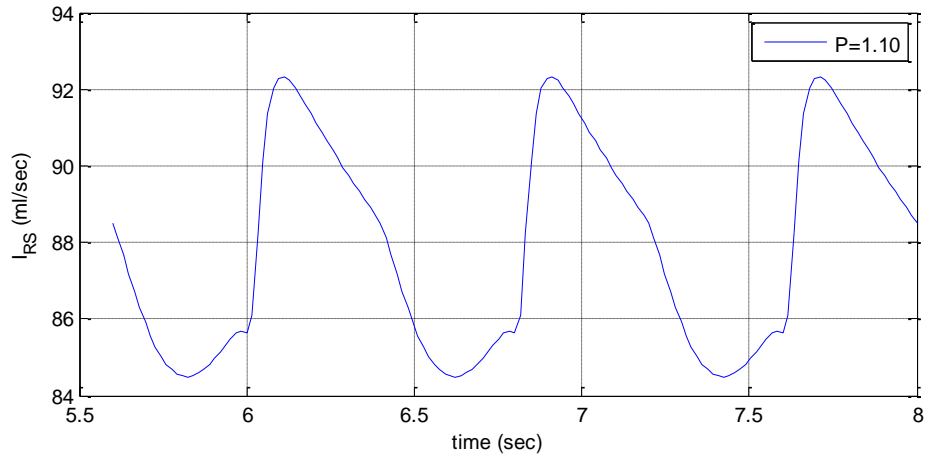
Again the case of a mild heart failure and moderate level of activity case is used as a representative case to highlight another significant pattern in the systemic vascular flow signal. Figure 6.10 is the same as Figure 6.7(b), but with a wider range of pump motor power values used and a smaller step. The range of  $P_E$  that is used in this simulation starts from 0.2W to 1.6W, with a step of 0.1W. The solid red traces in the figure represent the pump power values below  $P_E^c$ . These flows seem to share the first of the two peaks in the flow during each cardiac cycle (see the arrow labeled  $P_1$  in the figure). The dashed blue traces are the flows that cause the aortic valve permanent closure to happen, and it can be seen that they neither share the first nor the second peak of the flow.

Finally, Figure 6.11 shows the systemic vascular flow of healthy heart (The cardiovascular model introduced in chapter one was used). This signal resembles the systemic vascular flow of heart failure patients when the aortic valve is operating normally, although in the case of healthy heart, it can be seen that the first peak is greater than the second peak.

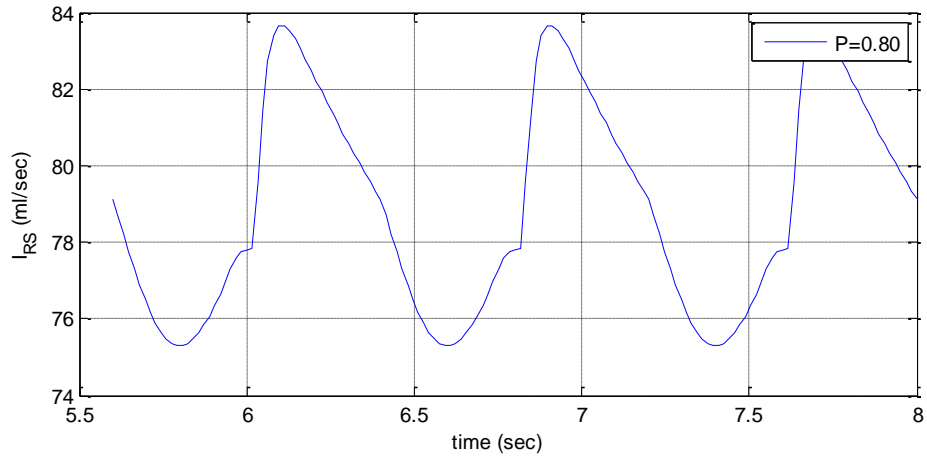




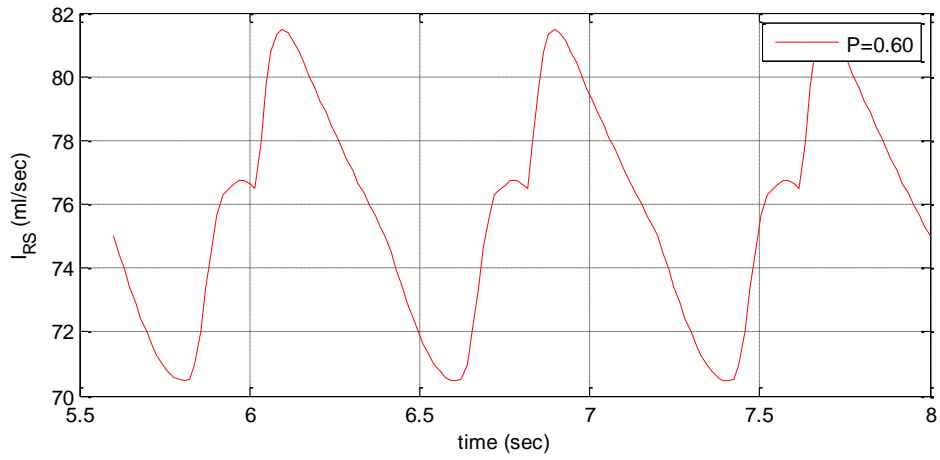
(a)



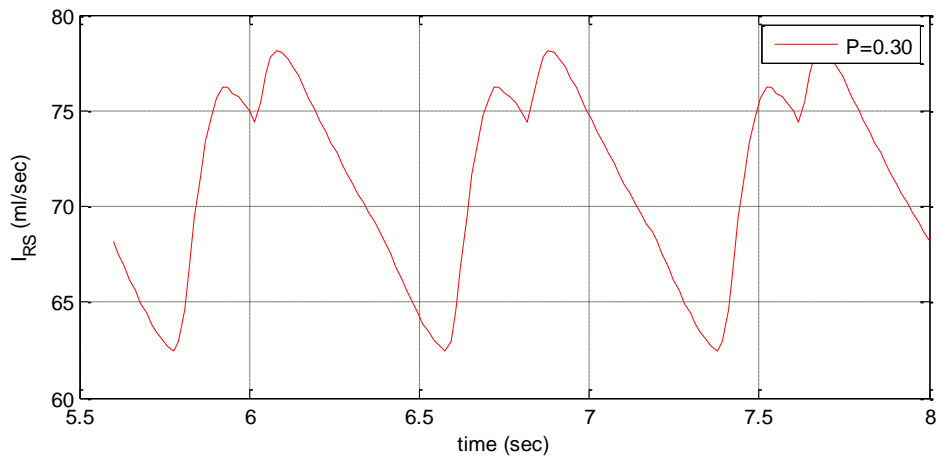
(b)



(c)

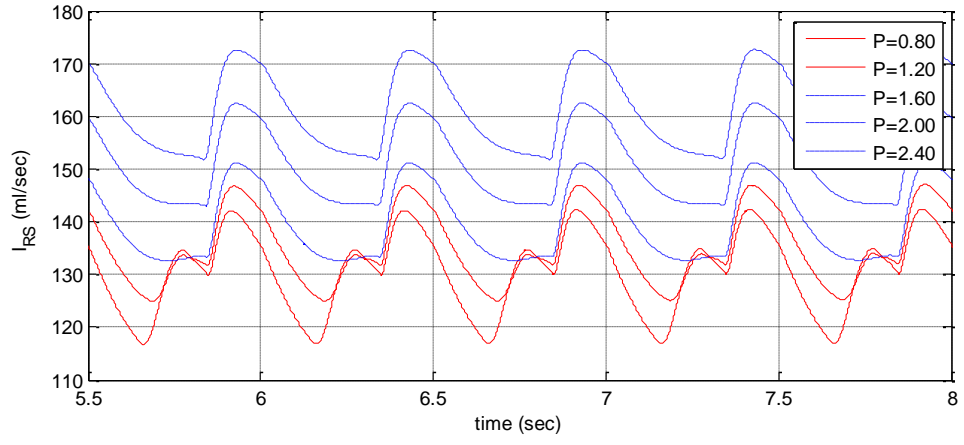


(d)

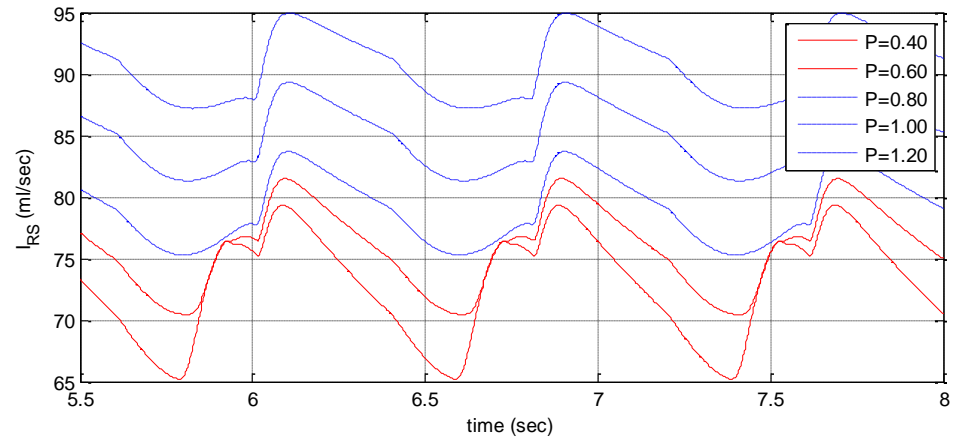


(e)

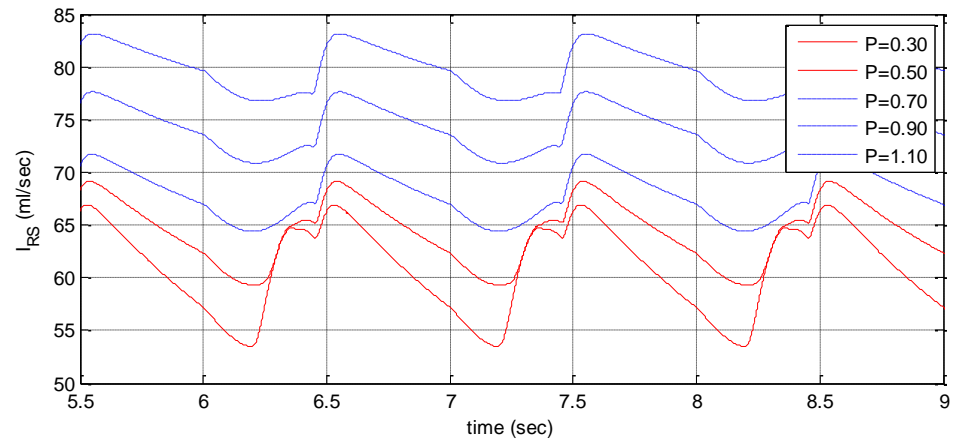
Figure 6.6: Systemic vascular current signal for mild heart failure with moderate level of activity. Pump motor power values shown are (a)  $P_E=1.4W$ , (b)  $P_E=1.1W$ , (c)  $P_E=0.8W$ , (d)  $P_E=0.6W$  and (e)  $P_E=0.3W$



(a)

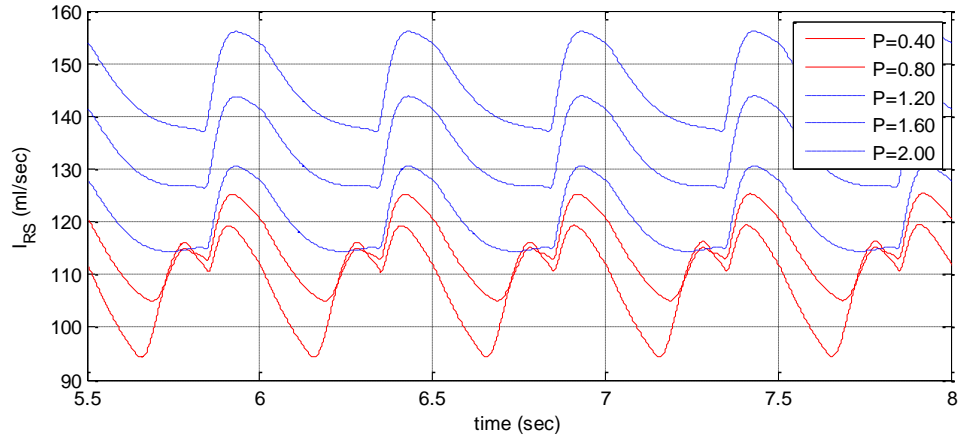


(b)

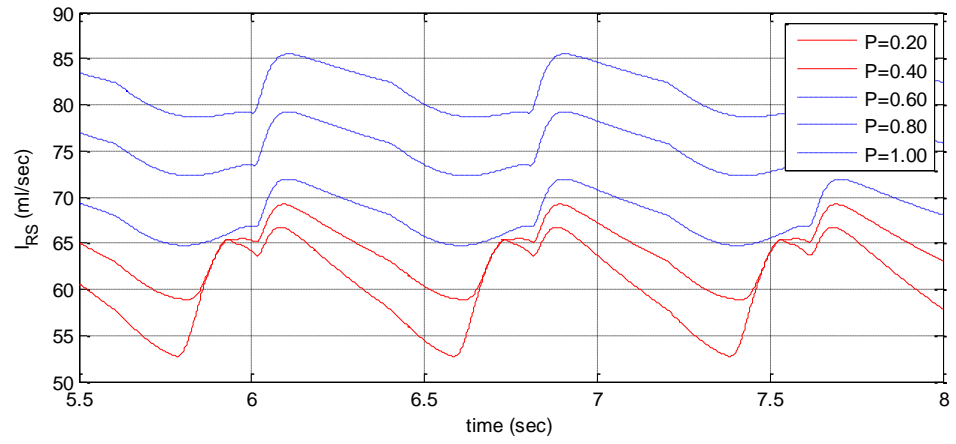


(c)

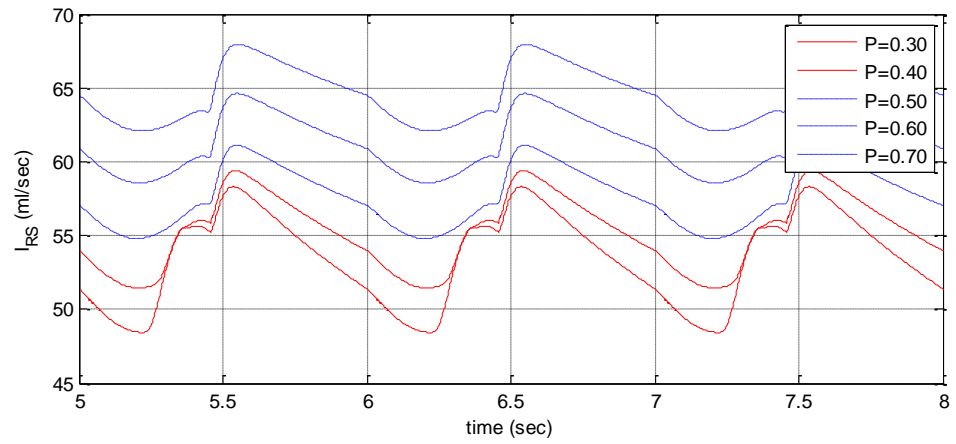
Figure 6.7: Systemic vascular of patient with mild heart failure and different levels of activity: (a) active, (b) moderately active, and (c) inactive.



(a)

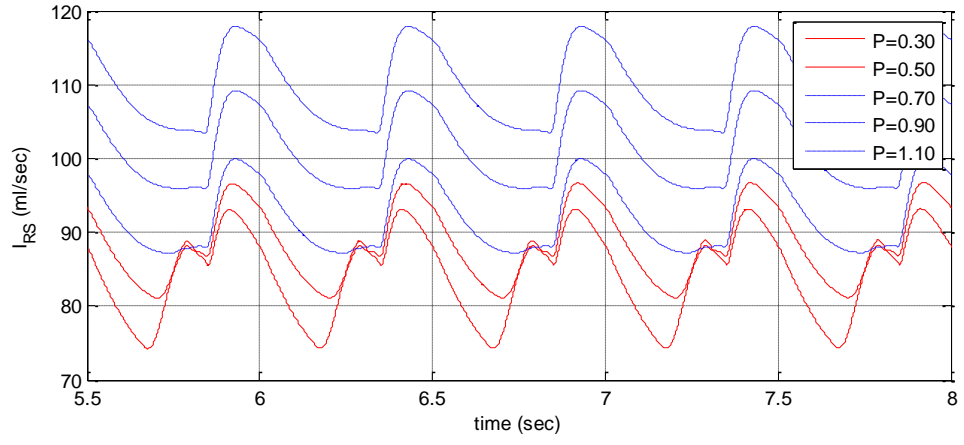


(b)

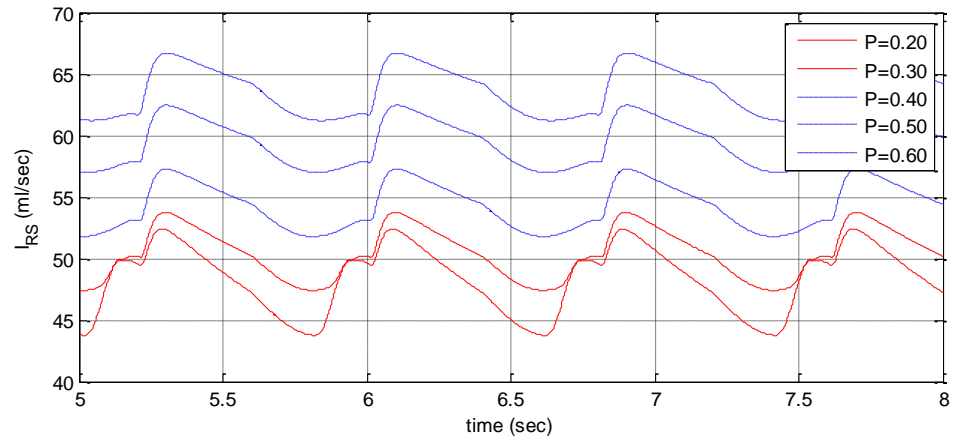


(c)

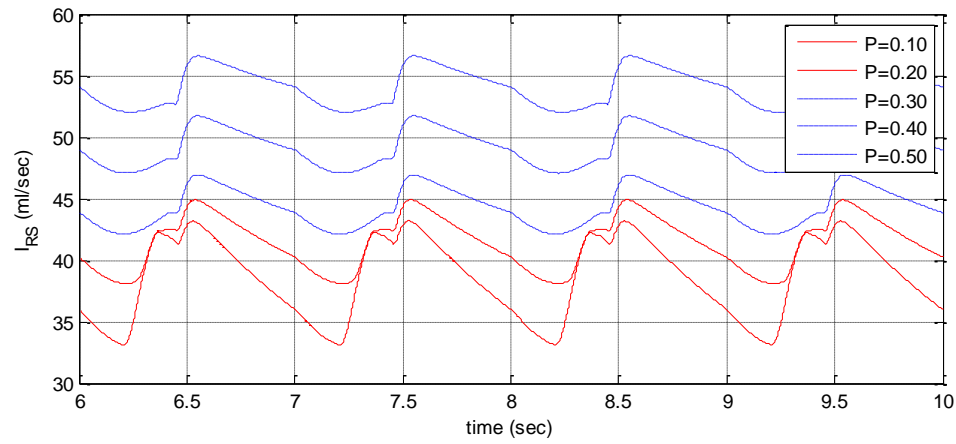
Figure 6.8: Systemic vascular of patient with moderate heart failure and different levels of activity: (a) active, (b) moderately active, and (c) inactive.



(a)



(b)



(c)

Figure 6.9: Systemic vascular of patient with severe heart failure and different levels of activity: (a) active, (b) moderately active, and (c) inactive.

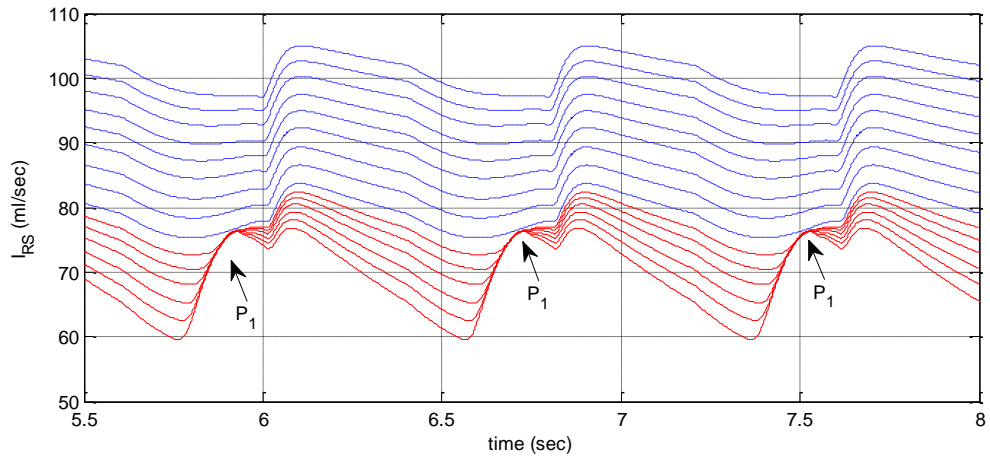


Figure 6.10:  $I_{RS}$  for mild heart failure and moderate level of activity.  $P_E$  range is from 0.2W to 1.6W .

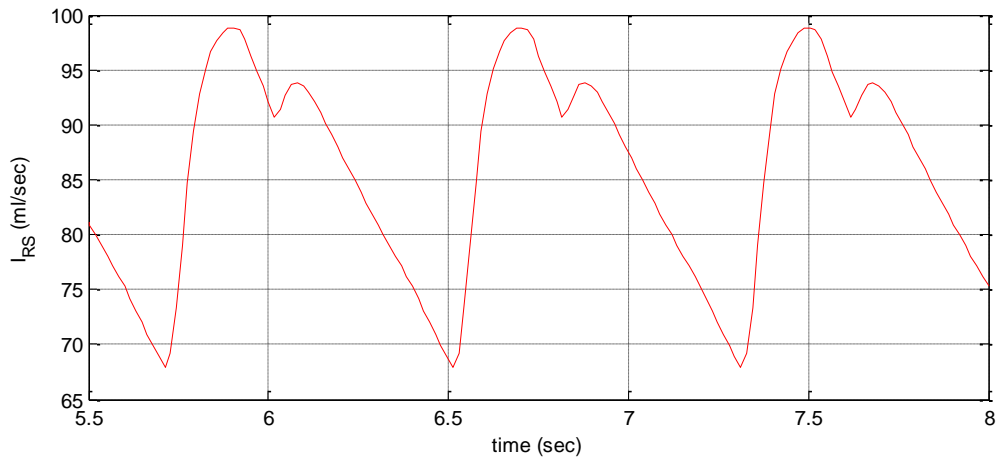


Figure 6.11: Systemic vascular flow for healthy heart with no LVAD used

#### 6.4. Summary

In this chapter, we used the data and simulation results from chapter five to further explore the effect of the aortic valve dynamics on the bridge to recovery treatments. The problems that occur because of the permanent closure of the aortic valve are listed. The aortic valve frequent opening was presented as a solution for these problems. Aortic valve opening duration is examined as the pump motor power is increased. The results show that the active patient with mild heart failure case has the highest pump motor power value at which the permanent closure occurs. This essentially means that the pump can be operated in a wide range of values while the aortic valve is opening every cardiac cycle. Finally, we presented simulation results suggesting that the systemic vascular flow is a good candidature to be a feedback variable for a controller that can keep the aortic valve dynamics operating normally.

## **CHAPTER 7: SUMMARY, CONCLUSION AND FUTURE WORK**

In this chapter, we summarize the research work while highlighting the conclusions that have been made in this dissertation. This chapter also presents possible future work directions where improvements are needed to shape the work presented here in a more practical form.

### 7.1. Summary and conclusion

The research presented in this dissertation attempted to provide a treatment-specific approach in the analysis and control of the LVAD in a heart failure patient. A modified combined cardiovascular-LVAD model that can accurately represent the system was used in obtaining the simulation results.

First, an introduction about cardiovascular system was presented in Chapter One. An overview of the heart, cardiac cycle and different circulations was discussed from the physiological point of view. Then we reviewed a previously developed fifth order model of the cardiovascular system that focuses on the left side of the heart.

In the second chapter we reviewed the heart failure problem and the different treatment options. One of these treatment options is the use of the LVAD, which is the main focus of this research. We explained the differences between the two generations of the LVAD, the different components of the device, and the treatment strategies of the LVAD usage. We continued to build on the model presented in Chapter One by adding the LVAD pump model in parallel to the native left ventricle of the patient. This resulted in the combined cardiovascular-LVAD system. This model used the pump speed as the control variable. It is important to note that this



combined (i.e. the cardiovascular-LVAD system) model was completely developed by a previous work of another research group.

In Chapter Three, we improved this model by selecting the pump motor power to be the control variable of the model. This is the first contribution of the dissertation, since the introduction of the pump motor power, instead of the pump speed, as the control variable made the existing model more practical. It may be acceptable from a theoretical perspective to have the pump speed as the control variable, but in reality the pump is controlled by the supplied power to the LVAD pump motor. We reformulate the sixth order model to have the pump motor power as the independent control variable. The relationship between the pump motor power and the pump speed was shown to be non-linear and is influenced by the pump flow. Simulation results concluded that the pump speed signal pattern changes as the LVAD operates in the suction range. Another conclusion from the simulation results was the effect of the severity of the heart failure on the pump speed and the pump flow signals. It was shown that the higher the value of  $E_{\max}$  (which is a representation of the contractility of the heart muscle), the larger the amplitude of both the pump speed and pump flow signals, while the pump power is kept constant. This essentially means that with the control variable of the pump being constant, the patient with less severe heart failure condition will have more blood flow as a result of the heart muscle ability to pump more blood.

Chapter Four presented the development of a feedback control that can be used in the bridge to transplant and destination therapy. This feedback controller is the second contribution by this dissertation. In this controller, the feedback variable is the spontaneous change (i.e. when pump motor power is kept constant) in the pump flow when the activity level of the patient

changes. When the controller detects a change in the pump flow, without any change in the pump motor power, an algorithm is employed to find the new  $R_s$  value that resulted from the change of the activity level. It should be noted here that  $R_s$  is the representation of the activity level of the patient in the model. Once  $R_s$  is identified, it is used in the fifth order model to calculate the physiological demand of blood flow of a health individual under the same level of activity. This physiological demand becomes the new blood flow target of the controller. The controller will use an optimization function to minimize the difference between the current pump flow and the target pump flow.

The third, and last, contribution of this research is presented in Chapters Five and Six. Chapter Five focuses, in general, on the effect of the pump performance on the aortic valve and the hemodynamic conditions of the patient. We developed a method to gather the data needed to study such effects, and we included a wide range of patient situations by varying  $E_{\max}$  (to represent different levels of heart failure severity), and  $R_s$  (to represent different levels of activity). The simulation results showed a change in the hemodynamic signals (such as: left ventricular pressure, aortic valve flow, and aortic pressure), when the aortic valve is closed during the entire cardiac cycle, also known as permanent closure. We showed that the envelope of the maximum values of the pump flow signal is continuously increasing as the pump motor power is increased while the aortic valve dynamics are normal. Once the aortic valve is in permanent closure state, that envelope of the maximum values has a slope of approximately zero.

Chapter Six used the data and simulation results from Chapter Five to provide a more detailed study on the aortic valve dynamics while focusing on the bridge to recovery treatment.

The permanent closure of the aortic valve can negatively impact the process of the heart recovery, thus we began the chapter with listing the problems associated with the valve permanent closure. We continued by explaining how the regular opening of the valve can contribute to avoiding the occurrence of such problems. The aortic valve opening duration as a percentage of the cardiac cycle was examined for the same patient situations listed in Chapter Five. We showed how the aortic valve opening percentage is comparable to that of a healthy heart when the pump motor power used is relatively low. The percentage decreases as we increase the pump motor power, until the permanent closure of the aortic valve happens when the pump motor power reaches its critical value. A comparison was made between the physiological demand of the patient and the blood flow when the pump is operated with the objective of keeping the aortic valve opening once every cardiac cycle. The purpose of the comparison was to show that in certain patient situations (such as: a patient with severe heart failure), it is not recommended to use this strategy (i.e. the aortic valve opening every cardiac cycle) since the critical pump motor power is so low that the blood flow by the pump is not sufficient for the patient. Finally, we suggested the use of the systemic flow signal to detect the permanent closure of the valve. This signal showed a different signature when the aortic valve is experiencing permanent closure. When the aortic valve is operating normally, the systemic vascular flow signal has two peaks with a small vertical separation between them. When the aortic valve is in permanent closure state, this vertical separation is large. Furthermore, in some cases when the pump motor power is very high, the first peak in the signal doesn't exist (i.e. the signal has one peak every cardiac cycle).

## 7.2. Future work

There are number of future research directions that can be based on the work presented in this research.

First, in Chapter Three we presented interesting observation of the amplitude change of the pump speed and pump flow signals when  $E_{\max}$  is changed.  $E_{\max}$  is a reliable index of the strength of the heart muscle of the patient. Estimating  $E_{\max}$  requires invasive sensors placement to measure pressure and flow signals [71]. Using the observation presented here in this dissertation, a less invasive method can be used to estimate  $E_{\max}$ . This will enhance the monitoring of the heart recovery process under the LVAD support (if the intended treatment is bridge to recovery).

Second, the development of a feedback controller that can use an algorithm to detect the permanent closure of the aortic valve, and change the pump motor power accordingly to keep the normal operation of the aortic valve. Initial efforts were done in developing a detection method using an indicator index ( $I_v$ ) that represents the relationship between the absolute value of the amplitude difference between the two peaks ( $P_1$  and  $P_2$ ) and the peak to peak amplitude ( $\Delta P$ ) of the signal [72]. That is:

$$I_v = \frac{|P_2 - P_1|}{\Delta P} \quad (7.1)$$

The ability of this method to detect the permanent closure of the aortic valve in simulation, allows it to be further validated in animal studies. Additionally, research needs to be

done to develop a feedback controller that can use this method and optimally adjust the pump motor power to meet the criterion of bridge to recovery treatment.

It is interesting to see that our future work focuses on the bridge to recovery treatment. This type of treatment has gained a lot of attention from different LVAD research groups. There is a great positive on the quality of life of the patient with a successful bridge to recovery treatment. In bridge to recovery treatment, the native heart regains its power to completely support the body, and then the LVAD can be removed. This treatment avoids the medical risks and financial burdens of having to go through heart transplant procedure (which is the case when the LVAD is used as a bridge to transplant device). It also avoids the inconvenience of being permanently supported by the LVAD device (as in the case of destination therapy), in addition to avoiding the risk of bleeding and thrombus formation when the LVAD is placed for a long period of time.

## REFERENCES

- [1] J. J. Batzel, F. Kappel, D. Schneditz and H. T. Tran, *Cardiovascular and Respiratory Systems: Modeling, Analysis and Control*, Philadelphia, PA: SIAM, 2007.
- [2] M. MacDonald, *Your Body: The Missing Manual*, 1<sup>st</sup> ed. Sebastopol, CA: O'Reilly Media, 2009.
- [3] A. C. Guyton and J. E. Hall, *Textbook of Medical Physiology*, 11th ed. Philadelphia, PA: W.B. Saunders, 2006.
- [4] Y. Wang, "A New Development of Feedback Controller for Left Ventricular Assist Devices," M.S. thesis, Dept. Elect. Eng., Univ. of Central Florida, Orlando, FL, 2010.
- [5] R. Aris, *Mathematical Modeling techniques*, Mineola, NY: Dover Publications, 1994.
- [6] T. A. Parlikar, "Modeling and Monitoring of Cardiovascular Dynamics for Patients in Critical Care," PhD dissertation, MIT, Boston, MA, 2007.
- [7] N. Westerhof, N. Stergiopoulos and M. Noble, *Snapshots of Hemodynamics*, Boston, MA: Springer Science, 2005.
- [8] M. A. Simaan, A. Ferreira, S. Chen, J. F. Antaki and D. G. Galati, "A Dynamical State Space Representation and Performance Analysis of a Feedback-Controlled Rotary Left Ventricular Assist Device," *IEEE Trans. Control Syst. Technol.*, vol. 17, no. 1, pp. 15-28, 2009.
- [9] A. Ferreira, S. Chen, M. A. Simaan and J. F. Antaki, "A nonlinear state space model for a combined cardiovascular system and a rotary pump," in *Proc. 44<sup>th</sup> IEEE Conf. Decision Contr. Eur. Contr. Conf.*, Seville, Spain, Dec. 12-15, 2005, pp. 897-902.

- [10] A. Ferreira, D. G. Galati, M. A. Simaan and J. F. Antaki, "A dynamical state space representation of a feedback controlled rotary left ventricular assist device," in *Proc. 2005 ASME Int. Mech. Eng. Congr.*, Orlando, FL, Nov. 5-11, 2005, paper IMECE2005-80973.
- [11] Y. -C. Yu, J. R. Boston, M. A. Simaan and J. F. Antaki, "Estimation of systemic vascular bed parameters for artificial heart control," *IEEE Trans. Autom. Contr.*, vol. 43, no. 6, pp. 765-779, 1998.
- [12] F. J. Haddy and J. B. Scott, "Cardiovascular Pharmacology," *Ann. Rev. Pharmacol.*, vol. 6, pp. 49-76, 1966.
- [13] F. J. Haddy, H. W. Overbeck and R. M. Daugherty, "Peripheral Vascular Resistance," *Ann. Rev. Med.*, vol. 19, pp. 167-194, 1968.
- [14] T. S. Hogan, "Exercise-induced reduction in systemic vascular resistance: A cover killer and an unrecognized resuscitation challenge?," *Medical Hypotheses*, vol. 73, pp. 479-484, 2009.
- [15] J. Melo and J. I. Peters, "Low systemic vascular resistance: differential diagnosis and outcome," *Critical Care*, vol. 3, pp. 71-77, 1999.
- [16] B. Oommen, M. Karamanoglu and S. J. Kovacs, "Modeling time varying elastance: The meaning of load independence," *Cardiovascular Engineering: An Intr. J.*, vol. 3, no. 4, pp. 123-130, 2003.
- [17] H. Suga and K. Sagawa, "Instantaneous pressure-volume relationships and their ratio in the excised, support canine left ventricle," *Circulatory Res.*, vol. 35, no. 1, pp. 117-126, 1974.

- [18] N. Stergiopoulos, J. Meister and N. Westerhof, “Determination of stroke volume and systolic and diastolic aortic pressure,” *Amer. J. Physiol.*, vol. 35, no. 1, pp. H2050-H2059, 1996.
- [19] D. Lloyd-Jones, R. J. Adams, T. M. Brown, M. Carnethon, S. Dai, G. De Simone, T. B. Ferguson, E. Ford, K. Furie, C. Gillespie, A. Go, K. Greenlund, N. Haase, S. Hailpern, P. M. Ho, V. Howard, B. Kissela, S. Kittner, D. Lackland, L. Lisabeth, A. Marelli, M. M. McDermott, J. Meigs, D. Mozaffarian, M. Mussolino, G. Nichol, V. L. Roger, W. Rosamond, R. Sacco, P. Sorlie, R. Stafford, T. Thom, S. Wasserthiel-Smoller, N. D. Wong and J. Wylie-Rosett, on behalf of the American Heart Association Statistics Committee and Stroke Statistics Subcommittee, “Heart disease and stroke statistics—2010 update: a report from the American Heart Association,” *Circulation*, vol. 121, pp. e46-e215, 2010.
- [20] E. P. Trulock, J. D. Christie, L. B. Edwards, M. M. Boucek, P. Aurora, D. O. Taylor, F. Dobbels, A. O. Rahmel, B. M. Keck and M. I. Hertz, “Registry of the International Society for Heart and Lung Transplantation: twenty-fourth official adult lung and heart-lung transplantation report-2007,” *J. Heart Lung Transplant.* vol. 26, no. 8, pp. 782-795, Aug. 2007.
- [21] B. Jana, *Essentials of Practice of Medicine*, 2<sup>nd</sup> ed. New Delhi, India: B. Jain Publishers, 1991.
- [22] R. Shah, S. Kommu, R. Bhuriya and R. Arora, “Left Ventricular Assist Devices: Emerging Modality for Long Term cardiac Support,” in *New Aspects of Left Ventricular Assist Devices*, G. Reyes, Ed., InTech Publishers, 2011, ch. 4, pp. 67-82.



- [23] E. J. Birks, "Left ventricular assist devices," *Heart*, vol. 96, pp. 63-71, 2010.
- [24] S. Takatani, "Beyond Implantable First Generation Cardiac Prostheses for Treatment of End-Stage Cardiac Patients with Clinical Results in a Multicenter," *Ann. Thorac. Cardiovasc. Surg.*, vol. 8, no. 5, pp. 253-263, 2002.
- [25] S. C. Horton, R. Khodaverdian, P. Chatelain, M. L. McIntosh, B. D. Horne, J. B. Muhlestein, J. W. Long, "Left Ventricular Assist Device Malfunction: An Approach to Diagnosis by Echocardiography," *J. Amer. Coll. Cardiol.*, vol. 45, no. 9, pp. 1435-1440. 2005.
- [26] H. M. Reul and M. Akdis, "Blood pumps for circulatory support," *Perfusion*, vol. 15, no. 4, pp. 295-311, 2000.
- [27] D. B. Olsen, "The History of Continuous-Flow Blood Pumps," *Artif. Organs*, vol. 24, no. 6, pp. 401-404, 2000.
- [28] G. S. Kumpati, P. M. McCarthy and K. J. Hoercher, "Left ventricular assist devices as a bridge to recovery: present status," *J. Card. Surg.*, vol. 16, no. 4, pp. 294-301, 2001.
- [29] E. J. Birks, P. D. Tansley, J. Hardy, R. S. George, C. T. Bowles, M. Burke, N. R. Banner, A. Khaghani and M. Yacoub, "Left Ventricular Assist Devices and Drug Therapy for the Reversal of Heart Failure," *N. Engl. J. Med.*, vol. 355, no. 18, pp. 1873-1884, 2006.
- [30] D. M. Mancini, A. Beniaminovitz, H. Levin, K. Catanese, M. Flannery, M. DiTullio, S. Savin, M. E. Cordisco, E. Rose and M. Oz, "Low Incidence of Myocardial Recovery After Left Ventricular Assist Device Implantation in Patients With Chronic Heart Failure," *Circulation*, vol. 98, pp. 2383-2389, 1998.

- [31] D. P. Mulloy, S. Mahapatra, and J. A. Kern, "Treatment of ventricular arrhythmias in patients undergoing LVAD therapy," in *Ventricular Assist Devices*, J. Shuhaiber, Ed., InTech Publishers, 2011, ch. 8, pp. 137-158.
- [32] E. A. Rose et al., "Long-term mechanical left ventricular assistance for end-stage heart failure," *N. Engl. J. Med.*, vol. 345, pp. 1435-1443, 2001.
- [33] K. Lietz et al., "Outcomes of left ventricular assist device implantation as destination therapy in the post-REMATCH era: implications for patient selection," *Circulation*, vol. 116, pp. 497-505, 2007.
- [34] S. H. Chen, "Baroreflex-Based Physiological Control of a Left Ventricular Assist Device," PhD. dissertation, Dept. Elect. Eng., Univ. of Pittsburg, PA, 2006.
- [35] M. A. Simaan, "Rotary Heart Assist Devices" in *Handbook of Automation*, E. S. Nof, Springer Verlag, 2009, ch. 79, pp. 1409-1422.
- [36] H-J. Wagner and J. Mathur, *Introduction to Hydro Energy Systems: Basics, Technology and Operation*, Springer, 2011.
- [37] G. Faragallah, Y. Wang, E. Divo and M. A. Simaan, "A new current-based control model of the combined cardiovascular and rotary left ventricular assist device," in *Proc. Amer. Contr. Conf.*, San Francisco, CA, Jun. 29 – Jul. 1, 2011.
- [38] D. G. Mason, A. K. Hilton and R. F. Salamonsen, "Reliable suction detection for patients with rotary blood pumps," *Amer. Soc. Artif. Internal Organs (ASAIO) J.*, vol. 54, no. 4, pp. 359-366, 2008.

- [39] M. Vollkron, H. Schima, L. Huber, R. Benkowski, G. Morello and G. Wieselthaler, "Development of a suction detection system for an axial blood pumps," *Artif. Organs*, vol. 28, no. 8, pp. 709-716, 2004.
- [40] A. Tanaka, M. Yoshizawa, P. Olegario, D. Ogawa, K. Abe, T. Motomura, S. Igo and Y. Nose, "Detection and avoiding ventricular suction of ventricular assist devices," in *Proc. 27<sup>th</sup> Annu. Conf. IEEE Eng. Medicine and Biology.*, Shanghai, China, Sep. 1-4, 2005.
- [41] K-W. Gwak, "Application of extremum seeking control to turbodynamic blood pumps," *ASAIO Journal*, vol. 53, no. 4, pp. 403-409, 2007.
- [42] A. Ferreira, M. A. Simaan, J. R. Boston and J. F. Antaki, "Frequency and time-frequency based indices for suction detection in rotary blood pumps," in *Proc. Int. Conf. of Acoust., Speech and Signal Process.*, Toulouse, France, May 14-19, 2006.
- [43] Y. Wang, G. Faragallah, E. Divo and M. A. Simaan, "Feedback control of a rotary left ventricular assist device supporting a failing cardiovascular system," in *Proc 2012 Amer. Contr. Conf.*, Montreal, QC, Jun. 27-29, 2012.
- [44] P. Naiyanetr et al., "Cardiac contractility assessment in rotary blood pump recipients derived from pump flow," in *Proc. World Congr. of Int. Federation of Medical and Biological Eng.*, Munich, Germany, Sep 7-12, 2009, pp. 434-437.
- [45] H. Senzaki et al., "Single-beat estimation of end-systolic pressure-volume relation in humans. A new method with the potential for noninvasive application," *Circulation*, vol.94, no. 10, pp. 2497-2506, 1996.

- [46] M. Yoshizawa et al., “An approach to single-beat estimation of  $E_{\max}$  as an inverse problem,” in *Proc. 20<sup>th</sup> Int. Conf. IEEE Eng. In Medicine and Biology*, Hong Kong, Oct. 29 – Nov 1, 1998, pp. 379-382.
- [47] H. Suga, “Cardiac energetics: From  $E_{\max}$  to pressure-volume area,” *Clinical and Experimental Pharmacology and Physiology*, vol. 30, pp. 580-585, 2003.
- [48] P. Naiyanetr et al., “Continuous assessment of cardiac function during rotary blood pump support: A contractility index derived from pump flow,” *J. of Heart and Lung Transplantation*, vol 29, no. 1, pp. 37-44, 2010.
- [49] M. S. Slaughter et al., “Clinical management of continuous-flow left ventricular assist devices in advanced heart failure,” *J. Heart and Lung Transplantation*, vol. 29, no. 4S, pp. S1-S39, 2010.
- [50] H. Shima et al., “Noninvasive monitoring of rotary blood pumps: Necessity, possibilities and limitations,” *Artif. Organs*, vol.14, no. 2, pp. 195-202, 1992.
- [51] H. Konishi, J. F. Antaki and D. V. Amin, “Controller for an axial flow blood pump,” *Artif. Organs*, vol.20, no. 6, pp. 618-620, 1996.
- [52] G. Giridharan, G. Pantalos, S. Koenig, K. Gillars and M. Skliar, “Achieving physiological perfusion with ventricular assist devices: Comparison of control strategies,” in *Proc. 2005 Amer. Contr. Conf.*, Portland, OR, Jun 8-10, 2005, pp. 3823-3828.
- [53] S. Chen, J. F. Antaki, M. A. Simaan and J. R. Boston, “Physiological control of left ventricular assist devices based on gradient of flow,” in *Proc. 2005 Amer. Contr. Conf.*, Portland, OR, Jun 8-10, 2005, pp. 3829-3834.

- [54] K-W. Gwak, M. Ricci, S. Snyder, B.E. Paden, J. R. Boston, M. A. Simaan and J. F. Antaki, "In vitro evaluation of multiobjective hemodynamic control of a heart-assist pump," *Amer. Soc. Artif. Internal Organs (ASAIO) J.*, vol. 51, pp. 329-335, 2005.
- [55] C. D. Bertman, "Measurements for implantable rotary blood pumps," *Physiological Measurements*, vol. 26, pp. R99-R117, 2005.
- [56] G. Faragallah, Y. Wang, E. Divo and M. A. Simaan, "A new control system for left ventricular assist devices based on patient-specific physiological demand," *Inverse Problems in Sci. Eng. J.*, DOI: 10.1080/17415977.2012.667092, to be published.
- [57] G. Faragallah, Y. Wang, E. Divo and M. A. Simaan, "A new control system for left ventricular assist devices based on patient-specific physiological demand," in *Proc. Int. Conf. on Inverse Problems in Eng.*, Orlando, FL, May 4-6, 2011.
- [58] T. Akimoto, et al., "Rotary blood pump flow spontaneously increases during exercise under constant pump speed: results of a chronic study," *Artif. Organs*, vol.23, no. 8, pp. 797-801, 1999.
- [59] R. A. Dunlap, *The Golden Ratio and The Fibonacci Numbers*, 1<sup>st</sup> ed., World Scientific Publishing Co. Pte. Ltd., Singapore, 1997.
- [60] G. Faragallah and M. Simaan, "An engineering analysis of the aortic valve dynamics in patients with rotary left ventricular assist devices," *J. of Healthcare Engineering*, vol.4, no. 3, pp. 307-326, 2013.
- [61] A. P. Yoganathan, J. D. Lemmon and J. T. Ellis, "Heart Valve Dynamics" in *The Biomedical Engineering Handbook: Second Edition*, Joseph D. Bronzino, CRC Press LLC, Boca Raton, FL, 2000, ch. 29.

- [62] M. Navaratnarajah, et al. "Myocardial recovery following left ventricular assist device therapy" in *New Aspects of Left Ventricular Assist Devices*, G. Reyes, InTech Publishers, 2011, ch. 5, pp. 83-104.
- [63] S. Maybaum, G. Kamalakannan and S. Murthy, "Cardiac recovery during mechanical assist device support," *Thoracic and Cardiovascular Surgery*, vol. 20, pp. 234-246, 2008.
- [64] S. Bozkurt, et al., "A method to increase the pulsatility in hemodynamic variables in an LVAD supported human circulation system," in *International Conference on Advancement of Medicine and Healthcare Through Technology*, Cluj-Napoca, Romania, August 29 – September 2, 2011, pp. 328-331.
- [65] C. M. Carr, et al., "CT of ventricular assist device," *RadioGraphics*, vol. 30, pp. 429-444, 2010.
- [66] P. Posuwattanakul "The Biomechanical Evaluation of the Aortic Valve Leaflet Fusion in the LVAD-Assisted Heart" MSc. Thesis, San Diego State University, 2011.
- [67] J. A. Crestanello, et al., "Aortic valve thrombosis after implantation of temporary left ventricular assist device," *Interact Cardio Vasc Thorac Surg*, vol. 8, pp. 661-662, 2008.
- [68] J. Martina, "Aortic valve dynamics as a tool for pump speed assessment & management during left ventricular assist with continuous axial flow pumps," *Eindhoven University of Technology*, BMTE07.18.
- [69] E. Tuzun, et al., "Continuous-flow cardiac assistance: effects on aortic valve function in mock loop," *J. of Surgical Research*, vol. 171, no. 2, pp. 443-447, 2011.

- [70] Y. Wang, G. Faragallah and Marwan Simaan, "Detection of aortic valve dynamics in bridge-to-recovery feedback control of the left ventricular assist devices," in *Proc. Of 2014 Euro. Control Conf*, Strasbourg, France, June 24-27, 2014, pp. 140-145.
- [71] Y-C. Yu, et al., "Minimally invasive identification of ventricular recovery index for weaning patient from artificial heart support," in *Proc. Of the 39th Conf on Decision and Control*, Sydney, Australia, December 2000, pp. 1799-1803.
- [72] Y. Wang, and Marwan Simaan, "A new method for detecting aortic valve dynamics during control of the rotary left ventricular assist device support," in *Proc. Of 2014 Amer. Control Conf*, Portland, OR, June 4-6, 2014, pp. 5471-5476.